JIMMA UNIVERSITY

SCHOOL OF GRADUATE STUDIES

JIMMA INSTITUTE OF TECHNOLOGY

FACULTY OF CIVIL AND ENVIRONMENTAL ENGINEERING

STRUCTURAL ENGINEERING STREAM

Effect of Soft Storey Location on Seismic Performance of Reinforced Concrete Building

A Thesis Submitted to the Post Graduate Studies of Jimma University in Partial Fulfillment of the requirement for the Degree of MSc in Civil Engineering (Structure Engineering)

BY:

SHANBEL ZURIE

November, 2019

JIMMA, ETHIOPIA

JIMMA UNIVERSITY

SCHOOL OF GRADUATE STUDIES

JIMMA INSTITUTE OF TECHNOLOGY

FACULTY OF CIVIL AND ENVIRONMENTAL ENGINEERING

STRUCTURAL ENGINEERING STREAM

Effect of Soft Storey Location on Seismic Performance of Reinforced Concrete Building

A Thesis Submitted to the Post Graduate Studies of Jimma University in Partial Fulfillment of the requirement for the Degree of MSc in Civil Engineering (Structure Engineering)

BY:

SHANBEL ZURIE

MAIN ADVISOR: ENGR. ELMER C.AGON, ASSO.PROF

CO ADVISOR: ENGR. MENBERU ELIAS (MSc)

November, 2019

JIMMA, ETHIOPIA

CERTIFICATION

As a member of the examining board of the final MSc open defense. We certify that we have read and evaluated the thesis prepared by Shanbel Zurie Entitled "**Effect of soft storey location on seismic performance of reinforced concrete building**"; and recommended that it be accepted as fulfilling the thesis requirement for the degree of Master of Science in Structural Engineering.

Approved By Board of Examiners

Engr. Elmer C. Agon, Asso. Prof**.**

Advisor	Signature	Date
Engr. Menberu Elias (MSc)		
Co - Advisor	Signature	Date
Internal Examiner	Signature	Date
External Examiner	Signature	Date
Chair Person	Signature	Date

DECLARATIONS

I, the undersigned, declare that this thesis entitled "**Effect of soft storey location on seismic performance of reinforced concrete building**" is my original work, and has not been presented by any other person for an award of a degree in this or any other University, and all sources of material used for theses have been dually acknowledged.

Candidate:- - -

Shanbel Zurie

Signature_____

As Master research Advisors, we hereby certify that we have read and evaluate this MSc research prepared under our guidance, by Shanbel Zurie entitled: **"Effect of soft storey location on seismic performance of reinforced concrete building**" We recommend that it can be submitted as fulfilling the MSc Thesis requirements.

Engr. Elmer C. Agon, Asso. Prof

Main Advisor	Signature	Date

Engr.Menberu Elias (MSc)

Co- Advisor	Signature	Date

ACKNOWLEDGMENTS

This study was conducted under the supervision of the main advisor E**ngr. Elmer C. Agon, Asso. Prof. and co-advisor Engr.Menberu Elias.** I would like to express my sincere appreciation to the support, guidance and insights that they have provided me throughout the study. Their readiness for consultation at all times, their educative comments and inputs, their concern and assistance have been extremely helpful. I am also thankful to **Engr. Bisrat Ayalew** for his generous helps in various ways for the completion of this thesis.

Next, my gratitude goes for **Jimma Institute of Technology and Civil Engineering College** for facilitating and giving this chance.

At last but not least my gratitude towards my parents, I would also like to thank **God** for not letting me down at a time of crisis and showing me the silver lining in the dark clouds.

ABSTRACT

Reinforced concrete frames with masonry infill walls are a popular form of construction in seismic regions worldwide. The typical multi-story construction in Ethiopia comprises reinforced concrete frames with hollow concrete block masonry infill. Due to space requirements for meeting-hall, game zones, large reception rooms, open shopping areas, parking areas, the infill walls are removed or very large doors and windows are provided in reinforced concrete buildings. Unreinforced masonry infill wall panels may not contribute towards resisting gravity loads, but contribute significantly, in terms of enhanced stiffness and strength under earthquake loading. But the irregular distribution of infill crates soft storey; which is more affected by earthquake load. It is important to study the effect of irregular distribution of infill wall on the seismic performance of reinforced concrete buildings. This research determines the effect of soft storey location on seismic performance of reinforced concrete building with infill using pushover analysis.

A typical office and shopping use building located in severe seismic Zones of Ethiopia is analyzed and designed according to ESEN-2015 and Euro Code. Effect of soft storey location on seismic performance has been studied with the help of (G+7, G+10) total of 16 building models with soft storey at different locations. The infill was modeled using the equivalent diagonal strut and soft storey is modeled by removing in-plane diagonal struts. To study the effect of soft storey location on seismic performance of reinforced concrete building pushover analysis for lateral loads was done using ETABS 2017 software. The comparison of these models for different earthquake response parameters like pushover curve, target displacement and base shear at performance point, Story displacement, storey shear, storey drift and seismic performance assessment are carried out. Building with soft storey at the top has good seismic demand resistance.

Depending on the stiffness ratios for soft storey considered; the base shear resistances of the buildings increase by (23-39) % when soft storey located at the top than buildings soft storey at the bottom. The roof displacement of the building is the maximum displacement for exciting earthquake and converges at one point for buildings with soft storey at different locations. Buildings soft storey at the top has maximum storey shear which is increased by (21-68) % than buildings soft storey at the bottom level. The maximum drift ratio of the buildings decreases by (43-51) % and buildings soft storey located at top than bottom. Similarly, the base shear resistance at performance point is maximum and target displacement decrease by (17-36) %

Keywords: *Equivalent Diagonal Strut, Soft Storey, Soft Storey Location, Infill Wall, Plastic Hinge.*

Table of Contents

ACKNOWLEDGMENTS iii
ABSTRACT iv
List of Tables viii
List of Figures ix
SYMBOLS xiii
CHAPTER ONE 1
INTRODUCTION 1
1.1 Background of the Study 1
1.2 Statements of the Problems 3
1.3 Research Questions 4
1.4 Objective of the Study 4
1.4.1 Main Objective 4
1.4.2 Specific Objectives of the Study 4
1.5 Significance of the Study 4
1.6 Scope and Limitation of the Study 5
CHAPTER TWO 6
RELATED LITERATURE REVIEW 6
2.1 General 6
2.2 Soft Storey 6
2.3 Masonry Infilled RC Frame 9
2.3.1 Effect of Masonry Infill on the Seismic Behavior of Frame Structures. 9
2.3.2 Modeling of Masonry Infill 12
2.3.3 Perforated Panels 15
2.3.4 In-Plane Strength and Stiffness Evaluation of URM Infill 17
2.3.5 Masonry Infill Shear Strength 18
2.3.6 Masonry Infill Crushing Strength. 18
2.3.7 Load-Deformation Behavior of the Diagonal Strut 19

2.4 Frame Member 19
2.4.1 Stiffness 19
2.4.2. Load Effects on Seismic Behavior of Frame Elements.....20
2.5. Method of Structural Analysis 22
2.5.1. Elastic Methods of Analysis 22
2.5.2 Inelastic Methods of Analysis 23
2.5.2.1 Inelastic Time history Analysis……..23
2.5.2.2 Pushover Analysis……..23
2.6 Gaps in Research Areas 28
CHAPTER THREE 29
MATERIALS AND RESEARCH METHODOLOGY 29
3.1 Research Design 29
3.2 Study Variables 30
3.2.1 Dependent Variables 30
3.2.2 Independent Variables 30
3.3 Data Collection Processes 30
3.4 Data Quality Assurance 31
3.6 STRUCTURAL MODELING 31
3.6.1 Building Description 31
3.6.2 Structural Modeling Data 34
3.6.3 Modeling of Structural Elements 39
3.6.4 Modeling of Masonry Infill Wall 39
3.6.5 Modeling of Soft Storey 41
3.6.6 Frame Hinge Properties 42
3.6.7 Plastic Hinge Placement 43
3.6.8 Frame Member Stiffness 44
3.6.9 Masonry Infill Crushing Strength. 44

3.7 Structural Analysis 45
3.7.1 Nonlinear Static (Pushover) Analysis 45
3.8 Strengthening of Soft Storey 56
CHAPTER FOUR 57
RESULTS AND DISCUSSIONS.....57
4.1 General.....57
4.2. Analysis Results for Pushover Load in X-Direction 57
4.2.1 Base Shear vs Monitored Roof Displacement Curve.....57
4.2.2 Storey Displacement for All Models.....60
4.2.3 Storey Shear.....62
4.2.4 Storey Drift 64
4.2.5 Target Displacement and Base Shear at Performance Point 67
4.2.6 Seismic Performance Assessment.....70
4.2.7 Strengthening of Soft Storey 82
CHAPTER FIVE 85
CONCLUSIONS AND RECOMMENDATIONS 85
5.1 Conclusions.....85
5.2 Recommendation.....86
References 88
Appendix- A: Behavior factor calculation for frame system 92
Appendix- B: Modeling of the Frame.....93
Appendix C: Tabulated Results.....95
Appendix D. ETABS output of target displacement and base shear at performance point. 104
Appendix E. 3-D design detail of building models 112
Appendix F. Stiffness of building models from response spectrum analysis and soft storey stiffness ratio computation. 114
Appendix G: Outputs after Soft storey Strengthening.....115

List of Tables

Table2. 1 In-plane damage reduction factor.....16
Table3.1 Seismic load data and factors……35
Table3. 2 Properties of the material used for design and analysis 36
Table 4. 1 Target displacement and Base shear at performance point for regular plan buildings…67
Table4. 2 Target displacement and Base shear at performance point for irregular plan models 68
Table4.3 Number of hinges in each state of soft storey location for (G+7) plan regular building. .75
Table4. 4 Number of hinges in each state of soft storey location for (G+10) plan regular building77
Table4. 5 Number of hinges in each state of soft storey location for (G+7) plan irregular building.
.....78
Table4. 6 Number of hinges in each state of soft storey location for (G+10) plan irregular building.
.....80
Table B1.1 Physical properties of the frame and infill panel…….....93
Table C1. 1 Comparison of monitored displacement and base shear for (G+7) regular plan building…….95
Table C1. 2 Comparison of monitored displacement and base shear for (G+10) regular plan building. 96
Table C1. 3 Comparison of Monitored Displacement and Base shear for (G+7) irregular plan building. 97
Table C1.4 Comparison of Monitored Displacement and Base shear for (G+10) irregular plan building. 98
Table C1. 5Comparison of story displacement for (G+7, G+10) regular plan building.....98
Table C1. 6 Comparison of story displacement for (G+7, G+10) irregular plan building 99
Table C1. 7 Comparison of story shear for (G+7) regular plan building 99
Table C1. 8 Comparison of story shear for (G+10) regular plan building.....100
Table C1. 9 Comparison of storey shear for (G+7) irregular plan building 101
Table C1. 10 Comparison of storey shear for (G+10) irregular plan building.....101
Table C1. 11 Comparison of storey drift for (G+7, G+10) regular plan building.....102
Table C1. 12 Comparison of storey drift for (G+7, G+10) regular plan building.....102
Table F 1. 1 Stiffness of building models from response spectrum analysis…….114
Table G1. 1 Storey drift ratio after strength of soft storey & building without soft storey……...115
Table G1. 2 Storey displacements after strength of soft storey & building without soft storey….115

List of Figures

Figure1. 1 Failure of buildings due to soft storey (Kirac, Dogan, & Ozbasaran, 2011).....2

Figure 2. 1 Soft storey behavior of a building structure under lateral loading (Naphade, 2015)…...7

Figure 2. 2(A) Ground soft storey building & (B) Soft storey in above level building (Patnala & Ramancharla 2014).....8

Figure 2. 3 (A) Predominant frame action (B) Predominant truss action [15].....10

Figure 2. 4(A) Bare frame (B) frame with infill wall in all stories except ground floor [16].....10

Figure 2. 5 Pushover curve comparison for the bare and infilled frames [16].....11

Figure 2. 6 Displacement profile comparison for the bare and infilled frames [16] 11

Figure 2. 7 Equivalent diagonal strut model [19]. 14

Figure 2. 8 Perforated panel (Al-Chaar, 2002).....16

Figure 2. 9 Visual damage classifications (Al-Chaar, 2002) 17

Figure 2. 10Shear failure of masonry (Al-Chaar, 2002).....18

Figure 2. 11 Effects of lateral forces on a building (Paulay and Priestley, 1992).....21

Figure 2. 12 Generalized load-deformation relation for non-degrading components (Euro Code 8, 2005) 21

Figure 2. 13 Idealized flexural mechanisms in multi-story frames (Paulay and Priestley, 1992)...22

Figure 2. 14 Force-Deformation Relations for Plastic Hinge in Pushover Analysis (Habibullah and Pyle, 1998) 25

Figure 3. 1 Floor plan of (G+7) and (G+10) storey regular plan building models……..32

Figure3. 2 Sample of 3-D render view of regular plan building model.....33

Figure3. 3 Floor plan of (G+7) and (G+10) irregular plan building models.....33

Figure 3. 4 Sample of 3-D render view of irregular plan building model 33

Figure 3. 5 Sample designs of buildings in the plan view for regular plan model 38

Figure3. 6 Sample design of buildings in the plan view for irregular plan model 38

Figure3. 7 Sample design of buildings in the elevation view 39

Figure3. 8 Modeling of beam & column.....39

Figure3. 9 Connections of Compression Strut 40

Figure3. 10 diagonal strut modeling of walls using ETABS 2017 41
Figure3. 11 Sample Elevation view of soft storey modeling at ground floor 41
Figure3. 12 Plastic hinge placements 44
Figure3. 13Force-Deformation Relations for Plastic Hinge in Pushover Analysis 45
Figure3. 14Pushover load case for Gravity loads 50
Figure3. 15 Pushover load case for Pushover loads 51
Figure3. 16 Load application control for non-linear static analysis 51
Figure3. 17 Result saved for non-linear static load case 52
Figure3. 18 Hinge at both ends for columns 52
Figure3. 19Hinge Properties for Beams 53
Figure3. 20 Hinge Properties for Columns 53
Figure3. 21 User-defined hinge properties for diagonal strut 54
Figure3. 22 Hinge assignment for diagonal struts 54
Figure3. 23 Set Load Case to Run the Analysis 55
Figure3. 24 Graphical representation of capacity spectrum method 55
Figure3. 25 Cross-sectional dimension of X-steel bracing used and strengthening of soft storey ..56
Figure4. 1 pushover Curves for G+7 plan regular building for Push X –load..... 58
Figure4.2 Pushover Curves for G+10 plan regular building for Push X – load 58
Figure4. 3 Pushover Curves for G+7 plan irregular building for Push X – load 59
Figure4. 4 Pushover Curves for G+10 plan irregular building for Push X– load 59
Figure4.5 Comparison of Story displacements in (G+7) plan regular building for push X– load ...60
Figure4.6 Comparison of Story displacements in (G+10) plan regular building for push X – load ……61
Figure4. 7 Comparison of Storey displacements for (G+7) plan irregular building for push X– load ……61
Figure4. 8 Comparison of Storey displacements for (G+10) plan irregular building for push X– load……...61
Figure4.9 Comparison of Storey shears for (G+7) regular plan building for push X –load…….63
Figure4.10 Comparison of Storey shears for (G+10) regular plan building for push X load……...63

Figure4.11 Comparison of Storey shears for (G+7) irregular plan building for push X –load……64

Figure4.12 Comparison of Storey shear for (G+10) irregular plan building for push X–load…….65

Figure4. 13 Comparison of drift ratio for (G+7) regular plan building for push X–load 65

Figure4. 14 Comparison of drift ratio for (G+10) regular plan building for push X –load 65

Figure4.15 Comparison of drift ratio for (G+7) irregular plan building for push X –load.....66

Figure4. 16 Comparison of drift ratio for (G+10) irregular plan building for push X –load.....66

Figure4. 17 Base shear at performance point for plan regular building models 68

Figure4. 18 target displacement at performance point for plan regular building 68

Figure4. 21 Typical failure modes observed for (G+7) plan regular building models.....72

Figure4. 22 Typical failure modes observed for (G+10) plan regular building models 73

Figure4. 23 Typical failure modes observed for (G+7) plan irregular building models.....74

Figure4. 24 Typical failure modes observed for (G+10) plan irregular building models.....75

Figure D1. 1Results of target displacement & base shear for (G+7) regular plan building.. ……105

Figure D1. 2 Results of target displacement & base shear for (G+10) regular plan building 107

Figure D1. 3 Results of target displacement & base shear for (G+7) irregular plan building 109

Figure D1. 4Results of target displacement & base shear for (G+10) irregular plan building 111

Figure E 1. 1 design of building for (G+7) plan regular building……..112

Figure E 1. 2 design of building for (G+10) plan regular model 112

Figure E 1. 3design of building for (G+7) plan irregular model.....113

Figure E 1. 4 design of building for (G+10) plan irregular model 113

ACRONYMS

ADRS	Acceleration displacement response spectrum
ASCE	American Society of Civil Engineers
ATC	Applied Technology Council
CP	Collapse Prevention
FE	Finite Element
FEM	Finite Element Method
FEMA	Federal Emergency Management Agency
HCB	Hallow Concrete block
IO	Immediate Occupancy
LS	Life Safety
MDOF	Multi Degree of freedom
MMP	Multi-Modal Pushover
MPA	Modal Pushover Analysis
OGS	Open Ground Storey
PEER	Pacific Earthquake Research Center
PGA	Peak ground acceleration
RC	Reinforced concrete
SDOF	Single Degree of Freedom
URM	Unreinforced Masonry

SYMBOLS

Ec	Modulus of elasticity of concrete
γ_c	Unit weight of concrete
ν_c	Poisons ratio of concrete
Es	Modulus of elasticity of steel
γ_s	Unit weight of reinforcing steel
ν_s	Poisons ratio of steel
γ_{infill}	Unit weight of infill
ν_{infill}	Poisons ratio of infill
Ec	Young's modulus of the column in the bounding frame
E_m	Young's modulus of infill masonry
f_m'	Compressive strength of the masonry
R_{cr}	Masonry infill compressive strength
R_{shear}	Shear strength of infill
f'v	Masonry shear strength
Q_c	Strength of the structure of the component.
Q	The demand imposed by the earthquake load on structures
F	Storey shear force
I_c	Moment of inertia of the column
A_n	Net cross-sectional mortar area of infill panel along its length
I_b	Moment of inertia of the beam
g	Gravitational pull force
q	Behavior factor
I	Importance factor assigned on important structures
h	Clear height of infill wall
H	Height of column between centerlines of beams

L	Length of the infill wall
a_l	Length of contact between column and infill
a_h	Length of contact between beam and infill
a_o	Bedrock acceleration
d_{inf}	Diagonal length of the infill.
R_1	Strut width correction factor due to infill opening
R_2	Strut width correction factor due to infill wall damage
A_{open}	Area of the openings the infill
A_{panel}	Area of the infill panel
t	Thickness of infill wall
w	Width of equivalent strut
H_{inf}	Height infill
E_{inf}	Modulus of elasticity of infill
λ_h	Relative stiffness parameter for infilled frame
θ	Slope of the infill wall diagonal to the horizontal
Ω	Constant between young's modulus and compressive strength

CHAPTER ONE

INTRODUCTION

1.1 Background of the Study

Earthquake force is the basic lateral force which is the cause for loss of life, property and buildings. To overcome these problem different types of reinforced concrete buildings are built in different seismic zones of the world and similarly in Ethiopia. RC moment-resisting frame buildings are the most preferred type of construction in developing countries like Ethiopia. RC moment-resisting frame buildings consist of moment resisting frame with a masonry wall as infill. These walls are considered as nonstructural elements in construction practices but the infill has significant resistance for the lateral load.

Due to the space requirement for meeting hall, larger reception room, game zones, parking area and the interests of the population buildings are constructed with large openings and removal of walls. This improper distribution of the infill wall creates non-uniform distribution of lateral loads on the building because soft storey is developed on the building.

According to ESEN-1998 (2015) if the stiffness of a story is less than 70% of the stiffness of the storey constructed exactly above it or less than 80% of the average stiffness of three stories above it is called soft storey. Because of low stiffness in soft storey the lateral forces due to earthquake must be resisted by columns. The weakness of columns will lead to the severe damage or collapse of the building.

The study of Pavithra and Prakash (2018) defined that the collapse or the damage of the high rise building due to soft storey is very often. Since the distribution of the lateral forces in the high rise buildings depend on the mass and the stiffness of the building. The soft storey which has less stiffness depends upon the column to resist the lateral forces. Infill walls provide stiffness to the structures and improve the seismic performance of structures. The opening provided in the masonry infill wall reduces the lateral strength of the structure.

Soft storey mechanism is the most common reason for the failure of reinforced concrete buildings by earthquake load. In many buildings requirement of an open ground story called soft Storey for commercial purposes or for the use of car parking, open commercial areas, and meeting hall does not have masonry infill. Such buildings with only columns in the ground storey and both partition walls and columns in the upper storey has a relatively flexible ground storey; i.e., the relative

horizontal displacement in the ground storey is much larger than that of the stories above. The presence of walls in upper stories makes them much stiffer than the open ground storey. Thus, the upper stories move almost together as a single block and most of the horizontal displacement of the building occurs in the soft ground storey itself. Soft storey buildings are the most vulnerable structural types during severe earthquakes. Open ground story buildings have consistently performed poorly during past earthquakes across the world and a significant number have collapsed. A well-known example of buildings failed by earthquake due to soft storey is shown in Figure 1.1.

a.Turkey during sumatra earthquake 2004

Turkey during Izmit earthquake ,1999

Figure1. 1 Failure of buildings due to soft storey (Kirac, Dogan, & Ozbasaran, 2011)

This study focuses on determining the effect of soft storey location on seismic performance of RC buildings which are designed using Euro Code8 2004 mostly similar to ES EN 1998 – 2015 Code using pushover analysis. To consider the effect of infill wall on lateral load resistance macro modeling of infill wall was used. The infill wall modeled as a diagonal strut to resist the compression load. Soft storey modeling is done by removing these struts at different floor levels on G+7 and G+10 reinforced concrete moment-resisting frames. Then to investigate the effect of soft storey location on seismic performance of RC building pushover analysis was done using ETABS 2017 software. From pushover analysis comparison of pushover curve, target displacement and base shear at performance point, storey shear, storey drift and storey displacement is drawn for different location of soft storey on reinforced concrete buildings.

1.2 Statements of the Problems

In the past and present time impact of earthquake load is a serious case in developed and developing countries. Earthquakes occurred in the past are devastated buildings, loss of human life and properties. Know a day this serious problem occurred in Ethiopia specifically in seismic Zone 4 regions. To overcome this problem engineers are designing and constructing different lateral load resisting system such as RC moment resisting system with infill, shear wall systems and others.

Infill has been generally considered as non-structural elements in many Codes, but Eurocode-8 includes detailed procedures for designing infilled RC frames. Contrary to common practice, the presence of masonry infill influences the overall behavior of structures when subjected to lateral loads. Construction of high rise or multi-story building is common practice in the developed and developing countries due to limitation of space. Construction of multi-story building often has soft stories due to space requirement in the building. Open ground storey for parking or soft storey at other levels for commercial purposes such as meeting hall, larger reception rooms and game zones create storey irregularities in stiffness (soft storey). This soft storey is weak to resist lateral loads.

Smith (1962) used an elastic theory to consider the effect of infill wall and to propose the effective width of the equivalent strut and concluded that this width should be a function of the stiffness of the in-fill with respect to that of bounding frame. He investigates the dimensionless relative parameters to determine the degree of frame in-fill interaction and thereby, the effective width of the strut. Homles, M. (1961) also replacing the infill by an equivalent pin-jointed diagonal strut and determine empirical equation to find the effective width.

This study concerns on nonlinear static analysis with an emphasis on RC frame buildings with soft storey at different locations**.** In this study sixteen (16) models of RC office and shopping use building with soft storey at different locations are analyzed using ETABS 2017 software and the effect of soft storey location on seismic performance has been evaluated.

1.3 Research Questions

- What is the effect of soft storey location on RC buildings response at performance point?
- What is the effect of soft storey location on seismic demand of RC buildings such as pushover curve, storey shear, storey drift and storey displacement?
- What is the effect of soft storey location on the nonlinear overall performance (Plastic resistance) of RC buildings?

1.4 Objective of the Study

1.4.1 Main Objective

The present study focused on the investigation of the effect of soft storey location on seismic performance of reinforced concrete building using nonlinear static (pushover) analysis.

1.4.2 Specific Objectives of the Study

- To investigate the effects of soft storey location on building response at performance point (target displacement and base shear)
- To determine the effect of soft storey location on building response such as pushover curve (base shear Vs monitored displacement), storey shear, storey drift and storey displacements.
- To examine or evaluate the effect of soft storey location on nonlinear overall performance (plastic resistance) of reinforced concrete building.

1.5 Significance of the Study

The importance of this study is to create awareness on earthquake resistance behaviors of soft stories in RC moment-resisting frames and how their location affects earthquake load resistance of buildings. This study will help students and future researchers to understand pushover analysis using software to evaluate the seismic performance of RC buildings with soft storey at different locations.

1.6 Scope and Limitation of the Study

- The procedures presented in this document are applicable to all building structures that have been constructed using reinforced concrete frame structures with unreinforced hollow concrete block (HCB) masonry infill wall.
- buildings considered for the present study are office and shopping use building which is regular and irregular in plan having (G+7 and G+10) stories reinforced concrete frame having typical floor height and similar properties of the structures and infill thickness of 20cm and 15cm.
- This research focuses on nonlinear static analysis and the work is based on the Eurocode-2004. Hence, the new Ethiopian building Code standard is similar to it.
- This study only deals with the in-plane stiffness and strength of masonry infill macro models of infill panels are considered for the simplified analysis.
- Masonry infill frame with the soft storey at different locations is analyzed using ETABS 2017 software up to the failure and the load-deformation curves. In this study, default hinges are used for frames and user-defined hinges for diagonal struts.
- The present study is limited on the macro models of infill panels and the equivalent struts width estimated using equations derived by (Smith and Carter, 1970) and (FEMA306, 1998) for their consistently accurate predictions of infilled frame in-plane behavior.
- In this study modeling of soft storey is done only by removing in-plane diagonal struts and subjected to only for in-plane pushover load pattern in X- direction.
- Soil structure interaction is not considered in this study
- In the present study, only ductility class medium building is considered.
- This study is limited to consider infill wall damaged

CHAPTER TWO

RELATED LITERATURE REVIEW

2.1 General

Now a day many buildings are constructed with masonry infill for commercial, industrial and multi-family residential uses in seismic prone regions throughout the world for functional and architectural reasons. Masonry infill typically consists of brick, clay tile or concrete block walls constructed between columns and beams of RC frame. Usually, the RC frame is filled with the hollow concrete block (HCB) as non- structural wall for the partition of rooms, social and functional needs for vehicle parking, shops and reception.

Often, open-ground-story structures are also called soft storey building, even though their ground storey may be soft or weak. Generally, the soft or weak storey usually exists at the ground floor level, but it could be at any other floor level as well such as soft storey building is a multi-story building with wide doors, large unobstructed commercial spaces, meeting hall, game zone, gymnasium room. The behavior of soft storey building in seismic force is very significant because the soft storey structure is more flexible than the normal floor. In seismic condition vibration happens more in soft storey building as compared to normal building and therefore it becomes important to study its behavior during such a mishap.

To provide a detailed review of the literature related to modeling and analysis of structures in its entirety would be difficult to address in this chapter. A brief review of previous studies related to seismic performance soft storey building and modeling of a masonry wall to create soft storey in RC building and application of pushover analysis of structures is presented in this section.

2.2 Soft Storey

ES EN-1998-(2015) states that if the stiffness of a story is less than 70% of the stiffness of the story constructed exactly above or less than 80% of the average stiffness of three stories above it is called soft story. Because of low stiffness in the soft storey the lateral forces due to earthquake must be resisted by columns. This weakness of columns will lead to the severe damage or collapse of the building.

Patnala & Ramancharla (2014) studies that infill walls tend to interact with the frame when the structure is subjected to lateral loads, and also exhibit energy-dissipation characteristics under seismic loading.

Many building structures having soft storey suffered by major structural damages and collapsed by the earthquake.

Large open areas with less infill and exterior walls and higher floor levels at the ground level result in soft stories and hence damage. In such buildings, the stiffness of the lateral load resisting systems at those stories is quite less than the stories above or below (Naphade, 2015)**.** The lateral displacement diagram of a building with a soft storey under lateral loading is shown in Fig.2.1.

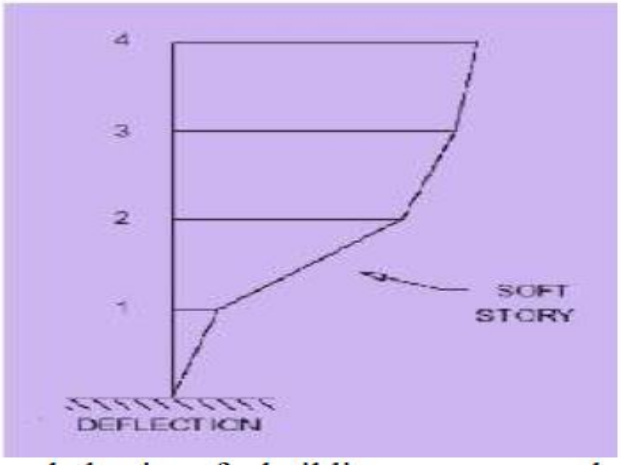

Figure2. 1 Soft storey behavior of a building structure under lateral loading (Naphade, 2015).

PATEL (2012) studies on earthquake resistant design of low rise open ground storey framed buildings using non -linear (pushover) analysis by modeling infill wall as a diagonal strut for (DL+0.25L) pushover load in X-and Y- direction. It is found that the maximum base shear and roof displacement capacity for buildings without-infill wall is less than that of building with-infill wall. This is true for both X- and Y- direction pushover load.

Kumar, Garg and Sharma (2014) Study on a 5 storey RC building subjected to seismic force for most appropriate location of a soft storey in moment resisting RC building using STAAD Pro software and the various analyses are performed for different location and height of the soft storey. The results of this study indicate that the structural forces and displacements are found to be higher when soft storey is located at first/second storey and the reinforcement quantity required in structure is found to be approximately 10% higher if soft storey is provided at first/second storey in comparison to soft storey provided at top storey.

According to Basavaraju and Babu (2016) Study on RC frames with 10 storey by pushover analysis using ETABS software for seismic zone 4 regions soft storey is considered at different levels along with the height of the frame. Soft storey is considered by varying the stiffness ratios as

1.0, 0.69, 0.46, 0.32and 0.23 respectively. The results show that the seismic performance of structures is very sensitive to the stiffness ratio and the lower the stiffness ratio of the soft storey more vulnerable. The earthquake excitations ductility capacity of the structure reduces when the structure becomes irregular in stiffness and also when the soft storey is placed at ground level.

Infill walls are generally seen as a nonstructural element and their effect is neglected by ignoring the stiffness of the infill wall during the modeling phase of the structure (analyzed as a linear bare frame) leading to substantial inaccuracy in obtaining the actual seismic response of framed structures **(**Pradhan, 2012).

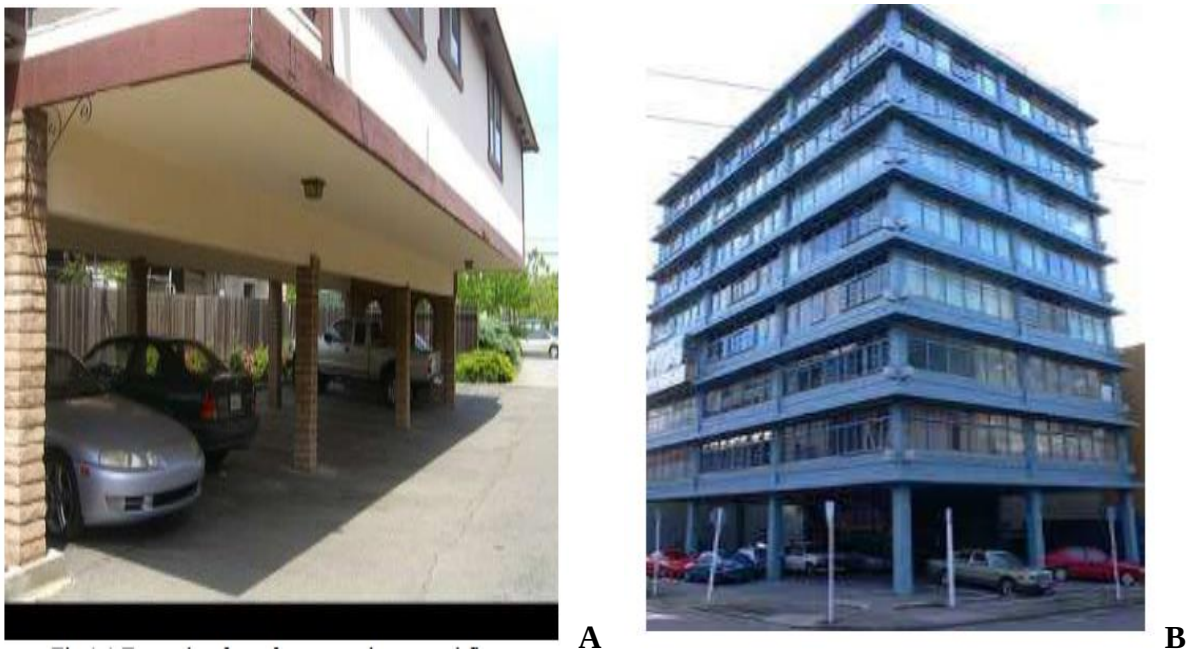

A **B**

Figure2. 2 (A) Ground soft storey building & (B) Soft storey in the above level building (Patnala & Ramancharla 2014)

Uruci and Bilgin (2016) study the effect of soft storey structural irregularity in reinforced concrete structures infilled frame, bare frame, Soft story due to increased ground story height (3 m to 4.5 m), Soft story due to absence of walls at ground story and Soft story due to increased height modeled and pushover analysis is done using ETABS. This study assesses the seismic performance of bare and masonry-in filled RC frames, frames with soft story due to the absence of masonry infill walls and higher height of the ground storey. The pushover analyses of this study show that infilled wall increase in initial stiffness, strength, and energy dissipation of the infilled frame than bare frame also the presence of soft story irregularity affect the seismic performance of the frame; it both weakens and softens the system. Soft story due to removal of masonry infill walls at the

ground storey is found to be more destructive than the soft storey due to the increased height of the storey in both low and mid-rise buildings.

Arunkumar and Devi (2016) studied four models with a soft storey at different levels on G+20 RC building and these models with the incorporation of shear walls are considered. Pushover analyses of the models with and without shear walls are carried out. This study highlights the poor seismic performance of G+20 RC building with the soft storey.

2.3 Masonry Infilled RC Frame

2.3.1 Effect of Masonry Infill on the Seismic Behavior of Frame Structures.

Reinforced concrete (RC) frame buildings with unreinforced masonry (URM) infill walls are commonly built throughout the world, including in seismically active regions. URM infill walls are widely used as partitions throughout Ethiopia, and despite often being considered as non-structural elements, they affect the structural performance of RC buildings.

Masonry infill is considered as nonstructural elements and their stiffness contributions are generally ignored in practice. But they affect the structural performance of the RC buildings during earthquake excitation. The existence of infill influences the distribution of lateral loads on the framed structures due to the increase in stiffness.

Considering the severity of the detrimental effects of infill can cause collapse. Proper modeling of URM infill walls within RC frames is essential for seismic evaluation and consequently for the selection of adequate retrofits solution to reduce damage and its consequences.

Grima (2017) study the seismic performance of reinforced concrete buildings with masonry infill by modeling infill walls using single diagonal struts. In this study, the comparison on seismic performance of bare frame and frame with infill wall are determined in terms of storey displacement, storey shear, base shear Vs roof displacement and evaluate the seismic performance of the two buildings using static pushover analysis. The result shows that; the storey shear calculated on the basis of the bare frame model gives a lesser value than the infilled frame. It was observed that a fully infilled frame is nearly 15% greater compared to the bare frame model in storey shear. Due to the introduction of infill, the displacement capacity of the infill frame decreases and the lateral displacement obtained from the bare frame model is the maximum which is about 60% greater than that of the infilled frame. Similarly, from the pushover analysis results

that fully-infilled frame has the lowest collapse risk than the bare frame for the induced earthquake.

The study of Siamak Sattar and Abbie B. Liel (2010) Predicted seismic performance utilizing nonlinear analysis models for the RC frame structures consist of the two-dimensional three-bay frame and concluded that the fully-infilled frame has approximately 15 times larger stiffness and 1.5 times greater peak strength than the bare frame.

According to the study of M and Jayalekshmi (2013) masonry infill have a very high initial in-plane lateral stiffness and low deformability. Infill wall has a significant contribution to lateral stiffness, strength, overall ductility and high energy dissipation capacity of the frame; however, under seismic loading, it can also create unimportant things such as torsion, soft storey effect and out-of-plane collapse. Therefore, under seismic loads, the whole lateral force transfer mechanism of the structure changes from a predominant frame action to predominant truss action which is shown in fig 2.3 A & B**.**

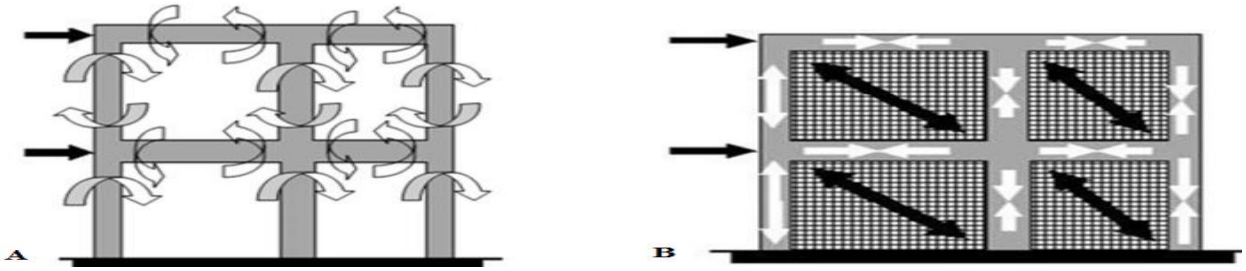

Figure2. 3 (A) Predominant frame action (B) Predominant truss action [15]

Gunay (2011) used pushover analysis in his study to determine the differences of behavior between a bare frame and the same frame with infill walls in all the stories but not on the ground floor, shown in Figure 2.4 below. The effect of the infill is simulated by a single diagonal compression strut in each bay.

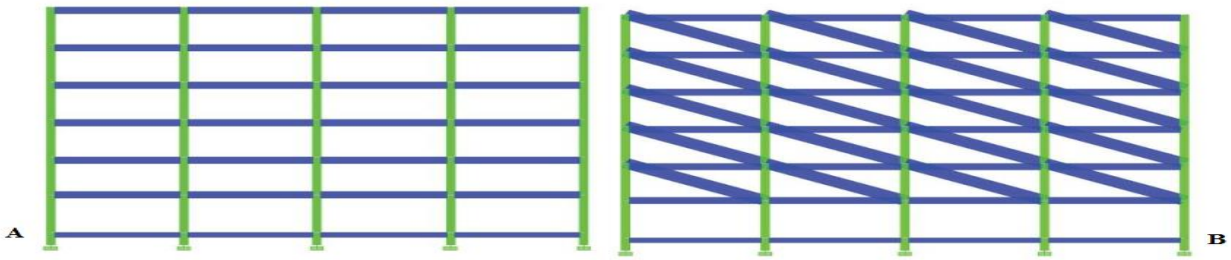

Figure 2. 4 (A) Bare frame (B) frame with infill wall in all stories except ground floor [16]

The pushover curves of the two frames are compared in Figure 2.5. The strength and stiffness of the infilled frame is significantly increased due to the presence of infill, but the displacement capacity decreases and a soft story develops, which showed in storey displacement as evidence in Figure 2.6 The deformation accumulates in the bottom storey that is the true behavior during an earthquake, when infill is considered in the analysis, rather than being distributed evenly over all stories when the designer not considers the infill during design of buildings.

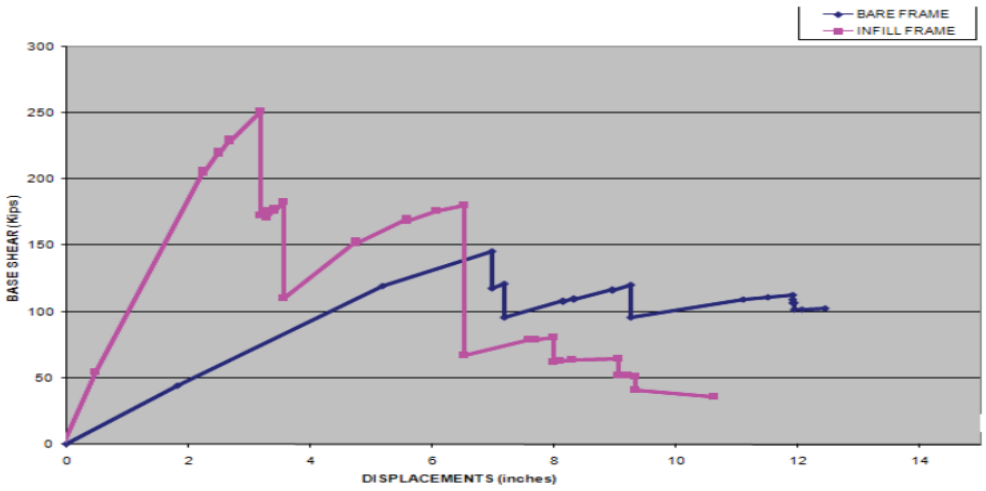

Figure 2. 5 Pushover curve comparison for the bare and infilled frames [16]

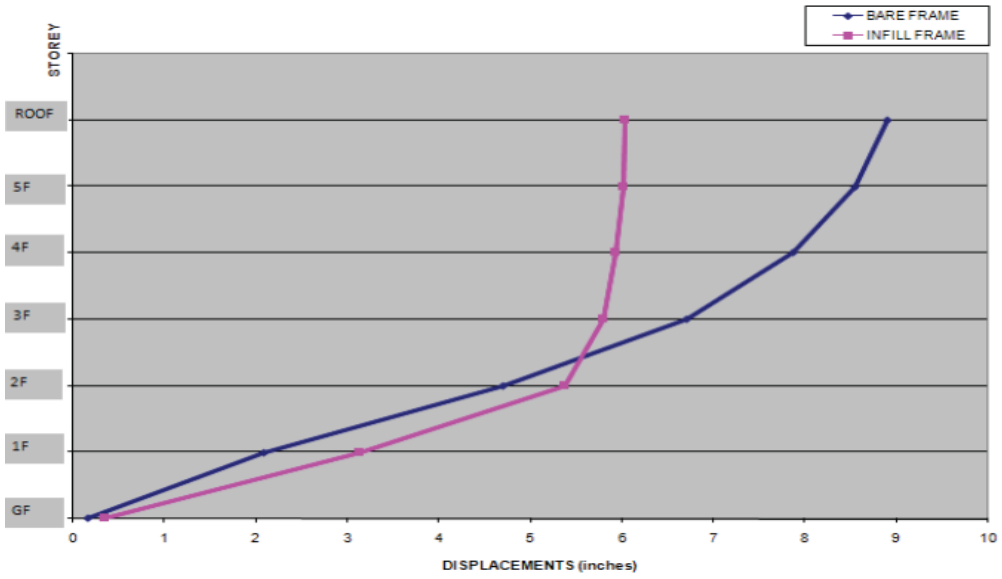

Figure2. 6 Displacement profile comparison for the bare and infilled frames [16]

So, based on those results on effect and advantage of infill walls they are properly taken into consideration in the design process and the failure mechanism is controlled (i.e., no weak story is allowed to occur). However, due to the interest of human beings soft storey can occurred at

different location on RC building. Therefore the effect of soft storey location for seismic load performance is studied in this research.

2.3.2 Modeling of Masonry Infill

Developing of Model for any structure is a very vital thing to obtain accurate results. However, it is difficult to model the as-built structures due to numerous constraints with as it is difficult to incorporate all physical parameters associated with the behavior of an infilled frame structure. Even if all the physical parameters, such as contact coefficient between the frame and infill, separation and slipping between the two components and the orthotropic of material properties are considered, there is no guarantee that the real structure behaves similar to the model as they also the structural behavior could also depend on the quality of material and construction techniques (Dorji, 2009)

However, to analyze the structural behavior of infilled frames, two types of modeling have been developed which are micro model and macro model. The micro model method is a finite element method (FEM) where the frames elements, masonry work, contact surface, slipping and separation are modeled to achieve the results. This method has seemed to be generating better results but it has not gained popularity due to its cumbersome nature of analysis and computation cost.

The macro models (equivalent diagonal strut) method was developed to study the global response of the infilled frames. In this method to study the behavior of the infill wall for earthquake load, one or more diagonal struts have been used.

2.3.2.1 Micro - Model

Finite element (FE) modeling divides the structural components into smaller sizes, maintaining the constitutive laws of material, boundary conditions, in order to improve the accuracy of results. However, this method most of the time is used to analyze small structures. Because requires computation equipment besides taking longer time. Relevant research on the infilled frames that were done in the past was reviewed and presented in this section.

The behavior of the infilled frame under an in-plane load was studied by (Dhanasekar and Page, 1987)**.** The results from biaxial tests on half-scale solid brick masonry were used to develop a material model for brick and the mortar joints which were then used to construct a non-linear finite element model. The result shows the behavior of the infilled frame significantly influenced by the

modulus of elasticity of the infill wall. However, the influence of Poison's ratio was found insignificant on the behavior of the structure.

Combescure and Pegon (2000) study on the effect of infill wall with and without a perfect contact between the infill wall and the reinforced concrete frame on single bay single storey structure by using FE modeling. It was reported, under unilateral contact conditions (frictionless), the forces between the frame and fill panel are transferred through compression corners at the ends of diagonal strut. However, there is no transfer of shear force from infill to frame.

2.3.2.2 Macro Model (Equivalent Diagonal Strut Model)

The main disadvantage of conducting finite element analysis for the global structural response study is due to computation cost and the nature of complexity in the model generation for larger structures. To overcome this problem the macro-model method has been developed based on the experimental and finite element analysis results, wherein, diagonal struts are used to represent the infill wall.

The study of Skafida et al. (2014) develops the concept of equivalent diagonal strut method by studying the infilled frame with three storey building. The cracks along the diagonal length of the panel give an insight into the strut behavior of an infill panel. The study stated that the stress from peripheral frame members to the infill was transferred only through the compression corners of the frame-infill interface.

A prominent among the most prevalent and known approaches is by replacing masonry infill by equivalent diagonal struts, the thickness of the strut which is equal to the thickness of masonry infill. The primary issue with this approach is to find the effective width. Numerous scientists have proposed different techniques for determining the width of the equivalent diagonal strut. Strut width leans on the length of contact between the columns and the wall (α_h) and between the beam and wall (α_L) (Yadunandan and N, 2017)

Homles (1961) conducts an experimental study on single storey single-bay infilled structure under in-plane loads to determine the width of equivalent strut. Based on his experimental study he proposed the width of the equivalent strut to be one-third of the diagonal length.

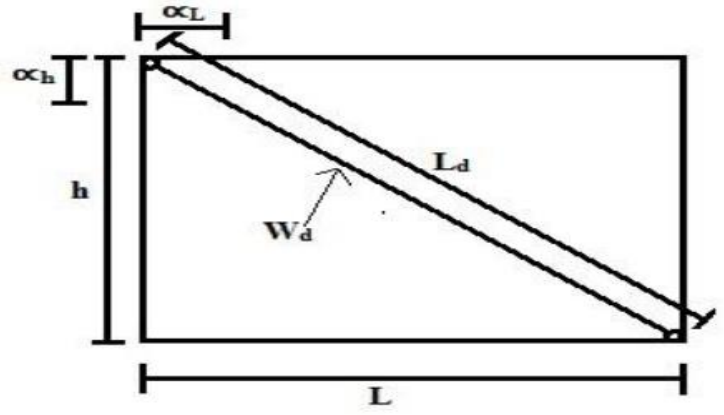

Figure2. 7 Equivalent diagonal strut model [19].

$W_d = L_d/3$ **2.1**

Where, L_d = Diagonal length of the panel

Smith (1962) conducted a study on infilled structure experimentally on a small scale specimen. The specimen had a steel frame and concrete mortar as infill. The in-plane load was applied at the top corner of the infilled specimen and was observed in a compression region within the infill panel which made the frame stiff and thus the concept of diagonal strut method was evolved. It was also reported that longer the contact length between the infill panel and the frame, wider the width of the strut.

Smith and Carter (1970) proposed nondimensional parameter to determine the interaction of the frame and infill wall.

$$\lambda_h = \sqrt[4]{\frac{Einf*\sin 2\theta}{4Ec\ Ic\ Hinf}} \qquad 2.2$$

Where: $\boldsymbol{H_{inf}}$ and $\boldsymbol{E_{inf}}$ are the height and the modulus of the infill respectively, θ is the angle between diagonal of the infill and the horizontal, E_c is the modulus of elasticity of the column, $\boldsymbol{I_c}$ is the moment of inertia of the columns, H is the total frame height, and $\boldsymbol{\lambda_h}$ is a dimensionless parameter (which takes into account the effect of relative stiffness of the masonry panel to the frame).

According to (Paulay and Priestley (1992) investigation the value of a modulus of elasticity of infill is a constant Ω times the compressive strength of infill. According to his study, the constant is equals to 750 for concrete block and 500 for clay brick.

$$E_{m(infill)} = \Omega f_m' \qquad 2.3$$

FEMA 306 (1998) develops an equation to determine the width of the infill wall thickness which is represented by equivalent strut.

$$W = 0.175\, d_{inf}\, ((\lambda_h H_{inf})\text{-}0.4 \qquad 2.4$$

Where, d_{inf} = Diagonal length of the infill

Mallick (1971) Study the effects of the location of opening on the lateral stiffness of the infilled frame and had recommended possible locations for door and window. The recommended location and stiffness reduction of the infill are;

1. Structure with a shear connector but having an opening at either end reduces the stiffness by 85 to 90%.
2. Structure Without shear connector but having an opening at either end the stiffness was reduced by 60 to 70%.
3. When the opening is placed at the center of the infill wall the stiffness reduces by 25 to 50%.

Thus, the suggested position for the door is at the center of the lower half of the infill wall while the window can be placed at the middle height of the infill wall at either side.

2.3.3 Perforated Panels

Al-Chaar (2002) studies the effect of perforated panels and infill damage to determine strut width. For perforated masonry panel, the equivalent strut is assumed to act in the same manner as for the fully infilled frame. Then strut should be placed at a distance l_{column} from the face of the beam as shown in Figure 2.9. The equivalent strut width (w) shall be multiplied by a reduction factor to account for the loss in strength due to the opening, $(R_1)i$, which is calculated using Equation 2.10.

$$(R_1)i = 0.6\left(\frac{Aopen}{Apanel}\right)^2 - 1.6\left(\frac{Aopen}{Apanel}\right) + 1 \text{ ----------} 2.5$$

Where

A_{open} = Area of the openings

A_{panel} = Area of the infill panel

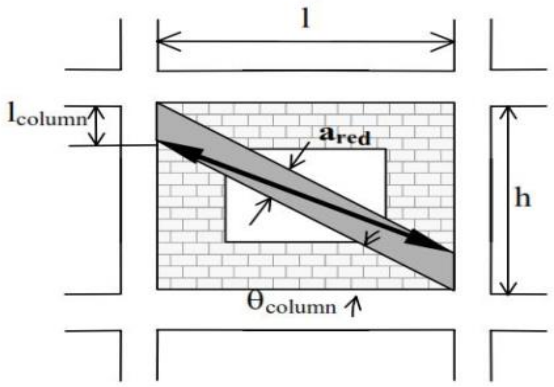

Figure2. 8 Perforated panel (Al-Chaar, 2002)

According to Al-Chaar (2002) if the area of the openings (A_{open}) is greater than or equal to 60 % of the area of the infill panel (A_{panel}), then the effect of the infill should be neglected, i.e., $(R_1)i = 0$.

Masonry infill panel property deteriorates as the elastic limit is exceeded. For this reason, it is batter to determine the severity condition of the infill and exceeded the elastic limit and, if so, by how much. The severity of existing infill damage can be determined by visual inspection of the infill. Existing panel damage (or cracking) must be classified as either: no damage, moderate damage, or severe damage as presented in Figure 2.10. If there is a difficulty to decide the severity level of infill damage considers the extreme case to be conservative. A reduction factor for existing panel damage $(R_2)i$ must be obtained from Table 2.1. (Al-Chaar, 2002). Notice that, if the slenderness ratio (h/t) of the panel is greater than 21, $(R_2)i$ is not defined and repair is required. For panels with no existing panel damage, the reduction factor $(R_2)i$ must be taken as 1.0.

Table2. 1 In-plane damage reduction factor

	$(R_2)i$ for the type of damage	
h/t	Moderate	Sever
≤21	0.7	0.4
≥21	Requires repair	

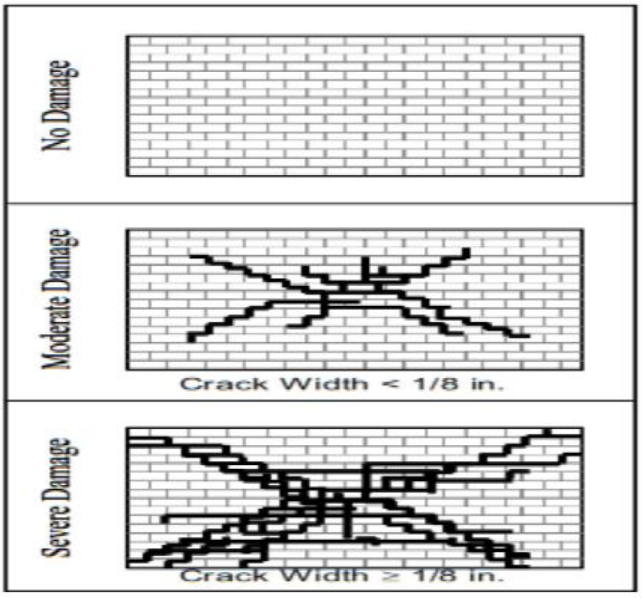

Figure2. 9 Visual damage classifications (Al-Chaar, 2002)

2.3.4 In-Plane Strength and Stiffness Evaluation of URM Infill

The lateral forces transfer across infilled frames causes non-uniform stress distribution within the infill and frame elements. As the lateral forces are increased, the stress distribution varies until failure of the infill occurs. Failure of the infill occurs when the applied shear and compression load exceeds its capacity.

The expected flexural and shear strength of the frame elements confining the infill panel must also be evaluated. Column and beam shear and flexural strengths must exceed the horizontal/vertical components of the force required for the failure of the infill. This procedure assures the failure of the infill before failure in the confining frame occurs.

The lateral load capacity of frame-infill systems should be found using a nonlinear finite element program which captures the nonlinear behavior of all material components: masonry, mortar and concrete. But this option is not available or is impractical in most situations. Then a simpler analytical pushover analysis of a frame containing equivalent struts that represent the masonry is used. The method can be used for fully infilled frames as well as partially infilled and perforated masonry panels. Using struts in this global analysis will yield infill effects on the column directly, which will deny the need to evaluate these members locally. This method relies on the development of plastic hinges to capture the nonlinearities of the structural system.

Great efforts have been invested, both analytically and experimentally to better understand and estimate the composite behavior of masonry-infilled frames. Skafida et al. (2014), Stafford-Smith (1961)**,** to mention just a few, formed the basis for understanding and predicting infilled frame in-plane behavior.

2.3.5 Masonry Infill Shear Strength

The tendency of infill wall for shear load resistance can be achieved in two ways these are by the bond shear strength and the friction between the masonry and the mortar. The concept of the bond shear strength is illustrated in Figure 2.11, where a typical stair-stepped shear crack is approximated by a single shear crack through a bed joint. This simplification is valid because the vertical component of the stair-stepped crack will be in tension, and its contribution to the shear strength should be neglected. Therefore, the horizontal lateral load required to reach the infill shear strength is calculated by Equation 2.11

$$R_{shear} = A_n f_v (R_1)_i (R_2)_i \quad \text{----------2.6}$$

Where:

An = net cross-sectional mortar/grouted area of infill panel along its length (cm^2)

f'_v = masonry shear strength (MPa)

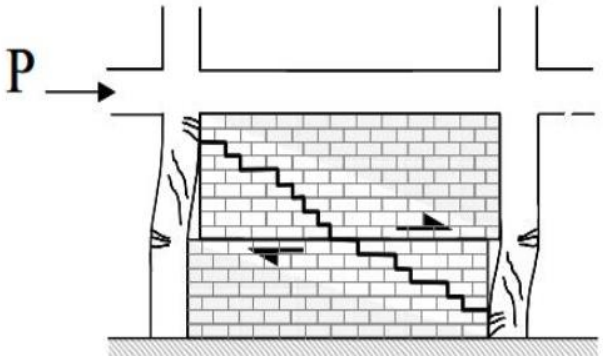

Figure 2. 10 Shear failure of masonry (Al-Chaar, 2002)

2.3.6 Masonry Infill Crushing Strength.

The masonry infill crushing capacity is the strength of infill that resists the applied compressive load before it is crushed (R_{cr}). This resistance can be determined using equation 2.7.

$$R_{cr} = w\, t_{eff}\, f_m' \quad \text{----------2.7}$$

Where

f_m' = Compressive strength of the masonry, Mpa

t_{eff} = Thickness masonry panel.

w = Effective width of strut

2.3.7 Load-Deformation Behavior of the Diagonal Strut

The diagonal equivalent strut used to model the masonry infill is pin-connected to the frame elements so that no moment transfer occurs. The stiffness of the strut will be governed by the modulus of elasticity of the masonry material (E_m) and the cross-sectional area (w x t_{eff}). The strength of the strut is determined by calculating the load required to reach masonry infill crushing strength (R_{cr}) (Equation 2.7).

2.4 Frame Member

2.4.1 Stiffness

The cracking and inelastic response of the frame member before yielding is depended on its stiffness value. Non-linearity properties of the frame arise from the stress-strain relation of the materials. The development of cracks in the concrete and secondary load-deflection (slenderness) effects lead to a situation in which the maximum load and bending moment induced in a column cannot readily be related to the loads acting on the structure. The strength of the frame member is affected by depends on the axial load of the moment variation along the length, the amount of reinforcement provided, the capacity of steel and concrete used and their critical strain values.

Many types of research are done on how to determine the stiffness of frame member and there are many code specifications that determine the stiffness value of members during the analysis of frame for the different load.

In ACI Code (1995) the stiffness value has been multiplied by a stiffness-reduction factor of 0.875, giving I = 0.35Ig. Two levels of behavior must be distinguished in selecting the *EI* of columns. The lateral deflections of the frame are influenced by the stiffness of all the members in the frame and by the variable degree of cracking of these members. Thus, the *EI* used in the frame analysis should be an average value. On the other hand, in designing an individual column in a frame, the *EI* used in calculating must be for that column. This EI must reflect the greater chance that a particular column will be more cracked, or weaker, than the overall average; hence, this *EI* will

tend to be smaller than the average *EI* for all the columns acting together. ACI Code gives this value multiplied by 0.875, *EI*=0.70EcIg or for this purpose.

Euro Code 8 (2005) states a more accurate analysis of the cracked elements. The elastic flexural and shear stiffness properties of concrete and masonry elements may be taken to be equal to one half of the corresponding stiffness of the uncracked elements. This study is based on J.Macgregor (1997) who recommends these two equations when carrying out second-order analysis. EI_{beam}= 0.35EcIg; EI_{column}= 0.7EcIg

According to ES EN 1998 (2015), the stiffness of the structural elements shall be evaluated taking into account both their flexural and shear flexibility and, if relevant, their axial flexibility. Uncracked elastic stiffness may be used for analysis or, preferably and more realistically, cracked stiffness in order to account for the influence of cracking on deformations and to better approximate the slope of the first branch of a bilinear force deformation model for the structural element.

In the absence of an accurate evaluation of the stiffness properties, determined by rational analysis, the cracked bending and shear stiffness may be taken as 1/2 of the cross-section of uncracked elastic stiffness.

From the above codes and researches to determine the stiffness of all members ES EN-2015 value of stiffness is used for the analysis of all models.

2.4.2. Load Effects on Seismic Behavior of Frame Elements

Gravity and lateral loads have a significant impact on the analysis of structures, so they should have considered this load during the analysis of structures.

During an earthquake, acceleration-induced inertia forces will be generated at each floor level, where the mass of an entire story may be assumed to be concentrated. Hence the location of a force at a particular level will be determined by the center of the accelerated mass at that level. The summation of all the floor forces, F_i (Figure 2.11) below and a given storey will then locate the position of the resultant force within that storey.

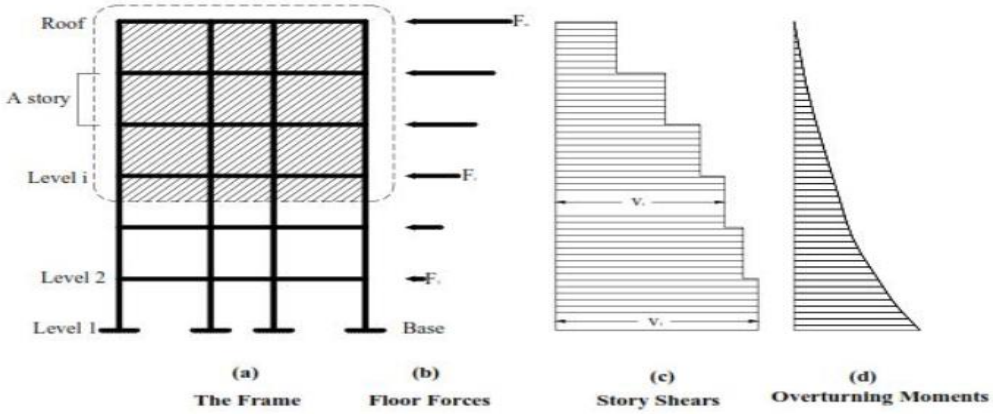

Figure2. 11 Effects of lateral forces on a building (Paulay and Priestley, 1992)

Figure 2.12 describes a generalized load-deformation relation which is appropriate for most concrete components. The relation is described by linear response from (unloaded component) to an effective yield point B, linear response at reduced stiffness from B to C, a sudden reduction in lateral load resistance to D, response at reduced resistance to E, and final loss of resistance thereafter (Fig 2.12a). Deformations beyond point E are not permitted because gravity load can no longer be sustained (Fig 2.12b). In some cases, initial failure at C will result in loss of gravity load resistance, in which case E is a point having deformation equal to that at C and zero resistance**.** The above main points are shown on the load-deformation relation of Figure2.13.

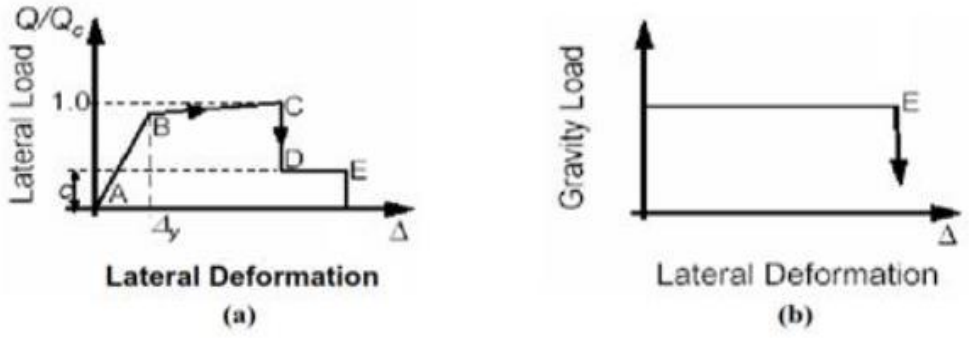

Figure2. 12 Generalized load-deformation relation for non-degrading components (Euro Code 8, 2005)

Where, Q_c - Refers to the strength of the component.

Q - Refers to the demand imposed by the earthquake

Lateral loads should be applied in predetermined patterns that represent predominant distributions of lateral inertial loads during critical earthquake response. When the size of the building increases; also the effects of lateral load damage increase. As a structure is displaced laterally, its lateral load stiffness usually decreases with increasing lateral displacement.

For the same maximum displacement at roof level, the overall ductility demand in terms of the large deflection is much more readily achieved when plastic hinges develop in all the beams (Fig 2.13b) instead of only in the soft-story column (Fig 2.13c). The column sway mechanism, also referred to as a soft-story, may impose plastic hinge rotations, which even with good detailing of affected regions, would be difficult to accommodate (Paulay and Priestley, 1992)

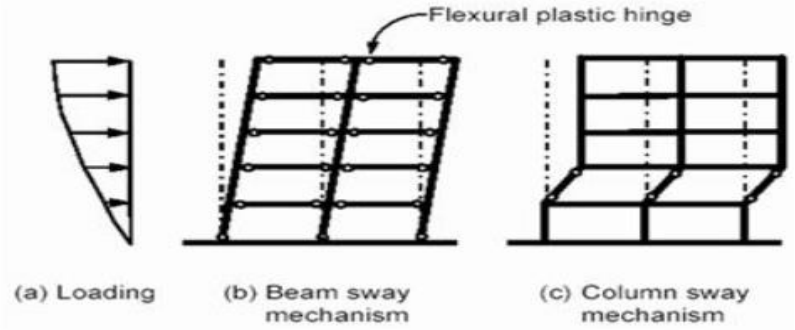

Figure2. 13 Idealized flexural mechanisms in multi-story frames (Paulay and Priestley, 1992)

2.5. Method of Structural Analysis

For seismic performance evaluation, a structural analysis of the mathematical model of the structure is required to determine force and displacement demands in various components of the structure. Several analysis methods are available to predict the seismic performance of the structures. These are:

1. Elastic Methods of Analysis
2. Inelastic Methods of Analysis

2.5.1. Elastic Methods of Analysis

The force demand on each component of the structure is obtained and compared with available capacities by performing an elastic analysis. Elastic analysis methods include

1. static (lateral) force procedure,
2. dynamic procedure

These methods are also known as force-based procedures which assume that structures respond elastically to earthquakes.

In static lateral force procedure, a static analysis is performed by subjecting the structure to lateral forces obtained by scaling down the smoothened soil-dependent elastic response spectrum by a structural system-dependent force reduction factor, "R". In this approach, it is assumed that the actual strength of structure is higher than the design strength and the structure is able to dissipate energy through yielding.

In the dynamic method of analysis, force demands on various components are determined by an elastic dynamic analysis. The dynamic analyses are response spectrum analysis and elastic time history analysis. A sufficient number of modes must be considered to have a mass participation of at least 90% for response spectrum analysis.

To determine the performance of structures force-based method of analysis is applicable. They have certain drawbacks. Structural components are evaluated for serviceability in the elastic range of strength and deformation. Post-elastic behavior of structures could not be identified by elastic analysis. However, post-elastic behavior should be considered as almost all structures are expected to deform in inelastic range during a strong earthquake. The seismic force reduction factor "R" is utilized to account for inelastic behavior indirectly by reducing elastic forces to inelastic. Force reduction factor "R" is assigned considering only the type of lateral system in most codes, but it has been shown that this factor is a function of the period and ductility ratio of the structure as well (Nassar and Krawinkler, 1991)

In order to determine the capacity of the structure elastic method of analysis is sufficient but not determine failure mechanisms and account for the redistribution of forces that will take place as the yielding progress. Moreover, force-based methods primarily provide life safety but they can't provide damage limitation and easy repair. The limitation of the above methods forced researchers to develop displacement-based procedures for seismic performance evaluation. Displacement-based procedures are mainly based on inelastic deformations rather than elastic forces and use nonlinear analysis procedures considering seismic demands and available capacities explicitly (Gupta B., 1999).

2.5.2 Inelastic Methods of Analysis

When the structures subjected to the strong ground motion they are undergoing inelastic deformation under a strong earthquake and dynamic characteristics of the structure change with time. To determine the performance of structures for this change requires an inelastic analytical method of analysis. Inelastic analytical procedure helps to understand the actual behavior of

structures by identifying failure modes and the potential for progressive collapse. Inelastic analysis procedures basically include:

1. Inelastic time history analysis and
2. Inelastic static analysis (pushover analysis)

2.5.2.1 Inelastic Time History Analysis

The inelastic time history analysis is the most accurate method to predict the force and deformation demands at various components of the structure. But the applicability of inelastic time history analysis is limited because the dynamic response is very sensitive to modeling and ground motion characteristics. It requires proper modeling of cyclic load-deformation characteristics considering the deterioration properties of all important components. Also, it requires the availability of a set of representative ground motion records that accounts for uncertainties and differences in severity, frequency and duration characteristics. Moreover, computation time, the time required for input preparation and interpreting voluminous output make the use of inelastic time history analysis impractical for seismic performance evaluation. Inelastic static analysis, or pushover analysis, has been the preferred method for seismic performance evaluation due to its simplicity. It is a static analysis that directly incorporates nonlinear material characteristics and geometric nonlinearity.

2.5.2.2 Pushover Analysis

Pushover analysis is a static nonlinear procedure using a simplified nonlinear technique to estimate seismic structural deformations. It is an incremental static analysis in case of force or displacement to determine the capacity curve of a structure. The analysis conducted through applying of horizontal loads in a well-defined pattern to the structure incrementally. Then plot the result in terms of base shear to displacement at each increment, until collapse condition (Oguz, 2011)**.**

Most of the simplified nonlinear analysis procedures utilized for seismic performance evaluation make use of pushover analysis and/or equivalent SDOF representation of actual structure. However, pushover analysis involves certain approximations that the reliability and the accuracy of the procedure should be identified. For this purpose, researchers investigated various aspects of pushover analysis to identify the limitations and weaknesses of the procedure and proposed improved pushover procedures that consider the effects of lateral load patterns, higher modes and failure mechanisms.

Model of the building is done by modeling software such as ETABS / SAP. Pushover analysis is done by subjecting the model for lateral load pattern (i.e., inverted triangular, uniform or modal). The intensity of the lateral load is slowly increased and the occurrence of cracks, yielding, plastic hinge formation and failure of various structural components is recorded. Number of iteration required to observe failure in structures. This iterative analysis and design process continue until the design satisfies a pre-established performance criterion. The performance criterion in pushover analysis is established as the desired state of the building given rooftop spectral displacement amplitude.

Documents of FEMA 356 (2000) and ATC–40(1996) describes the detail modeling procedures, acceptance criteria and analysis procedures for pushover analysis. These documents discuss force deformation criteria for potential locations of lumped inelastic behavior designated as plastic hinges used in pushover analysis. As shown in Figure 3.1 below, five points labeled A, B, C, D, and E are used to define the force deformation behavior of the plastic hinge, and three points labeled IO (Immediate Occupancy), LS (Life Safety) and CP (Collapse Prevention) are used to define the acceptance criteria for the hinge. In these documents, if all the members meet the acceptance criteria for a particular performance level, such as Life Safety, then the entire structure is expected to achieve the Life Safety level of performance.

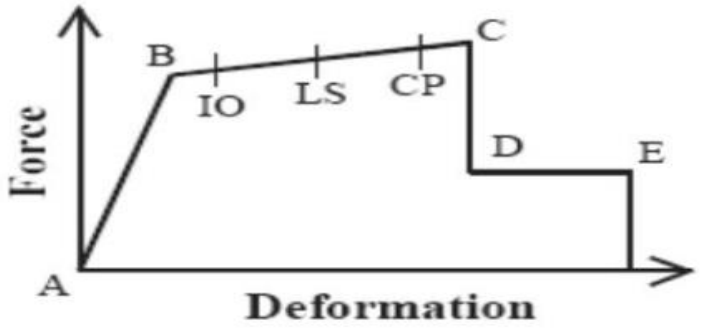

Figure2. 14 Force-Deformation relations for Plastic Hinge in Pushover Analysis (Habibullah and Pyle, 1998)

From figure 2.15 the following properties are described in pushover analysis,

- Point A is the unloaded condition,
- Point (A-B) elastic resistance
- Point B yielding of the element,
- Point (B-C) significant strength degradation begins
- Point (C-D) initial failure of the element

- Point (D-E) residual resistance of the frame element
- Point E maximum deformation and gravity load never sustained.

Inel M. et al (2003) conducted research to determine the accuracy of various lateral load patterns used in current pushover analysis procedures. First mode, inverted triangular, rectangular, "code", adaptive lateral load patterns and multimode pushover analysis were studied. Pushover analyses are done on four buildings consisting of 3- and 9-story regular steel moment-resisting frames using the above lateral load pattern. Peak values of story displacement, inter storey drift, story shear and overturning moment obtained from pushover analyses at different values of peak roof drifts representing elastic and various degrees of nonlinear response were compared to those obtained from nonlinear dynamic analysis. Nonlinear dynamic analyses were performed using 11 ground motion records selected from the Pacific Earthquake Research Center (PEER) strong motion database. Approximate upper bounds of error for each lateral load pattern with respect to mean dynamic response were reported to illustrate the trends in the accuracy of load patterns. Simplified inelastic procedures were found to provide very good estimates of peak displacement response for both regular and weak-story buildings. However, the estimates of inter-story drift, story shear and overturning moment were generally improved when multiple modes were considered. The results also indicated that simplifications in the first mode lateral load pattern can be made without an appreciable loss of accuracy.

Sasaki F. and Paret (1998) conducted a study on Multi-Mode Pushover (MMP) procedure to determine failure mechanisms due to higher modes of structures. In these study higher modes for different load patterns and a pushover analysis is performed and a capacity curve is obtained for each load pattern considering the modes of interest. Structure's capacity for each mode is compared with earthquake demand by using the Capacity Spectrum Method. Capacity curves and response spectrum are plotted in ADRS format on one plot and the intersections of capacity spectra with the response spectrum represent the seismic demand on the structure. A 17-storey steel frame damaged by 1994 Northridge earthquake and a 12-storey steel-frame damaged by1989 Loma Prieta earthquake were evaluated using MMP. For both frames, pushover analysis based only on the first mode load pattern was inadequate to identify the actual damage. However, pushover results of higher modes or combined of 1^{st} mode and higher modes matched more closely the actual failure mechanism of the structures. It was concluded that MMP can be useful in identifying failure mechanisms due to higher modes for structures with the significant higher-order modal response.

Krawinkler (1998) study a 4-storey steel building which was damaged in the 1994 Northridge earthquake to determine the accuracy of pushover analysis. The frame was subjected to nine ground motion records. Global seismic demands were calculated from pushover analysis results at the target displacement associated with the individual records. The comparison of a pushover and nonlinear dynamic analysis results showed that pushover analysis provides good predictions of seismic demands for low-rise structures having a uniform distribution of inelastic behavior over the height.

Chopra and Goel (2002) developed an improved pushover analysis procedure named Modal Pushover Analysis (MPA) which is based on structural dynamics theory. This method of analysis applied in linearly elastic and inelastic building systems. Then the analysis of an elastic building using MPA producer is the same as response spectrum analysis. The earthquake response of 9-storey inelastic building was determined by MPA procedure of nonlinear dynamic analysis and pushover analysis using uniform "code" and multi-modal load patterns. The comparison of results indicated that pushover analysis for all load patterns greatly underestimates the storey drift demands and lead to large errors in plastic hinge rotations. The MPA was more accurate than all pushover analyses in estimating floor displacements, story drifts, plastic hinge rotations and plastic hinge locations.

Babu (2015) conducted a study on the N2 method of pushover analysis. It is proposed that the pushover analysis of a 3-D mathematical model, which controls the target displacement at the mass center which is at the roof level and the distribution of deformations along with the height of the building, be combined with elastic dynamic (modal) analysis, which controls the torsional effects.

Inel and Ozmen (2006) done research on types and properties of hinges used on pushover analysis. Pushover analysis is carried out for either user-defined nonlinear hinge properties or default –hinge properties, available in some programs based on FEMA-356 and ATC -40 guidelines. Based on this study default –hinge properties provided in SAP2000 are suitable for modern code-compliant buildings; the displacement capacities are quite high for other buildings. The study also determines the user-defined hinge model is better than the default –hinge model in reflecting nonlinear behavior compatible with element properties. But if the default hinge model is selected due to simplicity, the user should be known what is provided in the program and should avoid the misuse of default-hinge properties.

2.6 Gaps in Research Areas

Many types of research are done on performance evaluation of reinforced concrete building with soft storey at the ground floor by increasing the height of storey to make soft. But the researches done on effect of soft storey location due to infill removal or larger door and window provision are not sufficient on performance evaluation of RC buildings. Also, most of the researches are done by using FEMA-356 and ATC-40 hinge properties to assign hinges on beams and column. But ES EN-2015 is mostly similar to Euro code 2005 and assigning of hinges using the Euro code is important for further study.

By considering this gap this research is done to determine the effect of soft storey location on seismic load performance of RC building. In this research RC building with soft storey at a different location is designed using ES-EN-2015 and Euro code 2004. Default hinges are assigned based on the ASCE table with EC8-2005 part 3 acceptance criteria by using ETABS 2017 software. Then pushover analysis is done to evaluate the performance of buildings with the soft storey at different location and comparison is drawn.

CHAPTER THREE

MATERIALS AND RESEARCH METHODOLOGY

This chapter presents and describes the approaches and techniques the researcher used to collect data and investigate the research problem. This section includes the research design of the study, the study variables, selection of specimens, data collection procedure, data quality assurance, data presentation and analysis.

3.1 Research Design

There are various methods that can be used to conduct research and these can be either quantitative, qualitative or combination of both. Based on this, the paper has a quantitative nature (comparative). In order to achieve the objectives of this research nonlinear static (pushover) analysis for earthquake load has done on G+7 and G+ 10 RC moment-resisting frames with soft storey at different locations on each building. The theoretical framework of effect of soft storey location in RC building for seismic performance evaluation has done using Finite element software ETABS 2017 using pushover analysis. The following things are the basic research design producers have been used to achieve the objectives of the study.

- Review of existing literature by different researchers related to subject area of the study
- Collecting of secondary data (allowed loads, material properties) available for modeling and design of the infilled frame with the soft storey from written documents basically from Code books such as ES EN -2015and Euro codes.
- Modeling and design of G+7 and G+10 plan regular and irregular RC moment-resisting frame with soft storey at different locations was done according to ES EN-2015 and Euro Code 2004 using ETABS 2017 commercial software.
- Beams and columns are modeled as rigid joint frame element and infill walls modeled as single diagonal strut and width of struts were estimated using equations derived by Smith and Carter, FEMA 306
- Modeling of soft storey is done by removing the in-plane diagonal struts at a different location and applying initial gravity loads and finally in-plane pushover loading in the negative X-direction
- After modeling and designing of G+7 and G+10 RC building models Pushover analysis is demonstrated using the computer software ETABS 2017. The mathematical model should be subjected to monotonically increasing lateral loads until the monitored displacement of

the design earthquake is reached or a failure mechanism forms. The monitored displacement should be 1% of the total height of the building.

3.2 Study Variables

3.2.1 Dependent Variables

The dependent variable of this study is:-

- Soft storey location

3.2.2 Independent Variables

The independent variable of this study is seismic performance of soft storey building in terms of

- Pushover curve
- Target displacement
- Storey displacement
- Storey Shear
- Storey drift
- Seismic performance (plastic resistance)

3.3 Data Collection Processes

In this research G+7 and G+ 10 RC moment resisting frames were analyzed for seismic performance effect of soft storey location using pushover analysis. Two are irregular in plan that is (L) shape and irregular in elevation due to soft storey and the others are irregular in elevation only due to the provision of soft storey. All stories of each building have 3m height. Modeling will be done on the interface of ETABS 2017 building design and analysis software. In these models, the soft storey is located at different locations of the models to evaluate the effect of soft storey location on seismic performance. The research data have been collected from secondary source and code books which are briefly discussed below**.** Models and modeling producers also discussed.

Justification for the selection of the samples

The samples selected for this study are based on their numerously constructed in the world and specifically in Ethiopia. Also, the model selected should be simple to minimize the manipulation time for pushover analysis in ETABS. When the modeling is complex the analysis complex and the output is unattainable.

3.4 Data Quality Assurance

In order to assure data quality of this study the following measures are taken:

- The ETABS software is checked for the known simple structural systems to check whether it is working well or not.
- The structural modeling, the loading and the different connections of the frame system and the diagonal struts are double-checked to remove errors.
- In case of any unreliable results due to some unobserved errors, the structure is re-modeled and reanalyzed.
- Due attention and care is taken when extracting results from ETABS and plotting them in Excel.

3.6 STRUCTURAL MODELING

It is very important to develop a mathematical model on which performance-based analysis is performed to determine the effect of soft storey location on RC buildings which is constructed in the seismic zone IV region. The first part of this chapter presents a summary of various parameters defining the computational models, the basic assumptions and the geometry of the selected building considered for this study. Infill walls are modeled as equivalent diagonal strut elements. The last part of the chapter deals with the computational model of the equivalent strut.

3.6.1 Building Description

Multi-storey rigid jointed frame of office and shopping use buildings (G+7, G+10) two rectangular in plan and the others are irregular in plan (L- shape) with the provision of soft storey at different location ware selected in seismic Zone IV region of Ethiopia. These Buildings designed based on Ethiopian Building Code Standard ESEN: 2015 and European Code-2004 almost similar to the new Ethiopian building code (as used by the software). ETABS 2017 was used for the analysis and design of the building by modeling as a 3-D frame system. Seismic performance is predicted by using performance-based analysis of simulation models of buildings with the provision of soft storey at different locations.

For the analysis work of this research, the following models of RC building have taken.

I. G+7 regular in plan RC building storey height of 3m
    a. Model 1:- soft storey at the ground floor
    b. Model 2:- soft storey at the 3rd storey level

c. Model 3:- soft storey at the 5th storey level

d. Model 4:- soft storey at the top (7th)storey level

II. G+10 regular in plan RC building storey height of 3m

a. Model 5:- soft storey at the ground storey

b. Model 6:- soft storey at the 4th storey level

c. Model 7:- soft storey at the 7th storey level

d. Model 8:- soft storey at the top(10th) storey level

III. G+7 irregular in plan RC building storey height of 3m

a. Model 9:- soft storey at the ground floor

b. Model 10:- soft storey at the 3rd storey level

c. Model 11:- soft storey at the 5th storey level

d. Model 12:- soft storey at the top (10th) storey level

IV. G+10 irregular in plan RC building storey height of 3m

a. Model 13:- soft storey at the ground floor

b. Model 14:- soft storey at the 4th storey level

c. Model 15:- soft storey at the 7th storey level

d. Model 16:- soft storey at the top (10th)storey level

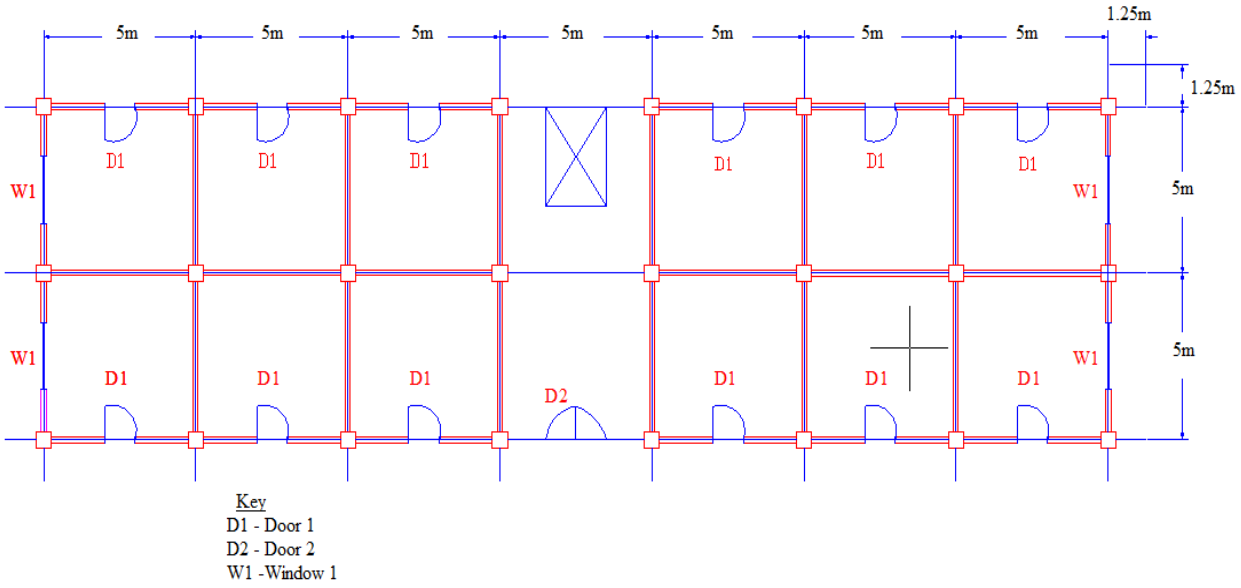

Figure 3. 1 Floor plan of (G+7) and (G+10) storey regular plan building models

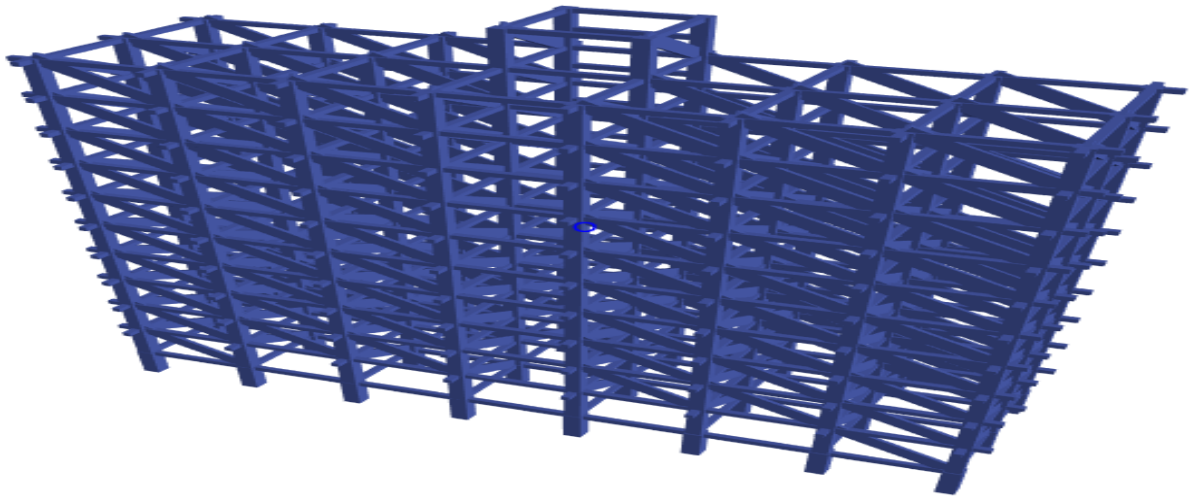

Figure3. 2 Sample of 3-D render view of regular plan building model

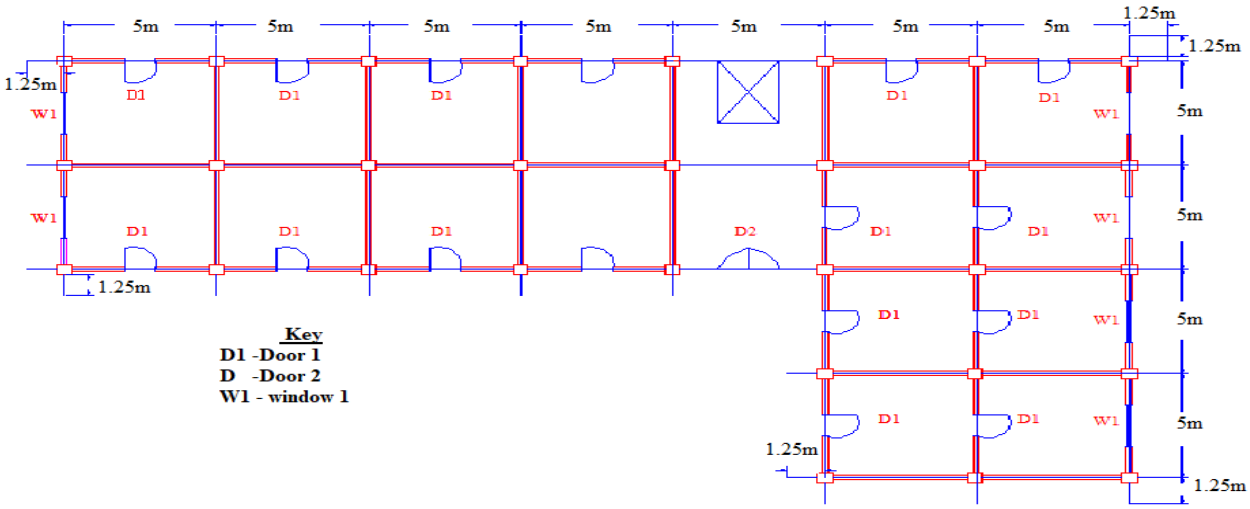

Figure3. 3 Floor plan of (G+7) and (G+10) irregular plan building models

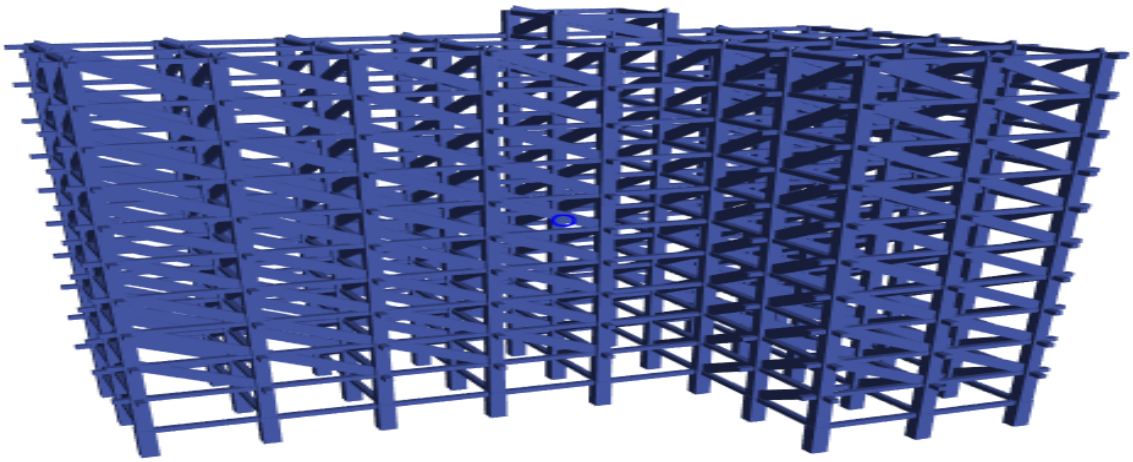

Figure 3. 4 Sample of 3-D render view of irregular plan building model

3.6.2 Structural Modeling Data

Modeling of buildings involves the modeling and assemblage of its various load-carrying elements. The model must ideally represent the mass distribution, strength, stiffness and deformability. Data required for modeling of buildings and loads applied for the study are discussed below.

- **Building Data**
  - Type of structure = Multi-storey moment-resisting frame
  - Frame Layout = as shown in figure 3.1 - 3.4
  - Number of stories = 7 and 10 storey
  - Height of Buildings = 23.5m and 32.5m
  - Floor to floor height = 3 m
  - External wall thickness = 20cm
  - Internal wall thickness =15cm
  - Depth of the slab =15cm

1. **Beam and Column sizes for G+7 models**
   - Size of all floor columns = 50x50cm
   - Size of all footing columns = 60x60cm
   - Size of all floor beams = 35×35cm
   - Size of all Grade beams = 30×50cm
   - Door and window opening size = 25% of wall panel
2. **Beam and Column sizes for G+10 models**
   - Size of all floor columns = 65x65cm
   - Size of all footing columns = 75x75cm
   - Size of all floor beams = 35×35cm
   - Size of all Grade beams = 30×50cm
   - Door and window opening size = 25% of wall panel

The following assumptions considered in this research.

- Modal damping 5% is considered.
- Beams and columns are modeled as frame elements and joined node to nodes.

- The effect of soil-structure interaction is ignored in the analysis. The columns are assumed to be fixed at the ground level.
- Plan dimension and beam size is kept similar to all Storey
- Beam column joints are taken as rigid joints
- Only the primary structural components and walls are assumed to participate in the overall seismic behavior.
- Ductility class medium only considered
- Geometric non –linearity (P- Δ) considered

- **Loading:**

For this research, the following loads are considered for the analysis and design of RC building models.

1. Live load: - Recommended by EN 1991-2015 for commercial building (office and shopping) are used.

- Slab live load = 4KN/m
- Stair live load = 4KN/m
- Flat roof live load = 0.5KN/m

2. Dead load

- Floor finish load (marble finishing)
- Self-weight of building
- External and internal wall load (hallow concrete block)

3. Seismic load Data

The following data are taken to consider earthquake load in the seismic Zone 4 region of Ethiopia recommended by ES EN 1998-2015.

Table3.1 Seismic load data and factors

Earthquake Data	
Seismic Zone	IV
bedrock acceleration ratio($\boldsymbol{\alpha_o} = \frac{ao}{g}$)(ratio of design bedrock acceleration to acceleration of gravity)	0.15g

Design PGA	1*0.15g = 0.15g
Importance factor, I	1
Behavior factor, q	depend on the structural system
Subsoil class	C
Spectrum type	1

Behavior factor (q) = 3.12 for moment-resisting high rise building irregular in elevation but regular in plan for ductility class medium from ES EN 1998-2015 and 3 for irregular in plan. The computation is put in appendix A.

- **Materials used**

For the design of RC structures models, the following materials are available

For beam and column = C-30/37

For slab = C-25 /30

Reinforcement bar = S-500

Wall part = HCB (hallow concrete block)

Table3. 2 Properties of the material used for design and analysis

Concrete material	
Grade of concrete	C-30 and C-25 according to their requirement
Poisons ratio of concrete (ν_c)	0.2
Unit weight of concrete(γ_c)	25kN/m3
Modulus of elasticity of concrete(Ec)	31GPa for C-30 and 30GPa for C-25
Coefficient of thermal expansion of concrete	10*10-6 per ^oC
Reinforcement bar	

Grade of steel(rebar)	S-500
Unit weight of reinforcing steel (γ_s)	77 KN/m^3
Coefficient of thermal expansion of steel	10*10-6 per ^oC
Modulus of elasticity of steel (Es)	200GPa
Poisons ratio of steel (ν_s)	0.3
HCB (hallow Concrete Block masonry wall	
Size of HCB	15 cm x 20cm x 40cm and 20 cm x 20cm x 40cm
Unit weight infill (γ_{infill})	14KN/m^3
Characteristic Compressive strength(fc)	3Mpa
Poisons ratio(ν_{infill})	0.15

Young's elastic modulus of masonry is calculated by the relation given by (T. Paulay and M. Priestley, 1992). The values for the modulus of elasticity of masonry in compression shall be taken as 750 and 550 times the expected masonry compressive strength for HCB and brick respectively.

$E_M = 750 x f_c = 750x3$ = 2250 MPa for HCB WALL

The dimensions of the building used in this research are designed using Euro Code 2004 which is encoding in ETABS 2017 design and analysis software. In the design of the above dimensions, loads listed in the above are considered and all load combination listed in the software according to Euro Code 2004 for earthquake and gravity loads are used. The sample detail design is shown in the figure below and the 3-D detail put in appendix E. The design of the building is safe as shown in the figure because there is no over-stressed member and the reinforcement required shown in mm^2.

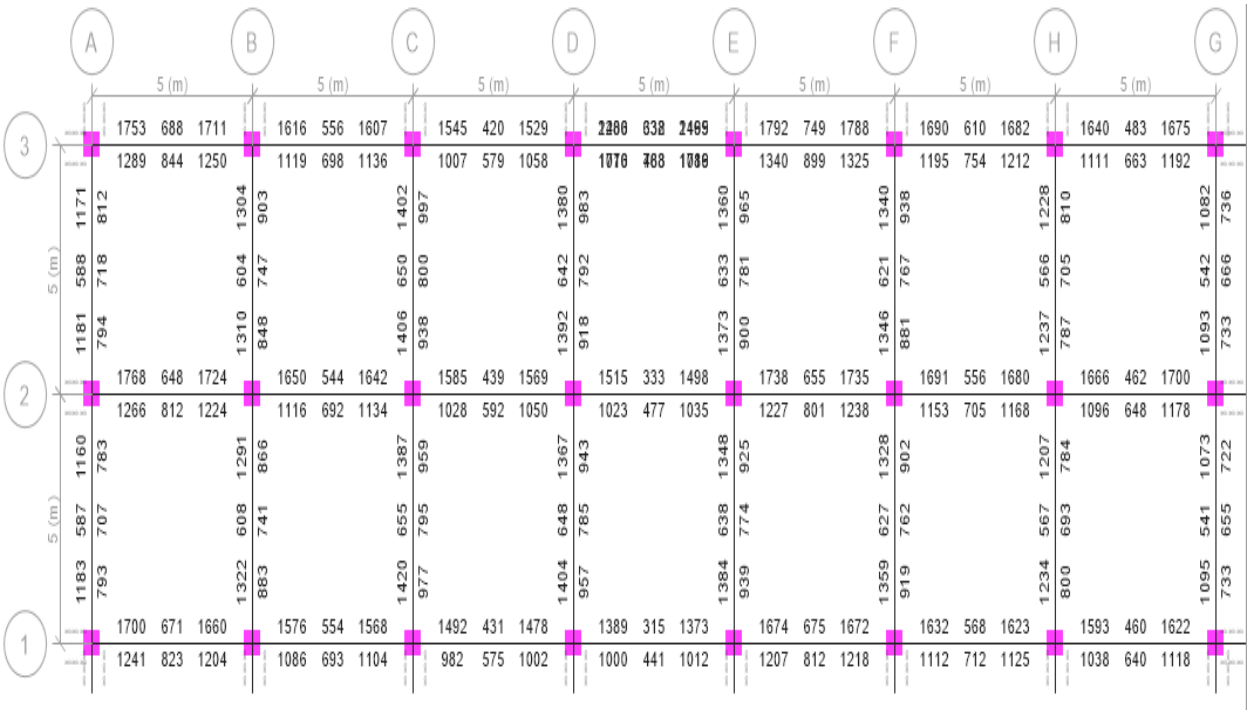

Figure 3. 5 Sample designs of buildings in the plan view for regular plan model

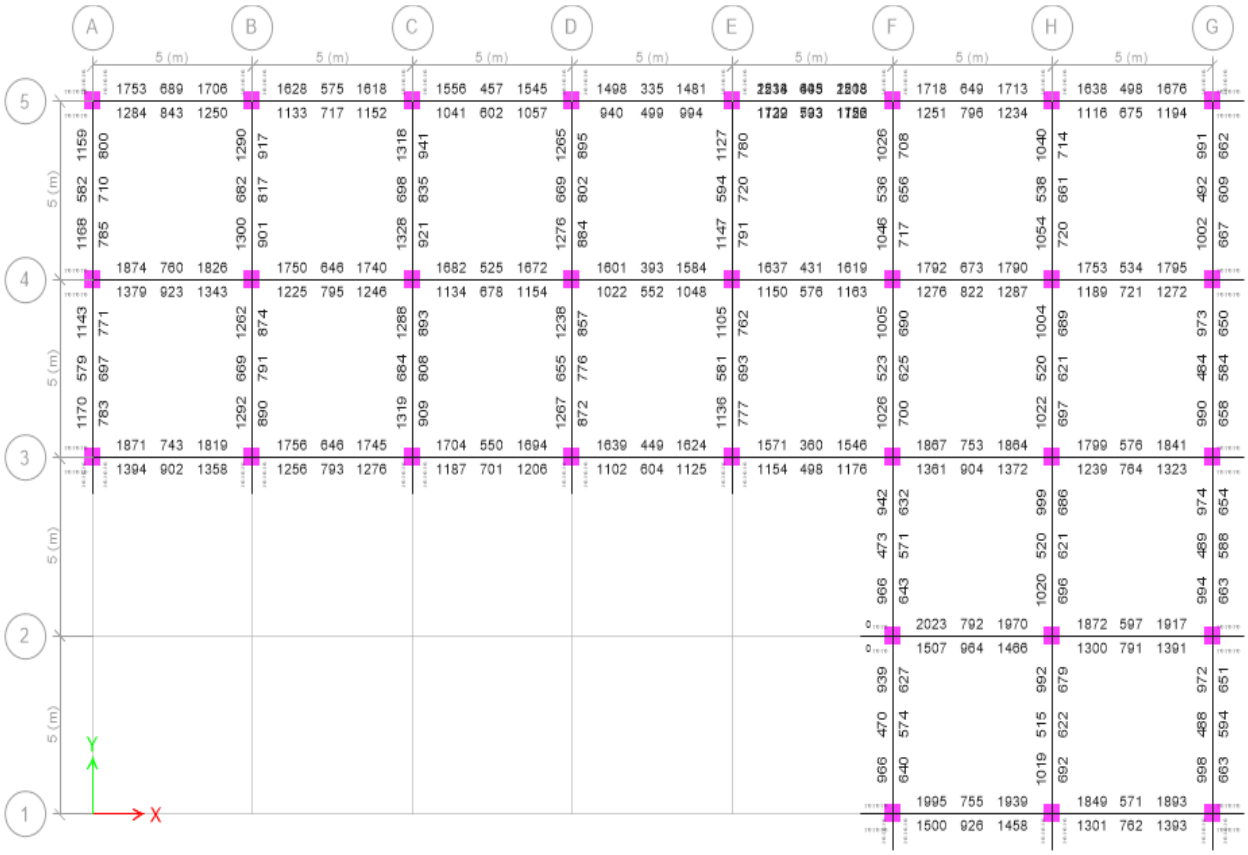

Figure3. 6 Sample design of buildings in the plan view for irregular plan model

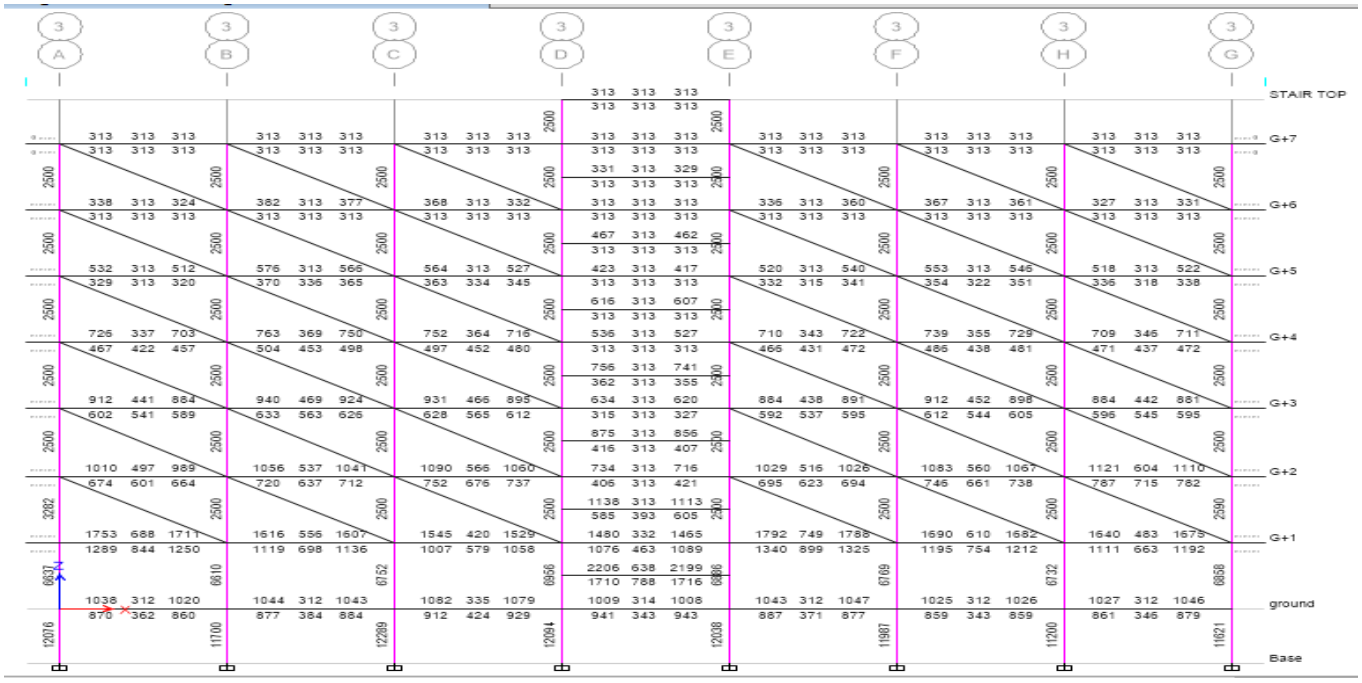

Figure3. 7 Sample design of buildings in the elevation view

3.6.3 Modeling of Structural Elements

Beams and columns are modeled as 3- D frame elements. The beam-column joints are modeled by giving end-offsets to the frame elements, to obtain the bending moments and forces at the beam and column faces. The beam-column joints are assumed to be rigid. Beams and columns in the present study were modeled as frame elements with the centerlines joined at nodes using commercial software ETABS 2017. The rigid beam-column joints were modeled as shown in (Figure 3.5). The weight of the slab was distributed on the beam.

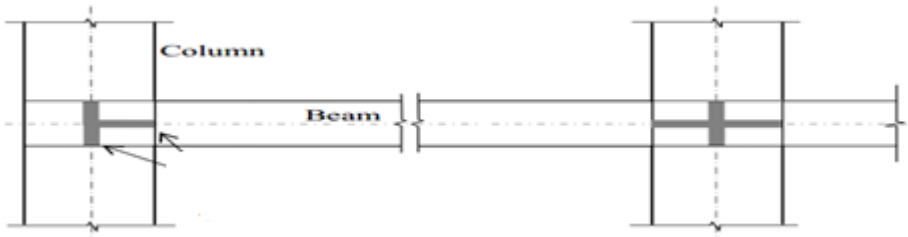

Figure3. 8 Modeling of beam & column

3.6.4 Modeling of Masonry Infill Wall

In the case of an infill wall located in a lateral load resisting frame, the stiffness and strength contribution of the infill is considered by modeling the infill as an equivalent compression strut. Because of its simplicity, several investigators have recommended the equivalent strut concept. In

the present analysis, a trussed frame model is considered. This type of model does not neglect the bending moment in beams and columns. Rigid joints connect the beams and columns, but pin joints connect the equivalent struts to columns.

Infill parameters (effective width and strength) are calculated using the method recommended by Smith and Carter, FEMA 306 described in chapter two sections 2.3.2.2. The length of the strut is given by the diagonal distance *d* of the panel and its thickness is given by the thickness of the infill wall. The initial elastic modulus of the strut *Ei* is equated to *Em* the elastic modulus of masonry is determined according to (T. Paulay and M. Priestley 1992) the value of a constant Ω equals to 750 for concrete block and 500 for clay brick.

3.6.4.1 Modeling of Equivalent Strut

For an infill wall located in a lateral load-resisting frame, the stiffness and strength contribution of the infill has to be considered. Non-integral infill walls subjected to lateral load behave like compression diagonal struts. Thus an infill wall can be modeled as an equivalent diagonal compression strut in the building model.

After modeling the bare frame, the equivalent diagonal struts are added to represent the masonry infill as shown in figure 4.6 and 4.7. Since most of the panels are fully infilled the struts should design to represent full infill panels and then multiplied by a proper reduction factor to account for door and window openings in the infill panel.

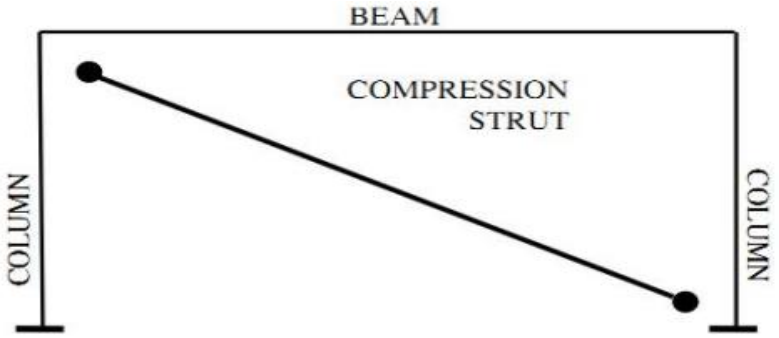

Figure3. 9 Connections of Compression Strut

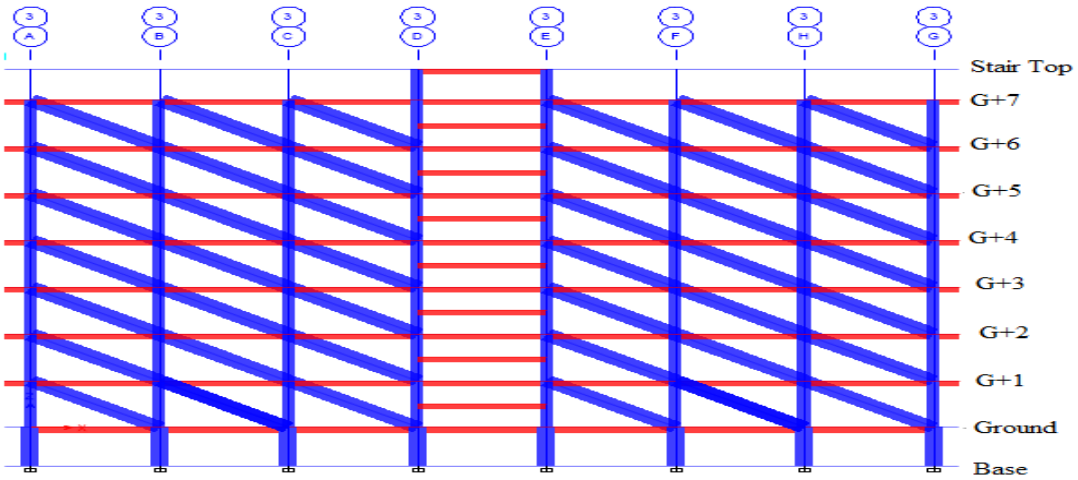

Figure3. 10 Diagonal strut modeling of walls using ETABS 2017

3.6.5 Modeling of Soft Storey

Soft storey irregularity refers to the existence of a building floor that presents a significantly lower stiffness than the others. It is commonly generates non-uniform system due to the elimination or reduction in the number of rigid non-structural walls in one of the floors of a building, or for not considering the structural design and analysis. If the soft story effect is not foreseen on the structural design, irreversible damage will generally be present on both the structural and nonstructural components of that floor. This may cause the local collapse, and in some cases even the total collapse of the building.

In in this research soft storey modeling is done by removing the diagonal strut which has in-plane lateral load resistance (X-axis) at different floor levels in order to determine the effect of soft/weak storey location for seismic load performance of RC building.

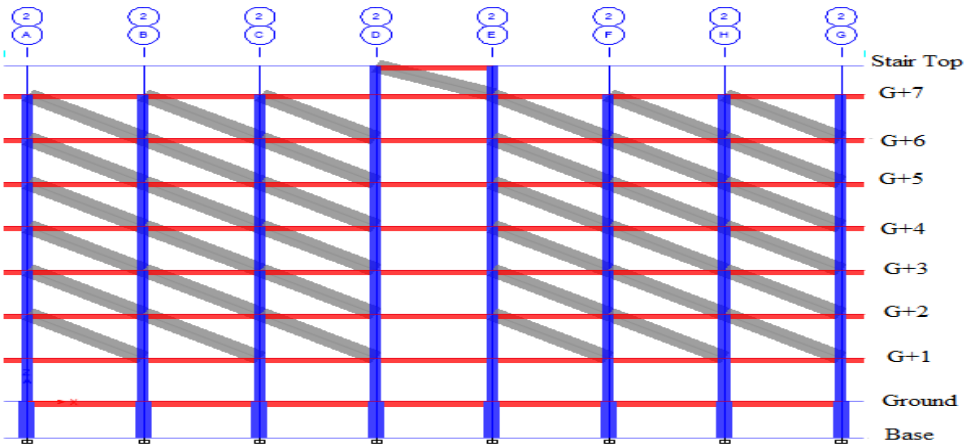

Figure3. 11 Sample Elevation view of soft storey modeling at ground floor

By the same principle, soft stories of all building models at the remaining location can be done by removing diagonal struts in the X-direction**.**

Stiffness of the building for different soft storey location is determined using the response spectrum method of analysis. And the ratio of stiffness used in this study calculated using the equations given below.

1. If $\frac{Ki}{Ki+1} < 0.7$

2. If $\frac{Ki}{(Ki+1+Ki+2+Ki+3)/3} < 0.8$

Then by using the above equation and stiffness outputs from response spectrum analysis the stiffness ratios in the X-direction for soft storey used in this study are.

1. For G+ 7 regular plans buildings

   0.54<0.8
2. For G+10 regular plans buildings

   0.71 <0.8
3. For G+7 irregular plan buildings

   0.51< 0.8
4. For G+10 irregular plan buildings

   0.71 <0.8

But using case one all stiffness ratios used in this study are above 0.7 and the detail calculation and stiffness are put in the appendix.

3.6.6 Frame Hinge Properties

The capacity of providing plastic hinges as discrete user-defined hinges along the clear length of the frame element introduced by SAP 2000/ETABS. And also the post-yield behavior in one or more degrees of freedom represented by plastic hinge. Uncoupled moment, torsion, axial force and shear hinge are available to be modeled along the frame element. Also, a P-M2-M3 hinge which yields based on the interaction of axial force and bending moments at the hinge location can be modeled. Sometimes more than one type of hinge can exist at the same location, for example, the user might assign both M3 (moment) and V (shear) hinge to the same end of a frame element.

For nonlinear analysis, user-defined hinge properties and automatic hinge properties can be assigned to the frame element. When user-defined or automatic hinge properties are assigned to

the frame element, the program automatically creates a generated hinge property for each and every hinges. User-defined hinge property can either be based on a hinge property generated from automatic, or it can be fully user-defined.

In SAP2000/ETABS there are two types of hinges that are user-defined and default hinge properties. A user-defined property is that typically the hinge properties are section dependent. Thus it would be necessary to mean that someone would need to define a large number of hinge properties. The definition of user-defined hinge properties requires moment-curvature analysis of each element.

In SAP2000/ETABS, the default-hinge model assumes the same deformation capacity for all columns regardless of their axial load and their weak and strong axis orientation. It takes the average values of hinge properties instead of carrying out the detailed calculations for each member. But, the hinge properties depend on the type of element, material property, shear span ratio and the axial load on the element.

In this study cross-sectional dimensions of beam and column are the same then default (Auto) hinge properties are used and user-defined hinges are used for diagonal struts.

3.6.7 Plastic Hinge Placement

In order to model nonlinear behavior in any structural element, a corresponding nonlinear hinge must be assigned in the building model. Nonlinear hinges were assigned to the following structural elements expected to undergo inelastic deformation.

To ensure gravity load-carrying capability at performance point, P-M_1-M_2 hinges are assigned at the ends of columns.

Plastic hinges in columns should capture the interaction between axial load and moment capacity. These hinges should be located at a minimum distance l_{column} from the face of the beam as shown in figure 4.9. Hinges in beams need only characterize the flexural behavior of the member. These hinges should be placed at a minimum distance l_{beam} from the face of the column.

For this study hinges located on columns and beam at (0.05, 0.95) According to Euro Code recommendation.

The equivalent strut only needs hinges that represent the axial load. This hinge should be placed at the mid-span of the member. In general, the minimum number and type of plastic hinges needed to capture the inelastic actions of an infilled frame are depicted in Figure 3.10.

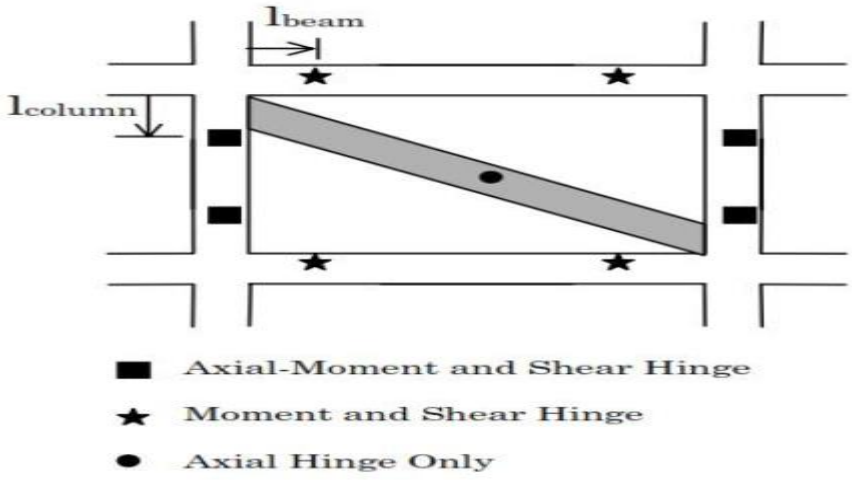

Figure3. 12 Plastic hinge placements

3.6.8 Frame Member Stiffness

Different codes recommended different values to undermine the effective stiffness of frame members in analysis. For this study ES EN 1998-2015 Code used

According to ES EN 1998-2015**,** the stiffness of the structural elements shall be evaluated taking into account both their flexural and shear flexibility. Uncracked elastic stiffness may be used for analysis or, preferably and more realistically, cracked stiffness in order to account for the influence of cracking on deformations and to better approximate the slope of the first branch of a bilinear force deformation model for the structural element.

In the absence of an accurate evaluation of the stiffness properties determined by rational analysis, the cracked bending and shear stiffness may be taken as 1/2 of the cross-section of uncracked elastic stiffness.

3.6.9 Masonry Infill Crushing Strength.

The masonry infill crushing capacity is the strength of infill that resists the applied compressive load before it is crushed (R_{cr}). This resistance can be determined using equation 2.12.

$$R_{cr} = w\, t_{eff}\, f_m' \quad \text{----------2.12}$$

Where

f_m' = Compressive strength of the masonry, Mpa

t_{eff} = net thickness masonry panel.

w = effective width of strut

The detail calculation of compressive strength used in this study is put in the appendix part including the reduction factor for openings.

3.7 Structural Analysis

3.7.1 Nonlinear Static (Pushover) Analysis

Pushover analysis is a static nonlinear procedure using a simplified nonlinear technique to estimate seismic structural deformations.it is an incremental static analysis in case of force or displacement to determine the capacity curve of a structure. The analysis conducted through applying of horizontal loads in a well-defined pattern to the structure incrementally. Then plot the result in terms of base shear to displacement at each increment, until collapse condition**.**

Model of the building is done in modeling software such as ETABS 2017. Pushover analysis is done by subjecting the model for modal lateral load pattern. The intensity of the lateral load is slowly increased and applied iteratively. This iterative analysis and design process continue until the design satisfies pre-established performance criteria. The performance criterion in pushover analysis is established as the desired state of the building given rooftop spectral displacement amplitude. In this study, the building model pushed by the load to a distance of 1% of the total building height.

FEMA-356 and ATC–40 documents describe the detail modeling procedures, acceptance criteria and analysis procedures for pushover analysis. As shown in Figure 3.1 below, five points labeled A,B, C, D, and E are used to define the force deformation behavior of the plastic hinge, and three points labeled IO (Immediate Occupancy), LS (Life Safety) and CP (Collapse Prevention) are used to define the acceptance criteria for the hinge. In these documents, the number of hinges with color code is determined and comparison is drawn for different locations of soft storey.

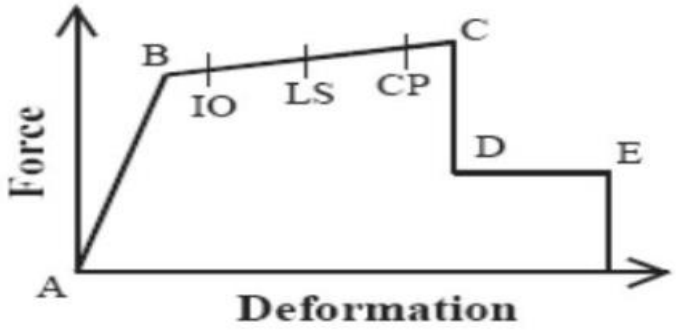

Figure3. 13 Force-Deformation Relations for Plastic Hinge in Pushover Analysis

3.7.1.1 Structural Performance Levels

3.7.1.1.1 Immediate Occupancy Performance Level

Immediate Occupancy, means the past-earthquake damage state in which only very limited structural damage has occurred. The basic vertical and lateral force-resisting systems of the building retain nearly all of their pre-earthquake strength and stiffness. The risk of life-threatening injury as a result of structural damage is very low.

3.7.1.1.2 Life Safety Performance Level

Life Safety means the past-earthquake damage state in which significant damage to the structure has occurred, but some margin against either partial or total structural collapse remains. Some structural elements and components are severely damaged, but this has not resulted in large falling debris hazards, either within or outside the building. Injuries may occur during the earthquake; however, it is expected that the overall risk of life-threatening injury as a result of structural damage is low. It should be possible to repair the structure; however, for economic reasons, this may not be practical.

3.7.1.1.3 Collapse Prevention Performance Level

Collapse Prevention means the building is on the verge of experiencing partial or total collapse. Substantial damage to the structure has occurred, potentially including significant degradation in the stiffness and strength of the lateral force-resisting system, large permanent lateral deformation of the structure and to more limited extent degradation in vertical-load-carrying capacity. However, all significant components of the gravity load resisting system must continue to carry their gravity load demands. Significant risk of injury due to falling hazards from structural debris may exist. The structure may not be technically practical to repair and is not safe for re-occupancy, as aftershock activity could induce collapse.

3.7.1.2 Load Pattern in Pushover Analysis

In non- linear static pushover analysis horizontal load is applied to the building to determine the performance of the building for earthquake excitation. Then lateral load pattern imitates seismic inertial forces at the center of mass at each floor of the structure and there is no unique way to define it. Three different load patterns are frequently used:

1. Triangular
2. Uniform

3. Modal

For this study, modal load pattern is used in ETABS 2017 building design and analysis software.

3.7.1.3 Pushover Analysis Using ETABS

Pushover analysis is an approximate analysis method in which the structure is subjected to monotonically increasing lateral forces with an invariant height-wise distribution until a target displacement is reached using ETABS 2017 software.

Nonlinear static analysis can be conducted in ETABS

- Force-controlled or
- Displacement-controlled.

In force-controlled pushover procedure, full load combination is applied as specified, i.e., force-controlled procedure should be used when the load is known (such as gravity loading). Also, in force-controlled pushover procedure, some numerical problems that affect the accuracy of results occur since target displacement may be associated with a very small positive or even a negative lateral stiffness because of the development of mechanisms and P-delta effects.

Pushover analysis has been the most selected method by engineers, maintenance and retrofitting guidelines and codes for seismic performance evaluation of structures due to its simplicity in computation.

ETABS menus and documentation refer to pushover analysis as static nonlinear analysis. The key points for conducting pushover analysis in this study can be summarized as follows.

1. Defining how nonlinearity is considered
2. Determining analysis cases
3. Defining loading
4. Selecting the type of load control
5. Analysis Results

3.7.1.4 Determining Nonlinearity

To get acceptable result proper modeling of the nonlinear properties of the structure is very mandatory. Very complicated models do not give accurate output. So when modeling structure as much as possible it is better not to be complicated in order to save analysis time and to obtain

accurate results. Many types of nonlinearity should undermine in pushover analysis but for this study, the following nonlinearity has been considered.

- Material nonlinearity (hinges in fame element and diagonal strut)
- Geometric nonlinearity (P-delta)

1. Material nonlinearity at discrete (default and user-defined hinges in frame/line elements should be considered. Plastic hinges can be assigned at any number of locations along the length of any frame element wherever yielding or other inelastic behavior is expected. The following hinge properties should be considered to assign hinge for frame elements in this study.

- Coupled P-M2-M3 hinge that considers the interaction of axial force and bending moments In columns
- Uncoupled moment **(**M_3**)** hinges for beams.
- Axial load (P) for diagonal struts

2. Geometric nonlinearity. In pushover analysis, geometric nonlinearity should be considered. So choose only P-delta effects or considering P-delta effects plus large displacements for geometric nonlinearity. Large displacement effects consider equilibrium in the deformed configuration and allow for large translations and rotations. However, the strains within each element are assumed to remain small. Most of the time the P-Delta effects option (without large deformations) is recommended and used for this study.

3.7.1.5 Determining Analysis Cases

Static nonlinear analysis can consist of any number of cases. Each static nonlinear case can have a different distribution of load on the structure. For this study the following typical static nonlinear analysis cases used.

- First applied gravity load to the structure
- Then applied modal lateral load pattern over the height of the structure until the target displacement achieved.

A static nonlinear case may start from zero initial conditions, or it may start from the results at the end of a previous case such as gravity loads.

1. Defining Loading

The distribution of load applied on the structure for a given static nonlinear case is defined as a scaled combination of one or more of the following.

- **Any Static Load Case.**

Uniform acceleration is acting on any of the three global directions. The force at each joint is Proportional to the mass assigned to that joint (i.e., calculated from the tributary area) and acts in the specified direction.

- **A modal Load**

The force at each joint is proportional to the product of the modal displacement (eigenvector), and the mass tributary to that joint, and it acts in the direction of the modal displacement.

The load combination for each static nonlinear case is incremental, meaning it acts in addition to the load already on the structure if starting from a previous static nonlinear case.

2. Selecting the Type of Load Control

ETABS has two distinctly different types of control available for applying the load. Each analysis case can use a different type of load control. The choice generally depends on the physical nature of the load and the behavior expected from the structure.

1. Force Control.

Force control should be used when the load is known (such as gravity load), and the structure is expected to be able to support the load in the elastic range.

2. Displacement Control

A single monitored displacement component (or the conjugate displacement) in the structure is controlled. The magnitude of the load combination is increased or decreased as necessary until the control displacement reaches a value that you specify. Displacement control should be used when specified drifts are sought (such as in seismic loading), where the magnitude of the applied load is not known in advance, or when the structure can be expected to lose strength or become unstable.

- **Steps used in this study for pushover analysis using ETABS2017 software are summarized below.**

i. **Develop Structural Model**

The development of modeling of the structure was the first step in pushover analysis and the three-dimensional models of the building were adopted in this research. The material property and cross-section of the structure were defined with the reinforcement obtained from the capacity design of the element.

ii. **Define new Load Pattern**

In this research defined new load patterns as Gravity-x, push-x in negative X-direction

- Go to Define > load pattern >Gravity-x/push x/ > Add new load > ok
- Define pushover Load Case

For the present study of pushover analyses, use the total dead load and 30% of the live load (1.0 DL + 0.3 LL). All dead loads in the building (structural components, partitions, architectural finishes and more) should be included in defining the total dead load. Masonry infill walls should be considered as dead loads, because the infill walls are structural elements.

A non-linear static load (Push X) case was defined in the X directions. In this step mass source, Acceleration load type, load application type and how the results are saved parameters were filled in the software.

- The load applied used to assess the performance of the structure was displacement controlled type.
- Go to Define > load case>Gravity x>Add new case >load case (nonlinear static) > it started from zero initial condition>load type (acceleration) (load pattern of (DL+0.3LL)>>load name Ux>scale factor 1> Geometric nonlinearity parameters as P-Delta>load application (Full load)>used monitor displacement U1 (kept as equal to 1% of the height of the building)>Result saved>Final states only.

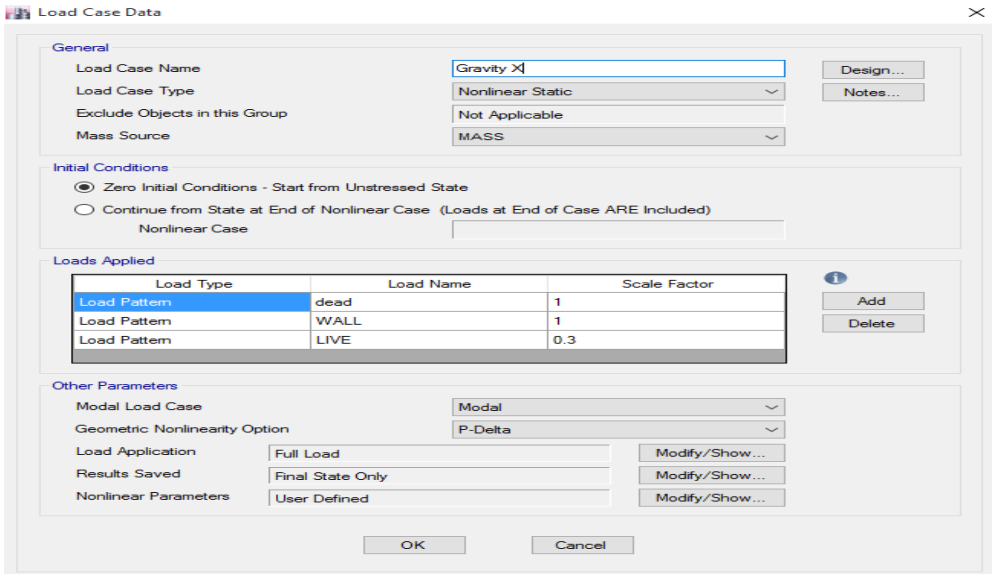

Figure3. 14 Pushover load case for Gravity loads

Go to Define > load case> push X>Add new case >load case (nonlinear static > continuous from state at end of nonlinear case >load type (acceleration) Ux >scale factor 1> Geometric nonlinearity parameters as P - Delta> load application (displacement control)>used monitor displacement U1 (kept as equal to 1% of the height of the building)>Result saved>Multiple states.

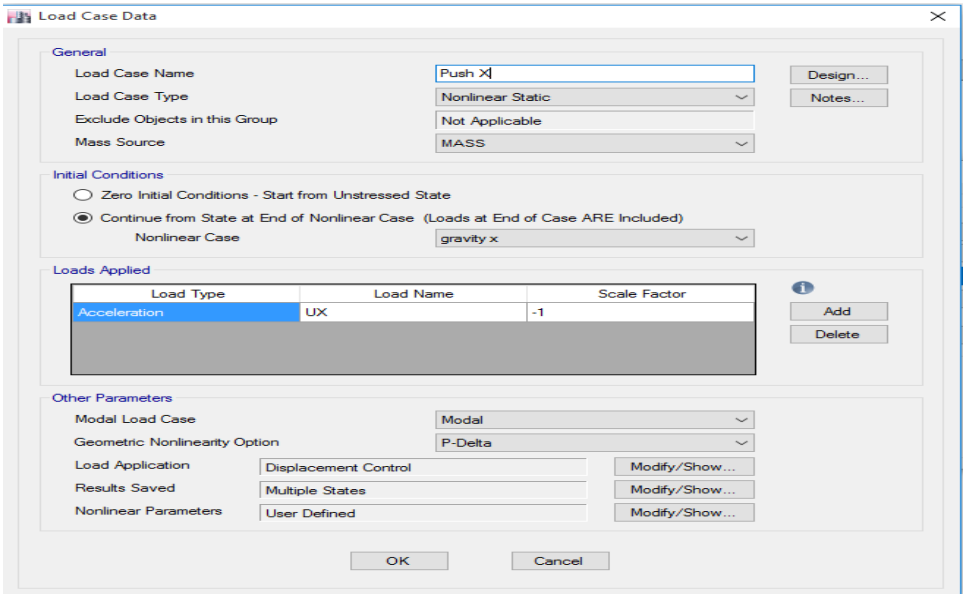

Figure3. 15 Pushover load case for Pushover loads

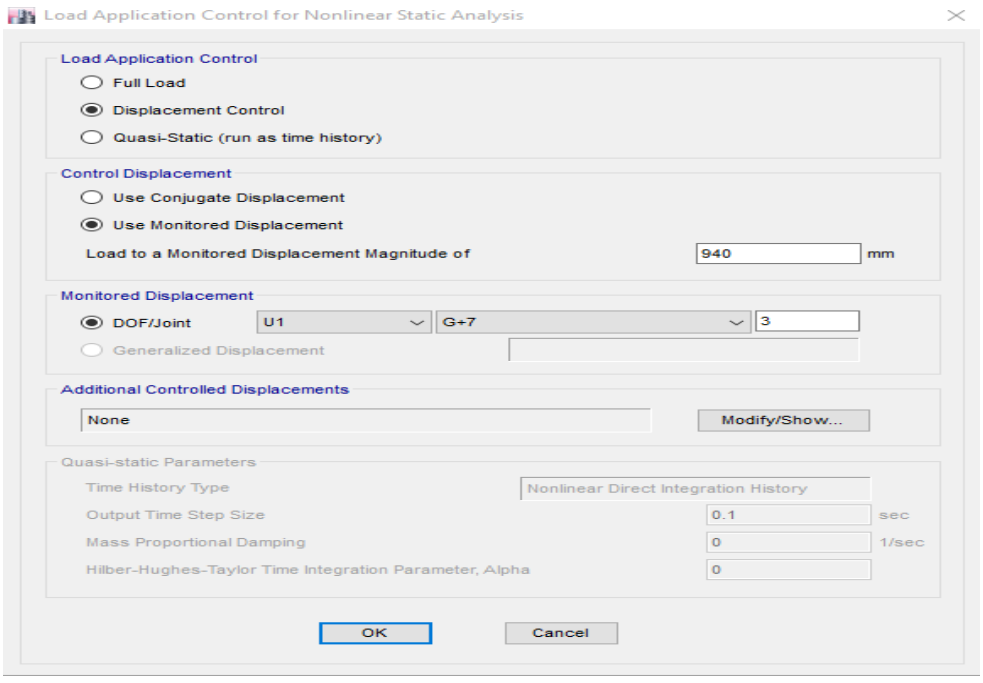

Figure3. 16 Load application control for non-linear static analysis

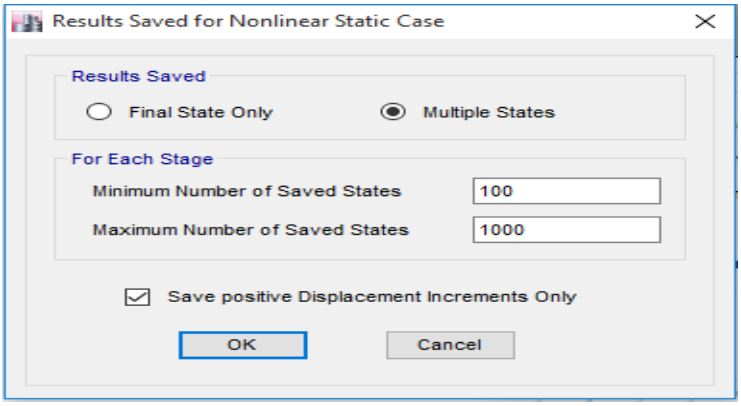

Figure3. 17 Result saved for non-linear static load case

iii. **Assignment of Hinges to the Frame Elements**

The plastic hinges formations in the nonlinear deformation of the building were concentrated or lumped in the critical length (single point) of the element

The modeling of the plastic hinges was performed at the end of beam element and the bottom end of the base column. When the plastic hinges were defined deferent assumptions are made and described as follows:

- Select all the beams in the model.
- Go to Assign>Frame>Hinges (the hinges assigned at both ends of the beam which means at the relative distance of 0.05 and 0.95.

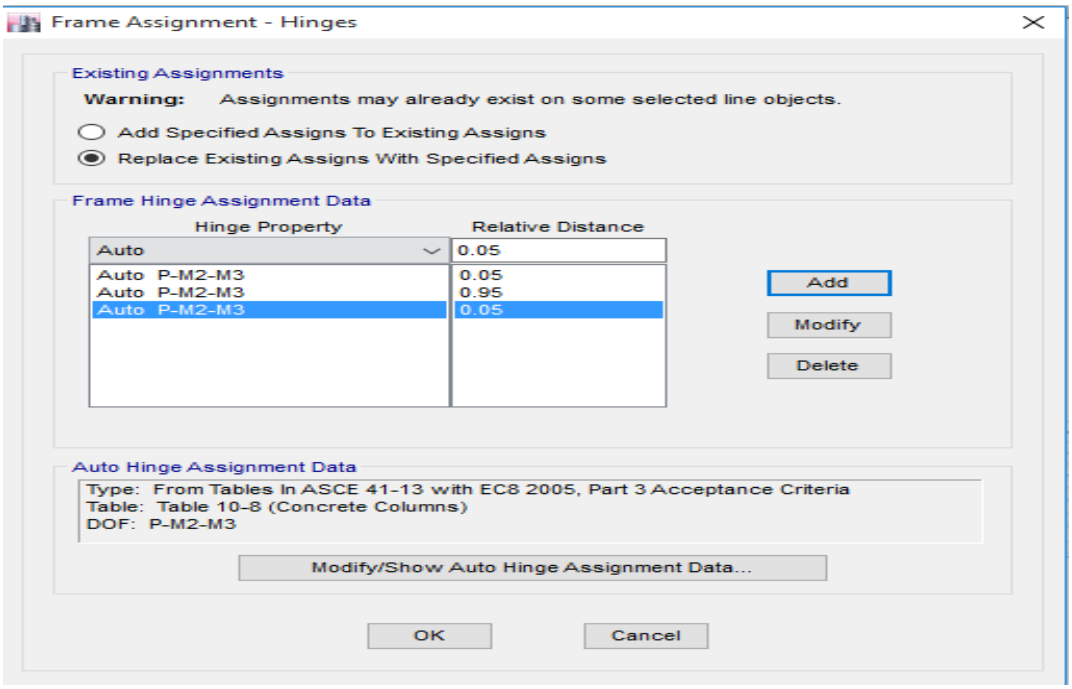

Figure3. 18 Hinge at both ends for columns

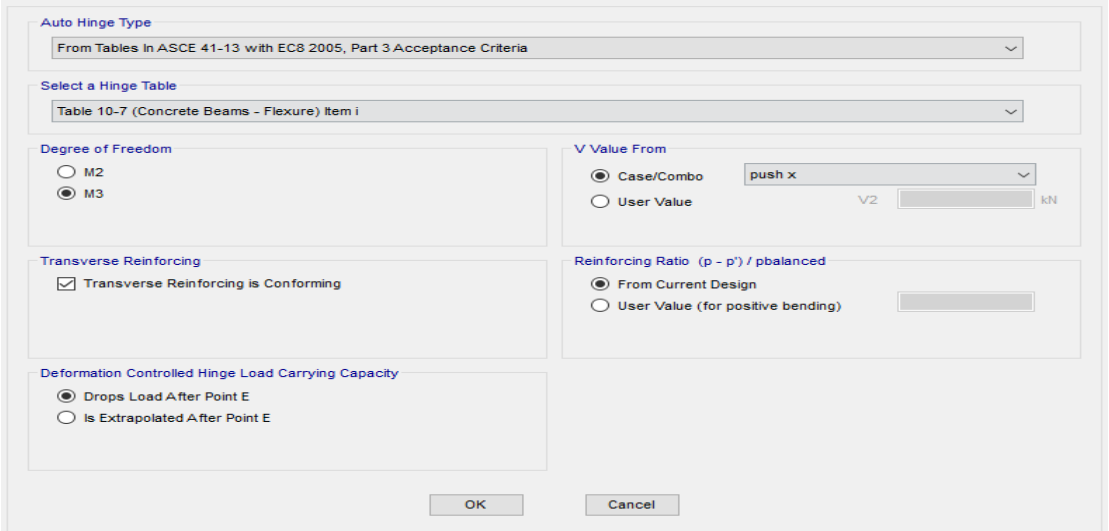

Figure3. 19 Hinge Properties for Beams

In a similar manner assigned hinges to all columns by repeating steps as previously carried out for beams, the only difference is that column assigned P-M_2-M_3 hinges instead of M_3 hinges for beams.

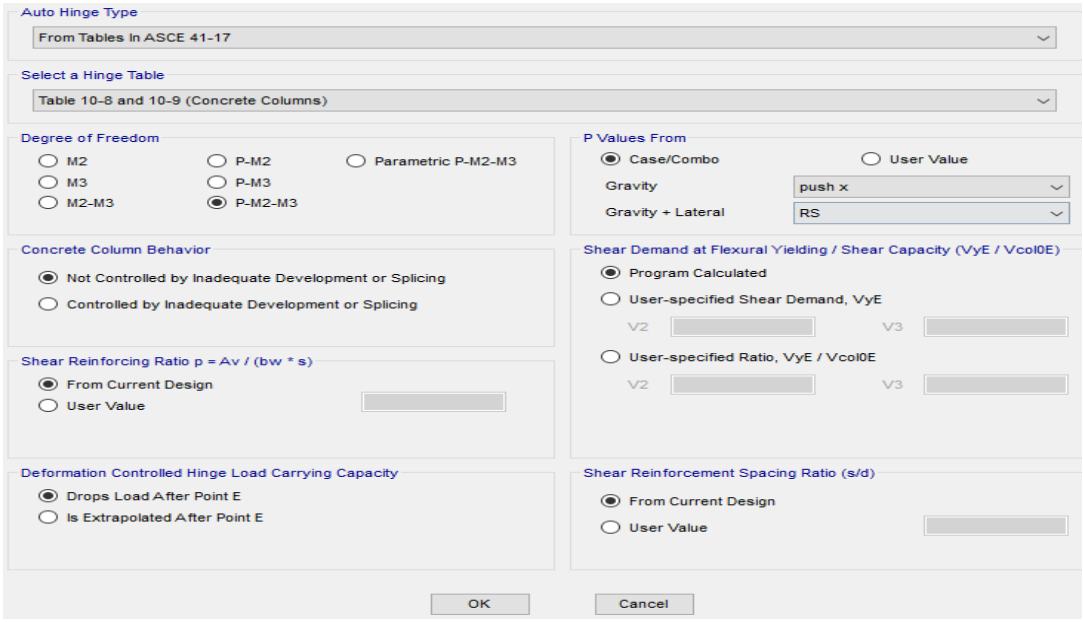

Figure3. 20 Hinge Properties for Columns

But for the equivalent strut user-defined hinges are provided for axial load and placed at mid-point of the strut.

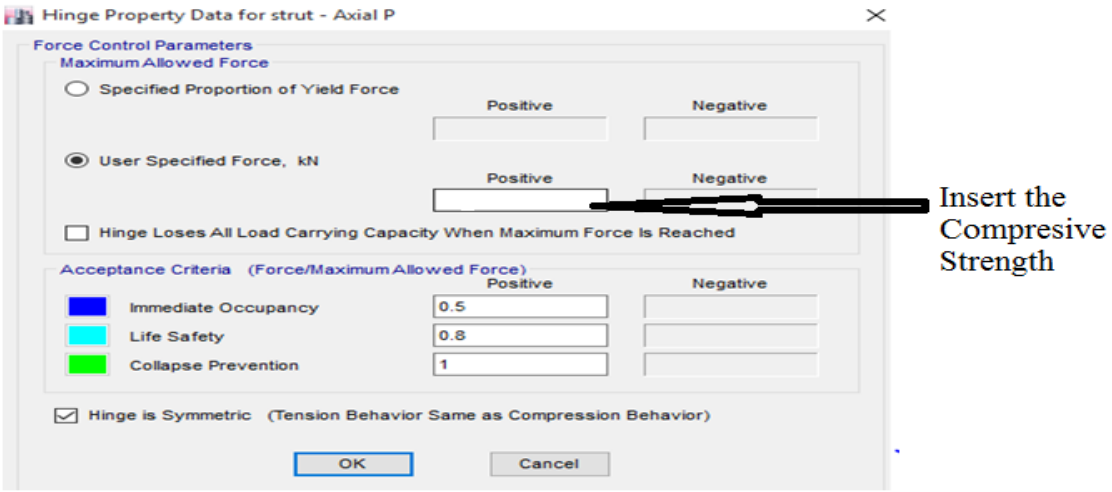

Figure3. 21 User-defined hinge properties for diagonal strut

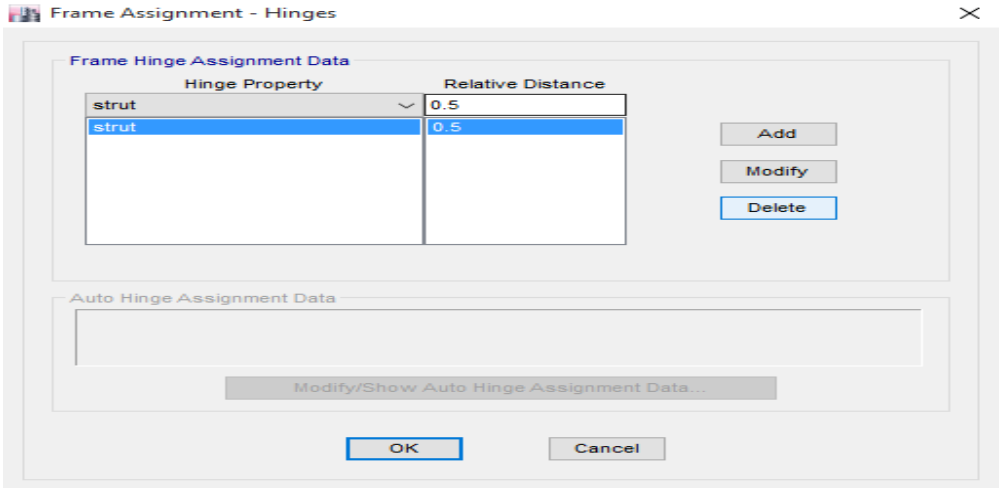

Figure3. 22 Hinge assignment for diagonal struts

iv. **Analysis of the Structure**

In this research, the analysis of the structures was performed by inserting the above data required and procedure. The structures that are designed with ductility class medium were analyzed and extract different parameters for the performance comparison of the structure.

- Go to Analyze>Set load case to run>don't run earthquake, modal load cases> Run now(only Gravity X, push X)

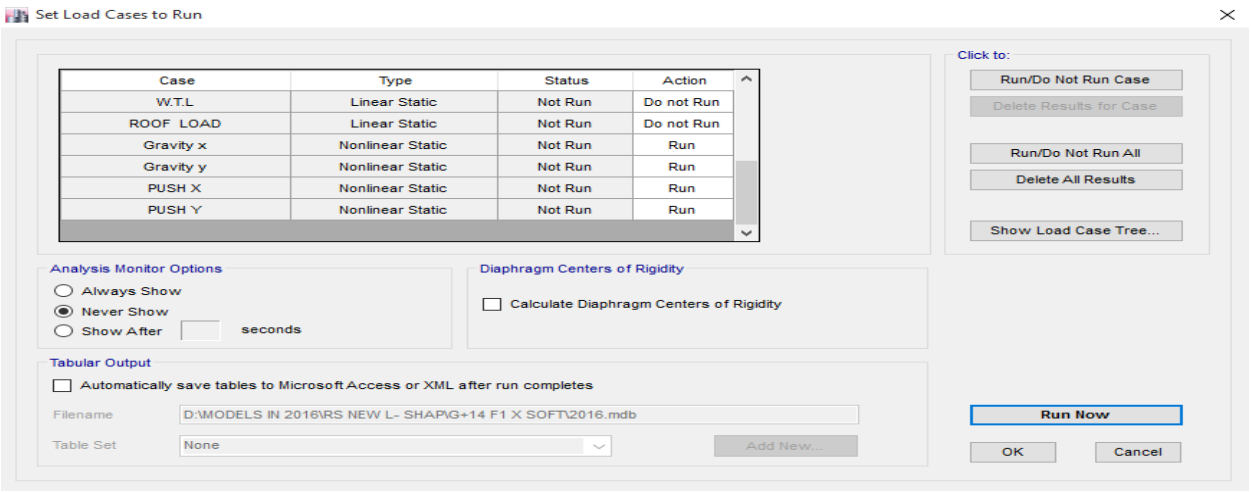

Figure3. 23 Set Load Case to Run the Analysis

3.7.1.6 Analysis Results

ETABS gives many results from the pushover analysis of structures. The following are some of the outputs determined in this study.

- The plot of Base shears Vs. Monitored Displacement (roof displacement).
- Tabulate the value of Base Reaction versus Monitored Displacement, number and properties of hinges at each iteration steps.
- According to EC8 2004 target displacement and by encoding the value of earthquake parameters ETABS draw the Capacity spectra {Base Reaction Vs. Monitored Displacement} and demand spectra in the ADRS format where the vertical axis is spectral acceleration and the horizontal axis are spectral displacement. The demand spectra can be superimposed on this plot. The plot shows the intersection of the two graphs which is called performance point. From this point can determine the value of base shear and target displacement.

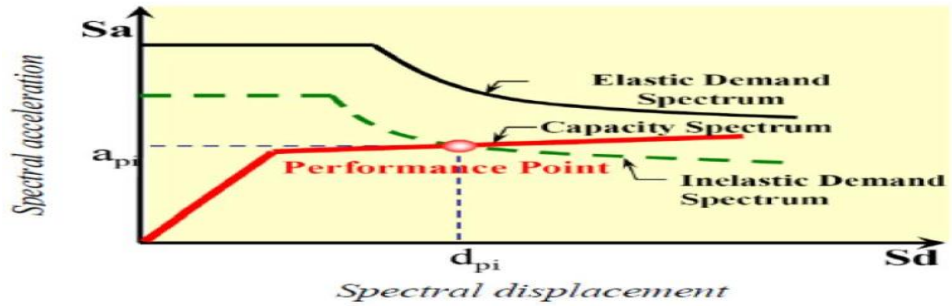

Figure3. 24 Graphical representation of capacity spectrum method

- The formation of the hinge and color-code state of each hinge is generated on the model of the building, which shows the performance level of the building. The color codes generated for each performance point are shown below.

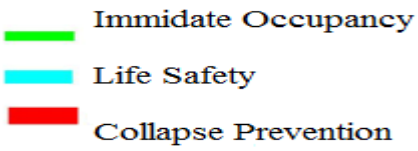

- Graphical and tabulated values of storey shear, storey displacement, storey drift for the applied pushover load.

3.8 Strengthening of Soft Storey

Strengthening strategy refers to options of increasing the strength, stiffness and ductility of the elements or the building as a whole. Several strengthening strategies may be selected under a retrofit scheme of a building. This are

1. Adding of Infill wall strengthening
2. shear wall strengthening
3. Steel bracing strengthening

In this study strengthening of the soft storey was done by providing X-steel bracing after determining the effect of soft storey location on seismic performance of RC buildings. X- steel bracing was provided at the top soft storey and ground soft storey building models. Then compression of this model had done within no soft storey building model for seismic performance using pushover analysis. The X- steel bracing used in this study has the same cross-sectional dimension for all models.

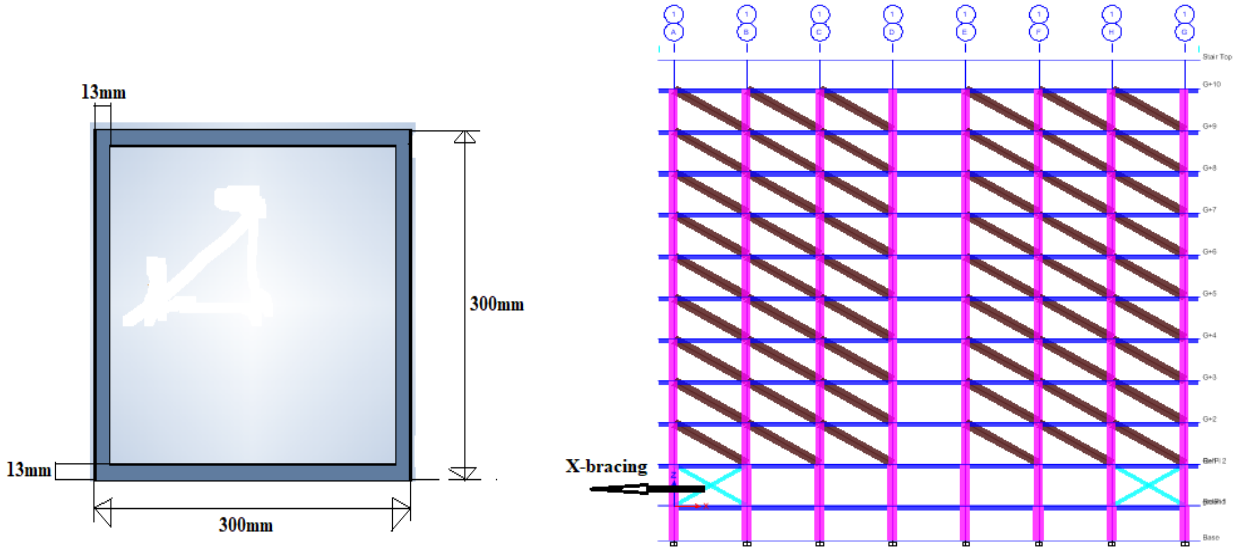

Figure3. 25 Cross-sectional dimension of X-steel bracing used and strengthening of soft storey

CHAPTER FOUR

RESULTS AND DISCUSSIONS

4.1 General

This chapter presents the results of pushover analysis of reinforced concrete frames with different locations of soft storey. Analysis of the models under the nonlinear static pushover load in the X-direction has been performed using ETABS 2017 software. All required data are provided in software and analyzed for total 16 models discussed above in section 3.6.1 and to get the result in terms of Base shear vs monitored (roof) displacement (pushover curve), target displacement and base shear capacity at performance point using EC8, Storey displacement, storey shear, storey drift and seismic performance assessment. Subsequently, these results are compared for reinforced concrete frames with soft storey at different locations.

4.2. Analysis Results for Pushover Load in X-Direction

In the present study, the non-linear response of reinforced concrete frames with different locations of soft /weak storey is modeled as per details discussed in Chapter 3 using nonlinear modeling under the loading has been carried out. Based on the results obtained from the Pushover loads in (X – Dir) by nonlinear static analysis using ETABS 2017, the effect of soft storey location on RC buildings are compared and described briefly in the next part. Thus 16 building models with different location of the soft storey which was modeled by removing the in-plane wall in the X direction is used for the analysis as discussed above.

4.2.1 Base Shear vs Monitored Roof Displacement Curve

All 16 building models with soft storey at a different location as described in chapter 3 are analyzed by pushover method in ETABS 2017 standard structural software and the static pushover curve is generated as shown in Figure 4.1 -4.4

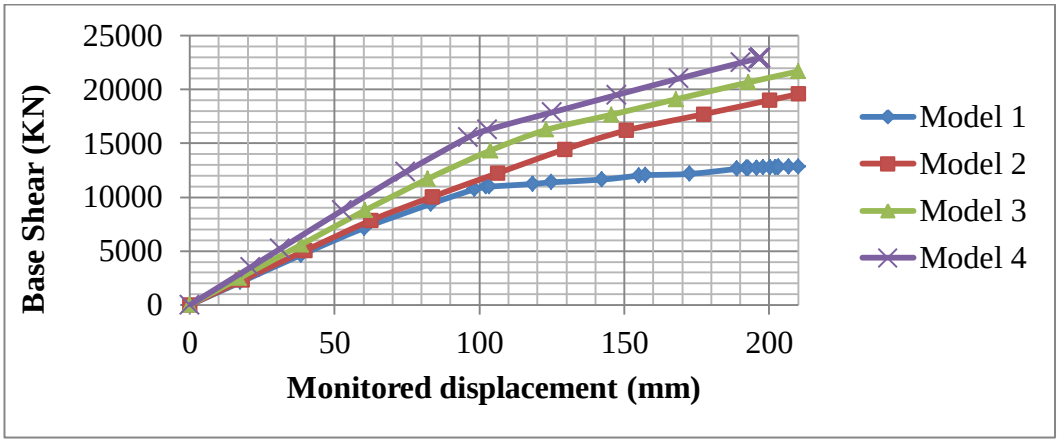

Figure4. 1 pushover Curves for G+7 plan regular building for Push X –load

Figure 4.1 and table in appendix C1.1 show the roof (monitored) displacement Vs base shear (pushover curve) of building with the soft storey at a different location for G+7 regular plan building models for iteratively applied pushover load in X-direction. From those graphs and appendix table, the flowing conclusions are draw.

The graph shows that the location of the soft storey changes from bottom to top the base shear resistance of the building increases. By considering the model of the soft storey at ground floor as control group the base shears resistance increases by 8.7%, 18% and 35% for model 2, model 3 and model 4 soft storey buildings respectively.

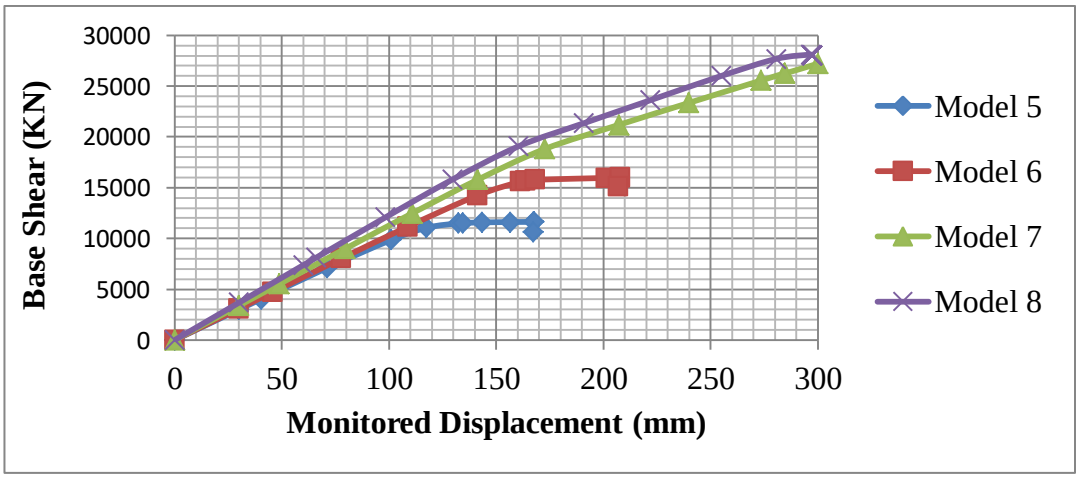

Figure4.2 Pushover Curves for G+10 plan regular building for Push X – load

Figure 4.2 and table in appendix C1.2 show the roof (monitored) displacement Vs base shear (pushover curve) of building with soft storey at different location for G+10 regular plan building models. From those graphs and appendix table, the flowing conclusion is draw.

The graph shows that the location of soft storey changes from bottom to top the base shear resistance of the building increases. By considering the model of the soft storey at ground floor as control group the base shear resistances increase by 3%, 13% and 23% for model 6, model 7 and model 8 soft storey buildings respectively.

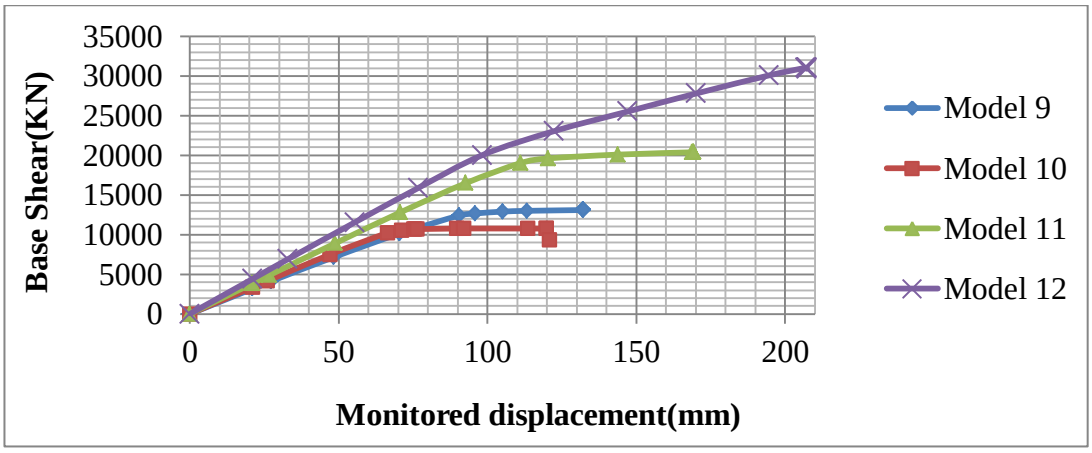

Figure4. 3 Pushover Curves for G+7 plan irregular building for Push X – load

Figure 4.3 and table in appendix C1.3 show the roof (monitored) displacement Vs base shear (pushover curve) of building with the soft storey at a different location for G+7 irregular plan building models. From those graphs and appendix table, the flowing conclusion is draw.

The graph shows that the location of the soft storey changes from bottom to top the base shear resistance of the building increases. By considering the model of soft storey at ground floor as control group the base shears resistance increase by 6%, 24% and 39% for model 10, model 11 and model 12 soft storey buildings respectively.

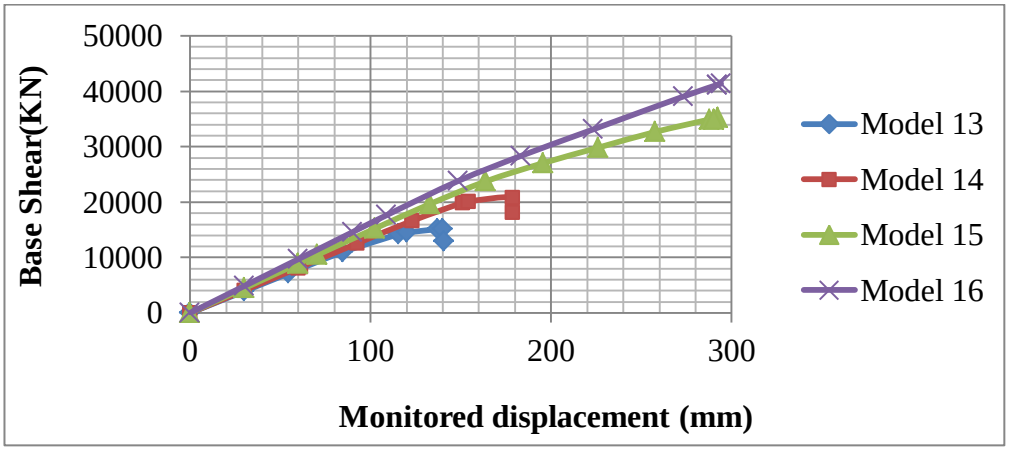

Figure4. 4 Pushover Curves for G+10 plan irregular building for Push X– load

Figure 4.4 and table in appendix C1.4 show the roof (monitored) displacement Vs base shear (pushover curve) of building with soft storey at different locations for G+10 irregular plan building models. From those graphs and appendix table, the flowing conclusions are draw.

The graph shows that the location of soft storey changes from bottom to top the base shear resistance of the building increases. By considering the model of soft storey at ground floor as control group the base shears resistance increase by 4%, 14% and 24% for model 14, model 15 and model 16 soft storey buildings respectively.

Generally from figure 4.1 - 4.4 and table in appendix C results of pushover curve the base shear resistance of the building increase when the location of soft storey changes from bottom to higher level. The base shear resistance of buildings with soft storey at the top has maximum value than others and increases by (23-39) % depending on the soft storey stiffness ratios considered. And also the graph shows that ground soft storey building yields first than the above location soft storey buildings. Therefore buildings with soft storey at the top floor level have a better base shear capacity.

4.2.2 Storey Displacement for All Models

After analyzing all models in ETABS 2017, the storey response results obtained in terms of storey displacement. Then the result is compared for different location of soft storey for all models and the conclusion is drawn. Results from static pushover analysis for all models are shown in Figure. 4.5 -4.8 and ETABS output list in Appendix Table C1.5-C1.6

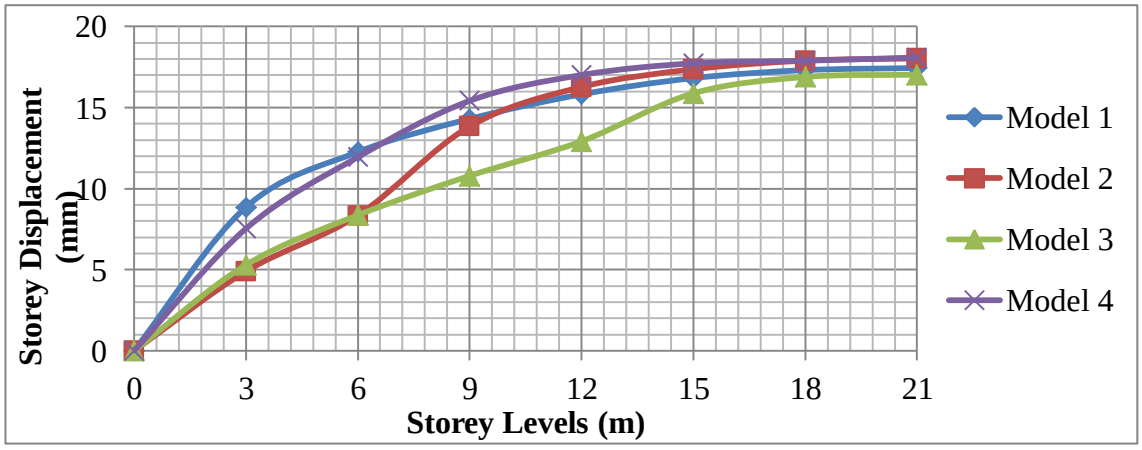

Figure4.5 Comparison of storey displacements in (G+7) plan regular building for push X– load

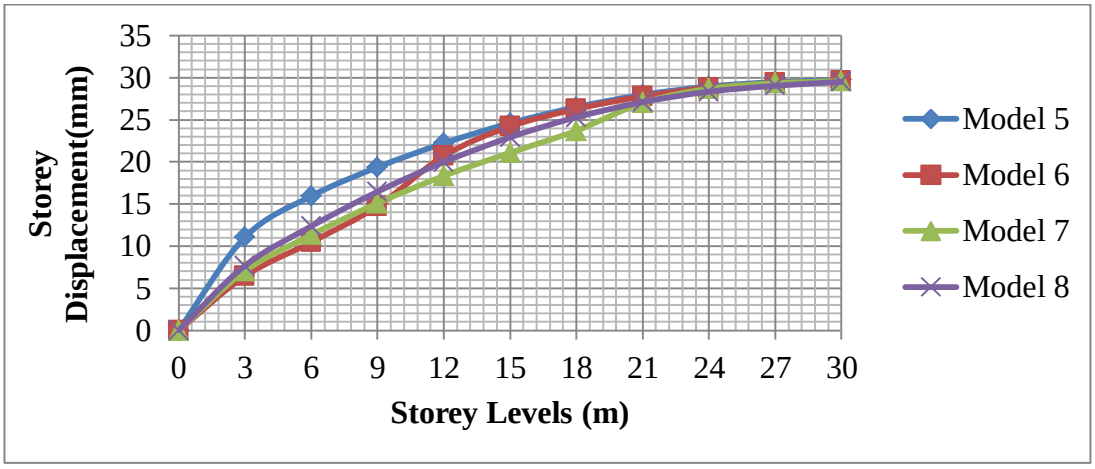

Figure4.6 Comparison of storey displacements in (G+10) plan regular building for push X – load

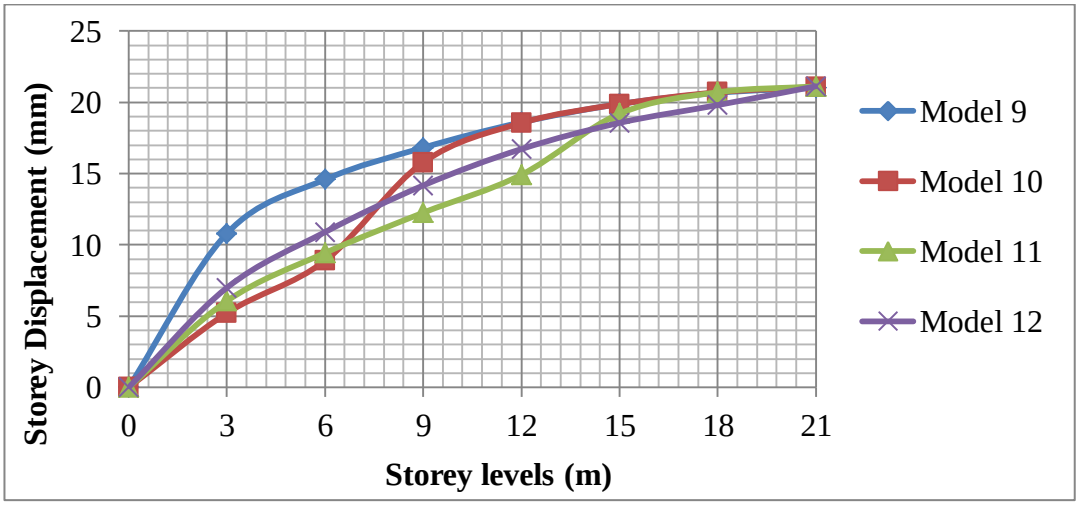

Figure4. 7 Comparison of storey displacements for (G+7) plan irregular building for push X– load

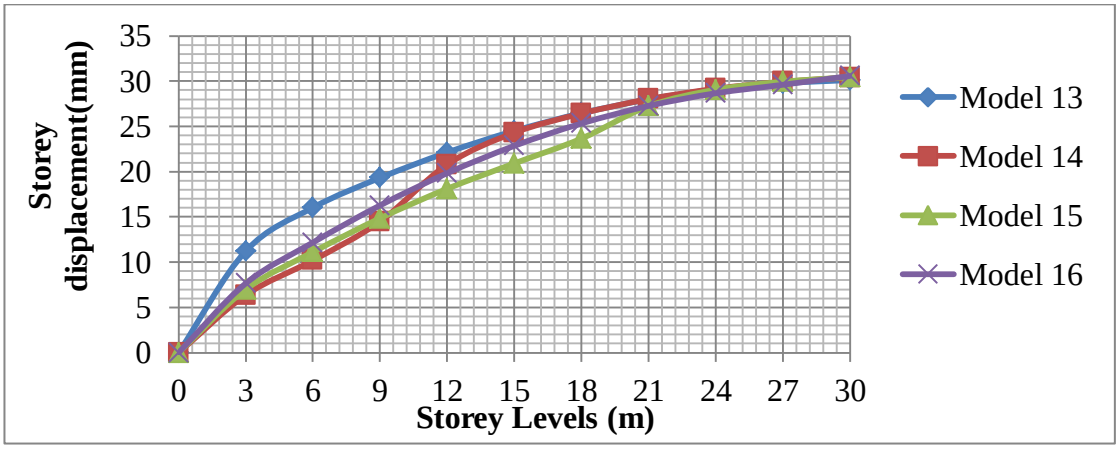

Figure 4.8 Comparison of storey displacements for (G+10) plan irregular building for push **X-** load

Figure 4.5-5.8 shows the comparative study of seismic demand in terms of storey displacement of all models with soft storey at different locations.

From the above graphs and tables in appendix (C1.5) the roof displacement of the building is the maximum displacement for the excited earthquake. The displacements of the roof for soft storey located at a different location is converged at one point as shown in the above graphs and almost have equal value of roof displacement for buildings soft storey at different locations subjected to pushover load in the X-direction.

Therefore the location of the soft storey has no impact on the maximum (roof) displacement of the building for pushover load.

4.2.3 Storey Shear

The lateral load distributed on the storey for different location of soft storey is shown figure 4.9-4.12.and in appendix table C1.7-C1.10

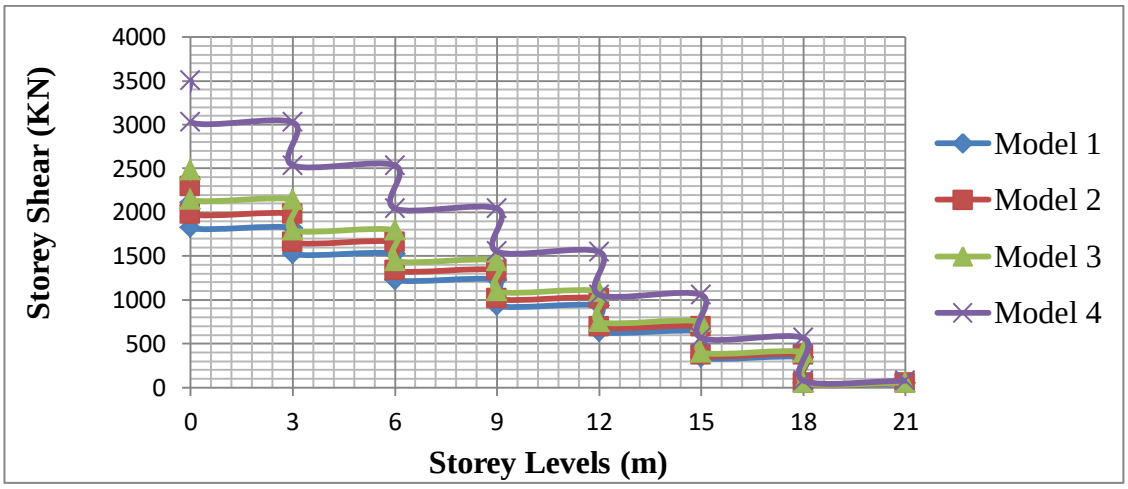

Figure4.9 Comparison of storey shear for (G+7) regular plan building for push X –load

Figure 4.9 and table in appendix C1.7 show the storey shear resistance of buildings with soft storey at different locations for (G+7) regular plan building models. From those graphs and appendix table results, the flowing conclusions are draw.

The graph shows that the location of soft storey changes from bottom to higher levels the storey shear resistance of the building increases. By considering the model of soft storey at ground floor as control group storey shear resistance increase by the average value of 8.8%, 18% and 68% for model 2, model 3 and model 4 soft storey buildings respectively.

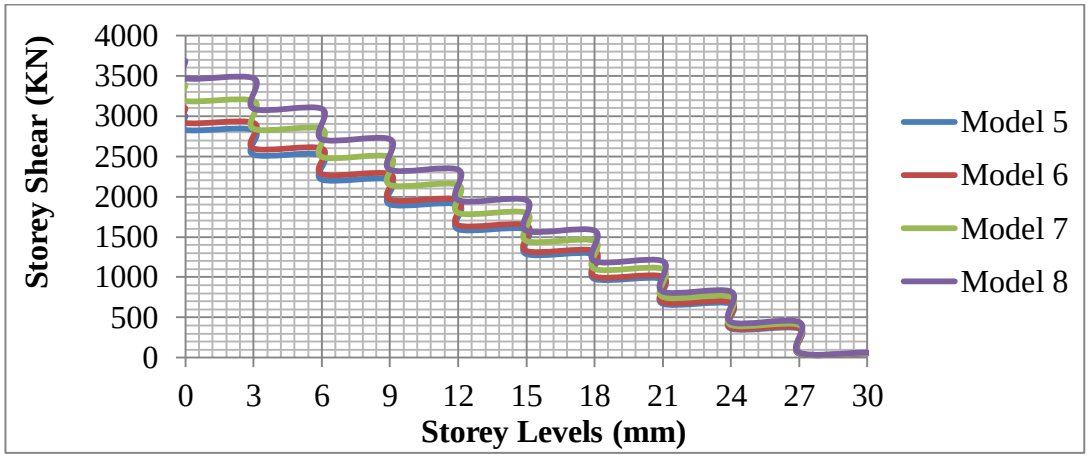

Figure4. 10 Comparison of storey shear for (G+10) regular plan building for push X –load

Figure 4.10 and table in appendix C1.8 show the storey shear resistance of buildings with soft storey at different locations for (G+10) regular plan building models. From those graphs and appendix table results, the flowing conclusions are draw.

The graph shows that the location of soft storey changes from bottom to higher levels the storey shear resistance of the building increases. By considering the model of soft storey at ground floor as the control group the storey shear resistances increase by the average value of 4%, 13% and 23% for model 6, model 7 and model 8 soft storey buildings respectively.

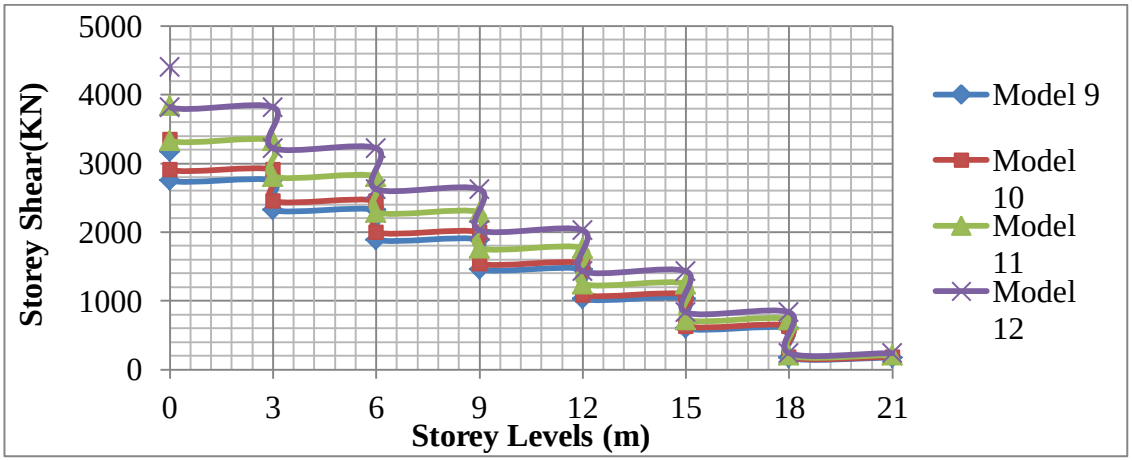

Figure4. 11 Comparison of storey shear for (G+7) irregular plan building for push **X** –load

Figure 4.11 and table in appendix C1.9 show the storey shear resistance of buildings with soft storey at different locations for (G+7) irregular plan building models. From those graphs and appendix table results, the flowing conclusions are draw.

The graph shows that the location of soft storey changes from bottom to higher levels the storey shear resistance of the building increases. By considering the model of soft storey at ground floor as control group the storey shear resistance increase by the average value of 5.8%, 21% and 39% for model 10, model 11 and model 12 soft storey buildings respectively.

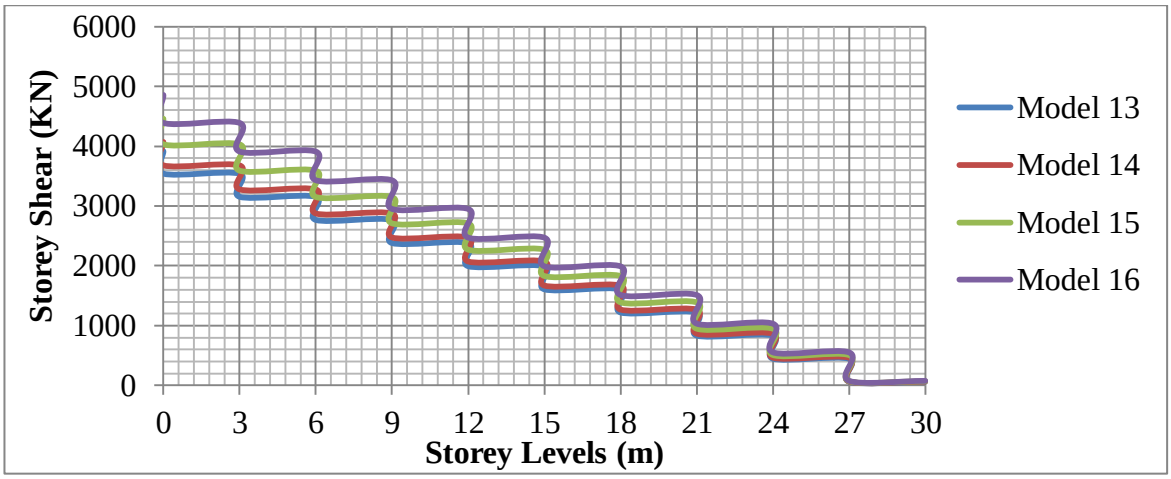

Figure4. 12 Comparison of storey shear for (G+10) irregular plan building for push X –load

Figure 4.12 and table in appendix C1.10 show the storey shear resistance of buildings with the soft storey at different locations for (G+10) irregular plan building models. From those graphs and appendix table results, the flowing conclusions are draw.

The graph shows that the location of the soft storey changes from bottom to higher levels the storey shear resistance of the building increases. By considering the model of soft storey at ground floor as control group the storey shears resistance increase by an average value of 4%, 14% and 24% for model 14, model 15 and model 16 soft storey buildings respectively.

Generally from figure 4.9 - 4.12 and table in appendix C results the storey shear capacity of the building increase when the location of the soft storey changes from bottom to higher level. The storey shear resistance of buildings with soft storey at the top has maximum value than others and increases by (23-68) % depending on soft storey stiffness ratio values considered. Therefore providing soft storey at the top level is better in terms of storey shear capacity.

4.2.4 Storey Drift

The relative displacement ratio of each storey determined in ETABS 2017 using pushover analysis for modal lateral load pattern in the X- direction for different soft storey location.

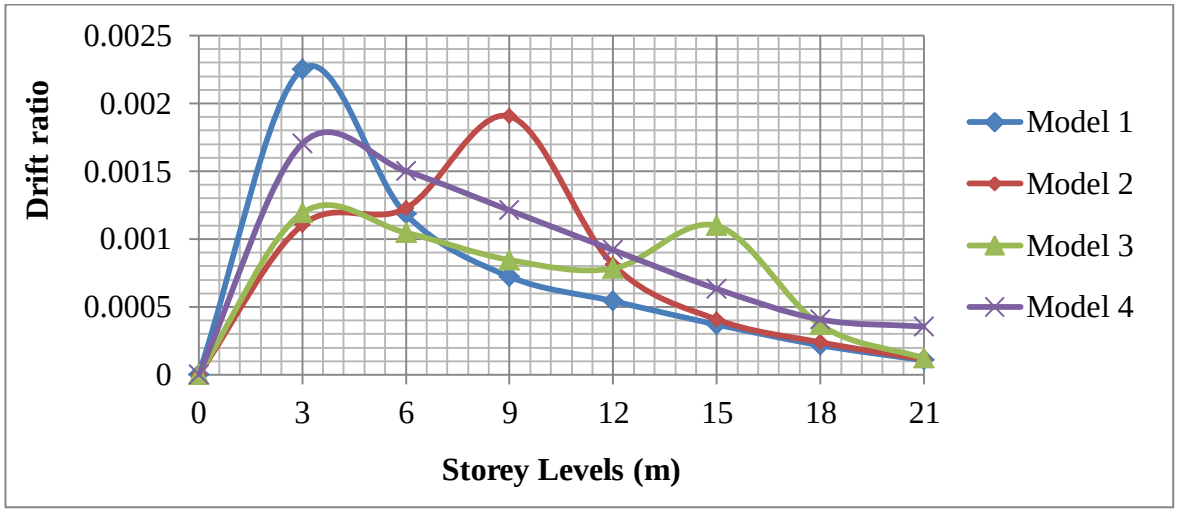

Figure4. 8 Comparison of drift ratio for (G+7) regular plan building for push X–load

Figure 4.13 and table in appendix C1.11 show the storey drift ratio of buildings with soft storey at different locations for (G+7) regular plan building models. From those graphs and appendix table results, the flowing conclusions are draw.

The graph shows that the location of soft storey changes from bottom to higher levels the maximum drift ratio of the building decreases. By considering the model of soft storey at ground floor as control group the maximum drift ratio decrease by average value of 15.5%, 51% and 24% for model 2, model 3 and model 4 soft storey buildings respectively. Therefore to minimize the maximum drift ratio it is better to provide soft storey near the top level.

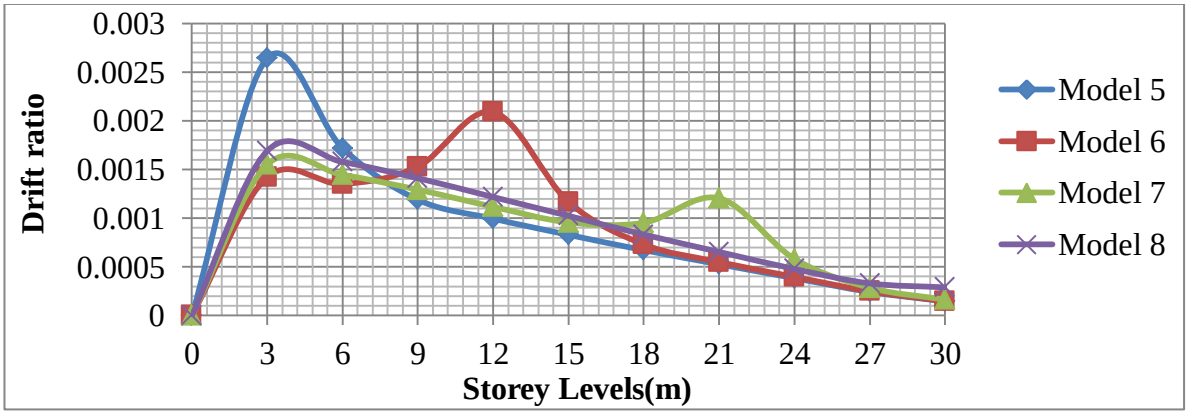

Figure4. 9 Comparison of drift ratio for (G+10) regular plan building for push X –load

Figure 4.14 and table in appendix C1.11 show the storey drift ratio of buildings with the soft storey at different locations for (G+10) regular plan building models. From those graphs and appendix table results, the flowing conclusions are draw.

The graph shows that the location of soft storey changes from bottom to higher levels the maximum drift ratio of the building decreases. By considering the model of soft storey at ground floor as control group the maximum drift ratio decrease by average value of 21%, 43% and 39% for model 6, model 7 and model 8 soft storey buildings respectively. Therefore to minimize the maximum drift ratio it is better to provide soft storey near the top level.

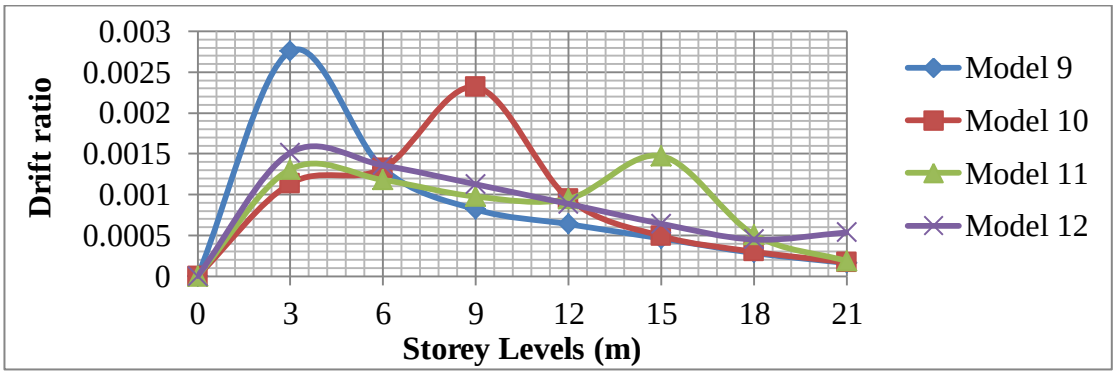

Figure4.10 Comparison of drift ratio for (G+7) irregular plan building for push X –load

Figure 4.15 and table in appendix C1.12 show the storey drift ratio of buildings with soft storey at different locations for (G+7) irregular plan building models. From those graphs and appendix table results, the flowing conclusions are draw.

The graph shows that the location of soft storey changes from bottom to higher levels the maximum drift ratio of the building decreases. By considering the model of the soft story at the ground floor as control group the maximum drift ratio decrease by average value of 15%, 48% and 44% for model 10, model 11 and model 12 soft storey buildings respectively. Therefore to minimize the maximum drift ratio it is better to provide soft storey near the top level.

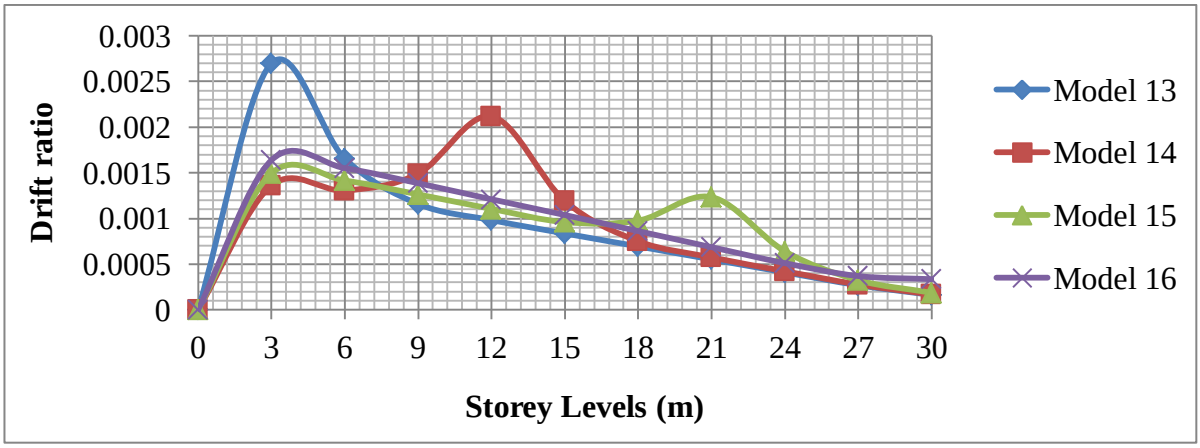

Figure4. 11 Comparison of drift ratio for (G+10) irregular plan building for push X –load

Figure 4.16 and table in appendix C1.12 show the storey drift ratio of buildings with soft storey at different locations for (G+10) irregular plan building models. From those graphs and appendix table results, the following conclusions are draw.

The graph shows that the location of soft storey changes from bottom to higher levels the maximum drift ratio of the building decreases. By considering the model of soft storey at ground floor as control group the maximum drift ratio decrease by average value of 19%, 46% and 38% for model 14, model 15 and model 16 soft storey buildings respectively. Therefore to minimize the maximum drift ratio it is better to provide soft storey near the top.

Generally from figure 4.13 - 4.16 and table in appendix C results the maximum drift ratio of the building decrease when the location of soft storey changes from bottom to a higher level. The maximum drift ratio of buildings with soft storey near the top has minimum value than others and decreases by (43-51) % based on the value of soft storey stiffness ratios considered. Then to minimize the maximum drift ratio it is better to provide soft storey near the top level.

4.2.5 Target Displacement and Base Shear at Performance Point

The target displacement of models in pushover analysis can be determined from the graph of spectral acceleration Vs spectral displacement. The intersection point of capacity curve and demand curve is called performance point which gives the value of target displacement and base shear for the inserted earthquake data. Using EC8 target displacement determination in pushover analysis and ETABS 2016 software the target displacement and base shear are determined at performance point. Then a comparison is drawn from this result at different locations of soft storey. Results from static pushover analysis for all models in table 4.1 and the comparison determined using the chart. The detail output of ETABS2016 and inserted data are listed in appendix D.

Table4. 1 Target displacement and base shear at performance point for regular plan buildings

G+7			**G+10**		
Soft storey location	Base shear (KN)	Target displacement(mm)	Soft storey location	Base shear (KN)	Target displacement(mm)
Ground floor	2001.91	16.50	Ground floor	2245.55	22.42
G+3	1513.56	11.91	G+4	1978.78	19.16
G+5	1648.52	11.32	G+7	2141.11	18.96
G+7	1746.26	10.45	G+10	2217.39	18.05

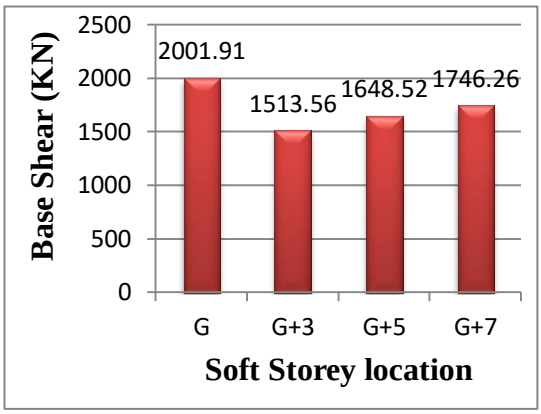

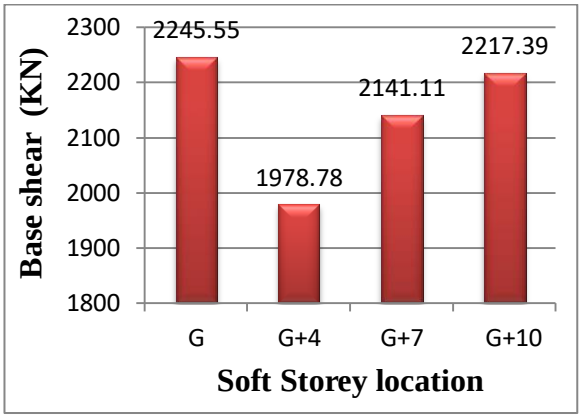

G+7 building G+10 building

Figure4. 12 Base shear at performance point for plan regular building models

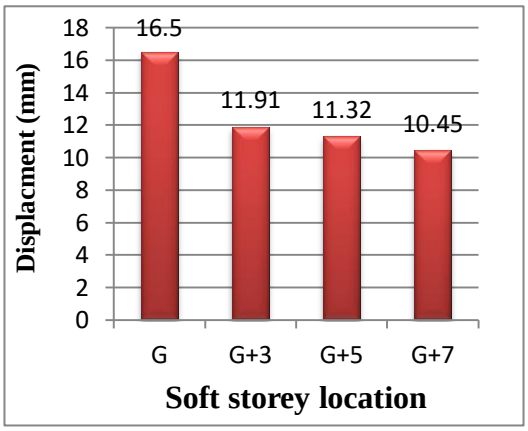

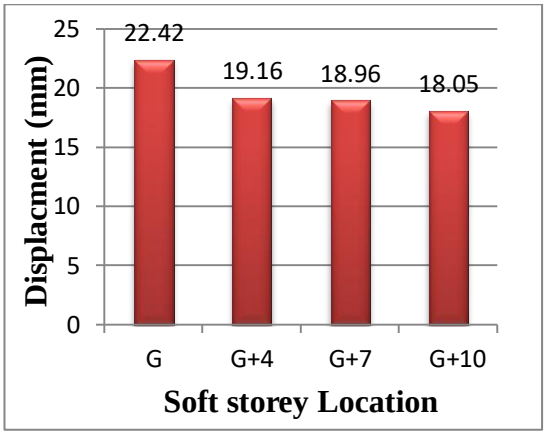

G+7 building G+10 building

Figure4. 13 target displacement at performance point for plan regular building

Table4. 2 Target displacement and base shear at performance point for irregular plan models

G+7			G+10		
Soft storey location	Base shear (KN)	Target displacement(mm)	Soft storey location	Base shear (KN)	Target displacement(mm)
Ground floor	2681.07	17.76	Ground floor	3088.78	23.65
G+3	2082.32	13.05	G+4	2713.48	19.99
G+5	2264.12	12.38	G+7	2909.95	19.57
G+7	2420	11.55	G+10	3015.29	18.62

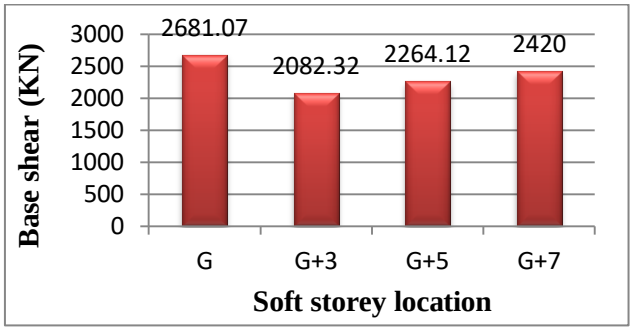

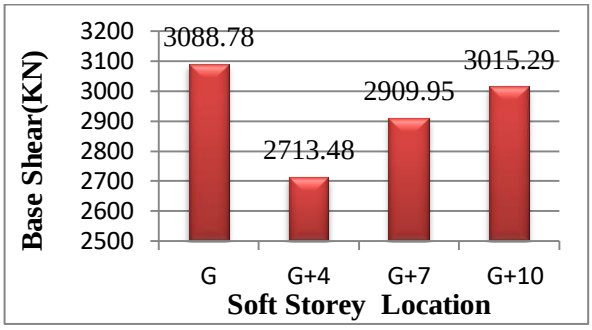

G+7 building G+10 building

Figure4. 19 Base shears at performance point for plan irregular building models

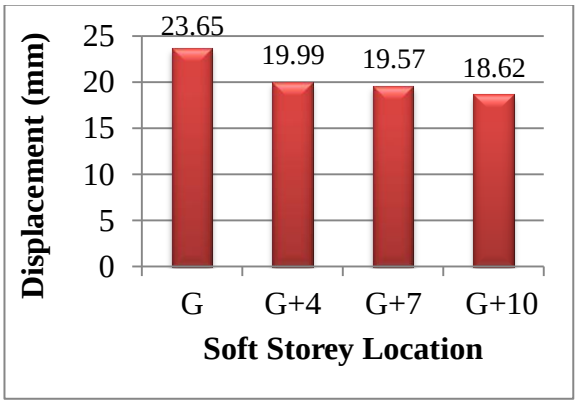

G+7 building G+10 building

Figure4. 20 target displacements at performance point for plan irregular building models

Figure 4.17, 4.20 and table4.1, 4.2 shows that the base shear value at performance point is relatively maximum for top soft storey building. Buildings with the soft storey at the ground floor have maximum base shear. Also, buildings with the soft storey at the top have maximum base shear at performance point than other location but not buildings soft storey at the ground. By considering the ground soft storey building as control group the following percentage decrements calculated for each model.

For G+ 7 regular building model the base shear decrease by 24%, 17%% and 12.7% for model 2, model 3 and model 4 respectively.

For G+ 10 regular building model the base shear decrease by 11 %, 4% and 1% for model 6, model 7 and model 8 respectively.

For G+ 7 irregular building model the base shear decrease by 22%, 15.5% and 9.7% for model 10, model 11 and model 12 respectively.

For G+ 10 irregular building model the base shear decrease by 12%, 6%and 2.4 % for model 14, model 15 and model 16 respectively.

But figure 4.18,4.20 and table 4.1,4.2 value of target displacement show that, the target displacement value decrease when soft storey location changed from bottom level to a higher level. By considering the ground soft storey building as control the following percentage decrement calculated for each model.

For G+ 7 regular building models the target displacement decrease by 27%, 31% and 36% for model 2, model 3 and model 4 respectively.

For G+ 10 regular building models the target displacement decrease by 14%, 15% and 20% for model 6, model 7 and model 8 respectively.

For G+ 7 irregular building model the target displacement decrease by 26%, 30% and 34 % for model 10, model 11 and model 12 respectively.

For G+ 10 irregular building model the target displacement decrease by 15.5%, 17.25% and 21.26% for model 14, model 15 and model 16 respectively.

The above numerical values show that buildings with the soft storey at the different location have different percentage decrement of target displacement and increment of base shear at performance point based on the soft storey stiffness ratios used. But from those values can be concluded that building soft storey at top level has less target displacement and decrease by (17-36) % than bottom soft storey building depending on the stiffness ratios considered for soft storey. And soft storey building at the top level has a maximum base shear capacity at performance point than other locations except ground soft storey building. Therefore providing soft storey at the top level has less target displacement than bottom soft storey building and maximum base sheer value for the exciting earthquake relatively.

4.2.6 Seismic Performance Assessment

The procedure for assessing seismic performance applies the methodology for performance-based earthquake engineering based on ASCE with EC8 document which presents performance-based engineering methods that rely on nonlinear static analysis procedures for prediction of

performance level. Lateral loads were applied according to the equivalent lateral force distribution specified by EC8.

Deflected shapes display the pushover deformed shape on step-by-step basis to view the pushover displacement shape and sequence of hinge formation (hinges appear when they yield and color-coded based on their state). The color of the hinges indicates the state of the hinge, i.e., where it is along its force-displacement curve. The state of the hinge is taken at the final step of pushover analysis for all models at different location of soft storey and the state of the hinge and deformed shape is shown in figure 4.21-4.24. A table also obtained which gives the coordinates of each step of the pushover curve and summarizes the number of hinges in each state (for example, between IO, LS, CP or between B and E). This data is shown in Table. 4.3 – 4.6

To determine the state of hinges developed and to evaluate the performance of the structures ETABS uses the following color Code with state of hinges.

Immidate Occupancy

Life Safety

Collapse Prevention

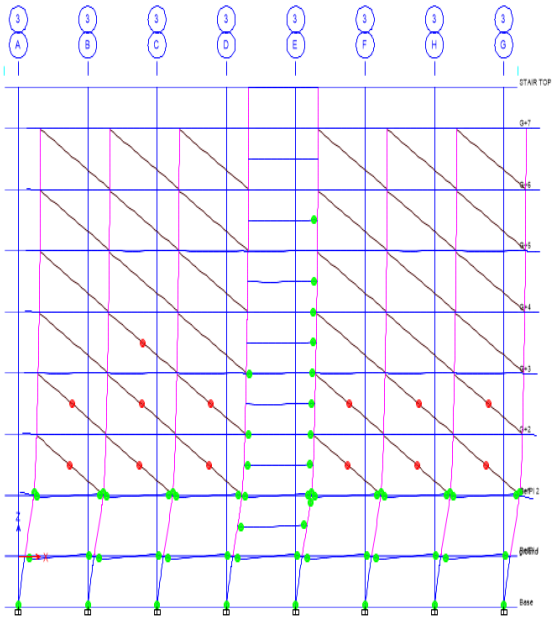

a. soft storey at ground storey

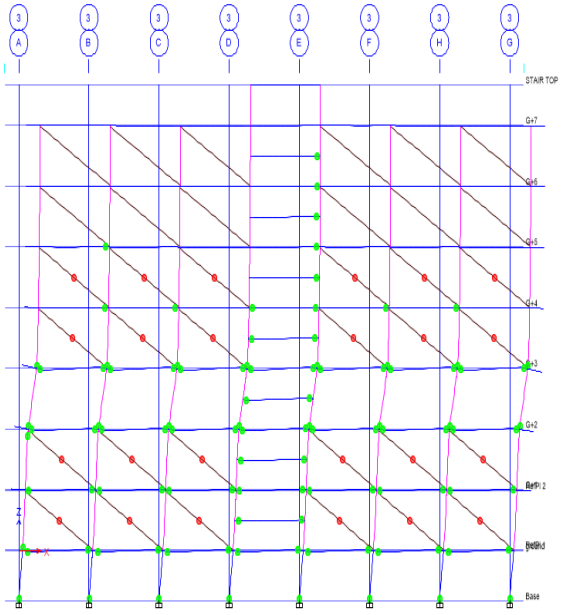

b. soft storey at 3rd storey

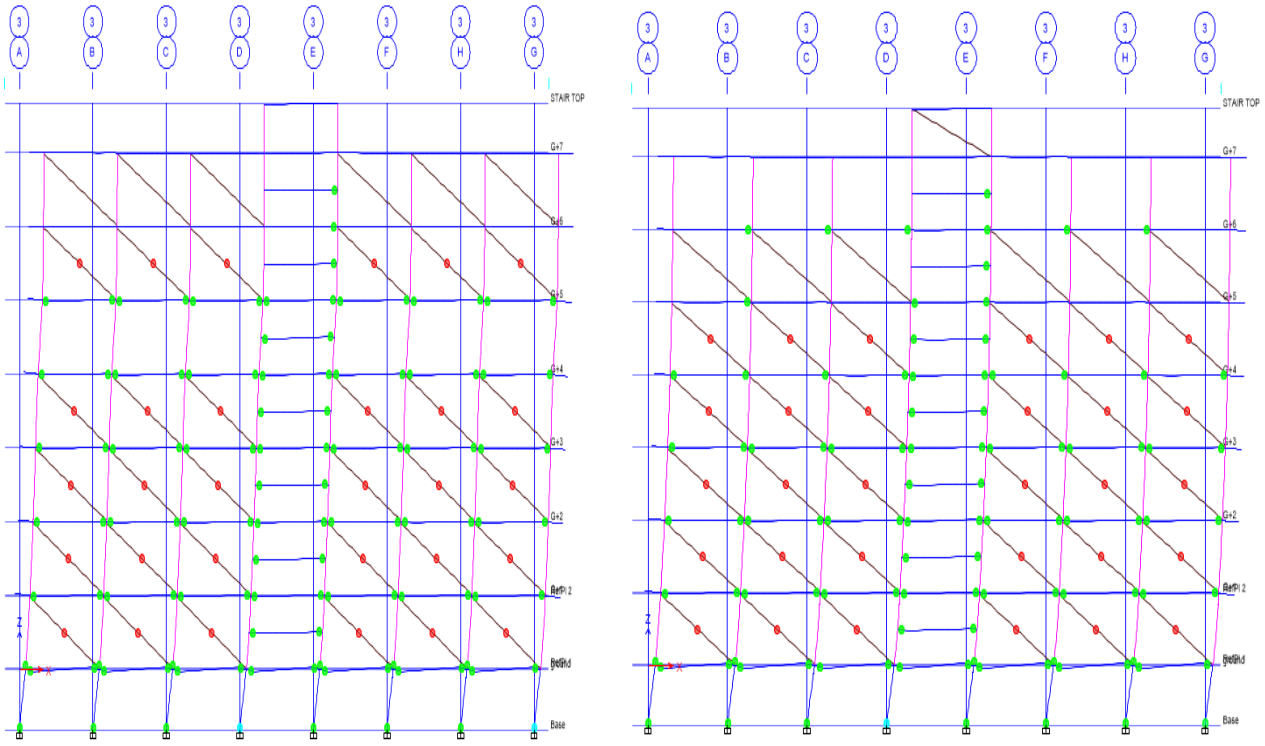

c. Soft storey at 5th storey

d. Soft storey at 7th storey

Figure4. 14 Typical failure modes observed for (G+7) plan regular building models

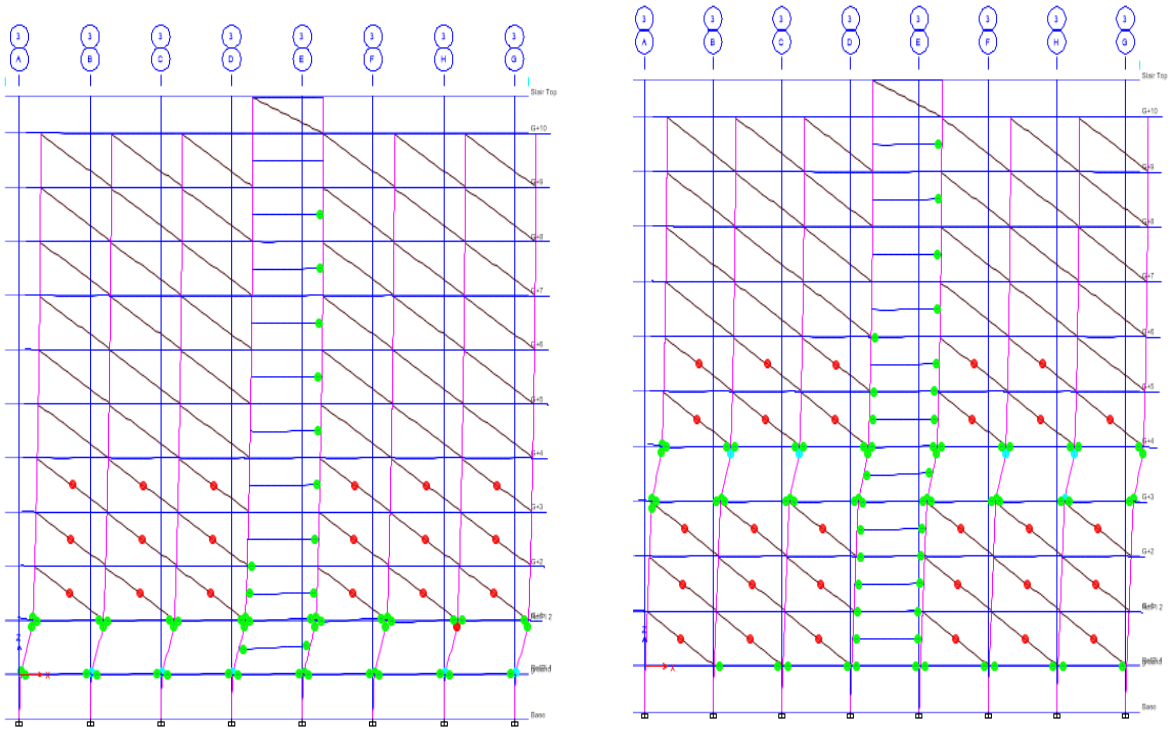

a. soft storey at ground storey

b. soft storey at 4th storey

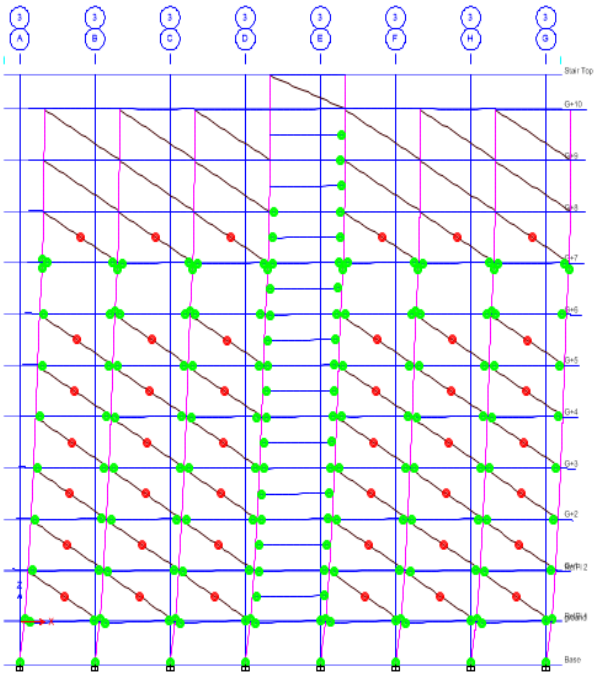

c. soft storey at 7th storey

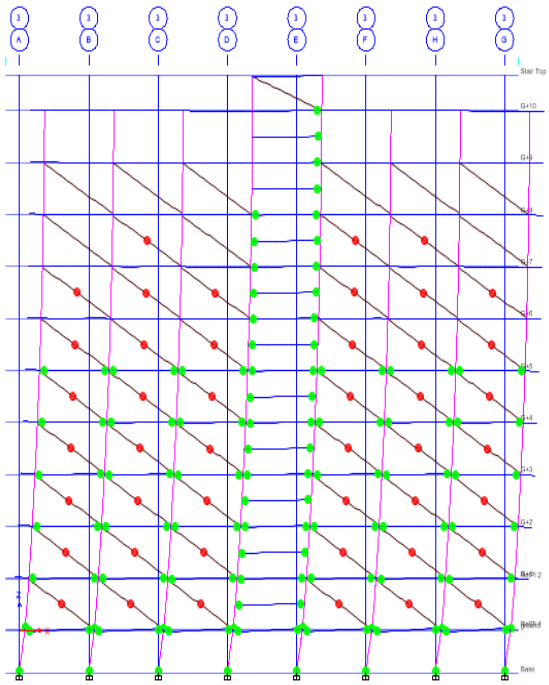

d. soft storey at 10th storey

Figure4. 15 Typical failure modes observed for (G+10) plan regular building models

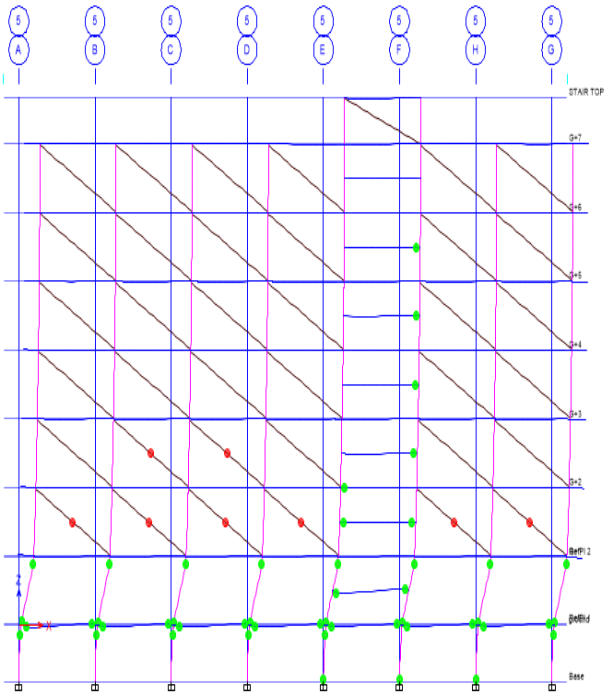

a. Soft storey at ground storey

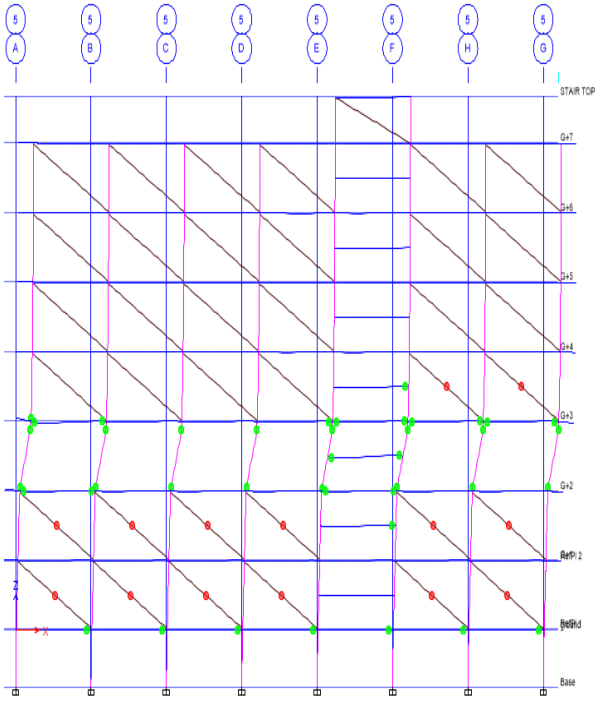

b. Soft storey at 3rd storey

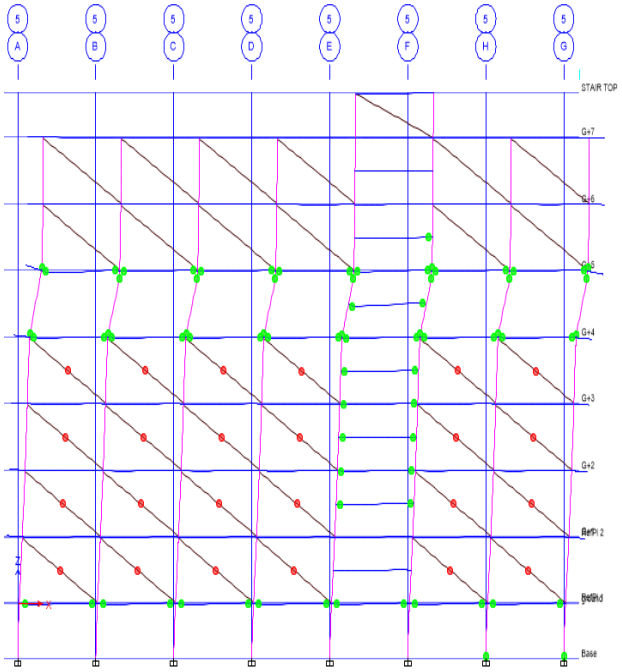

c. Soft storey at 5th storey

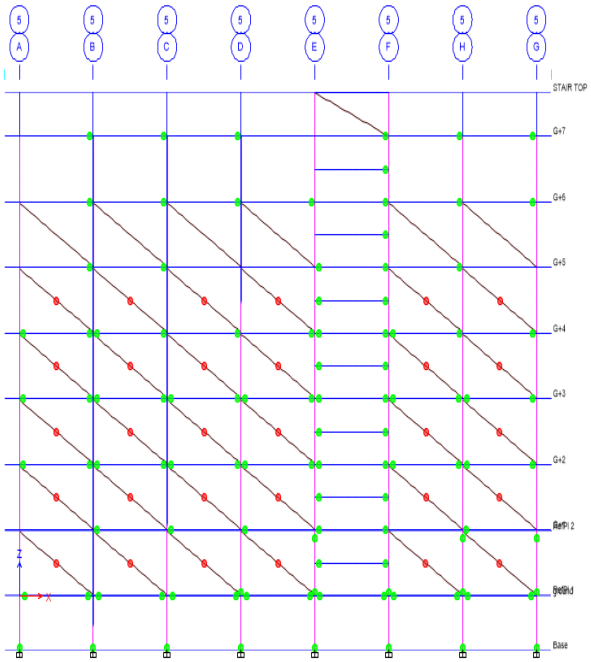

d. Soft storey at 7th storey

Figure4. 16 Typical failure modes observed for (G+7) plan irregular building models

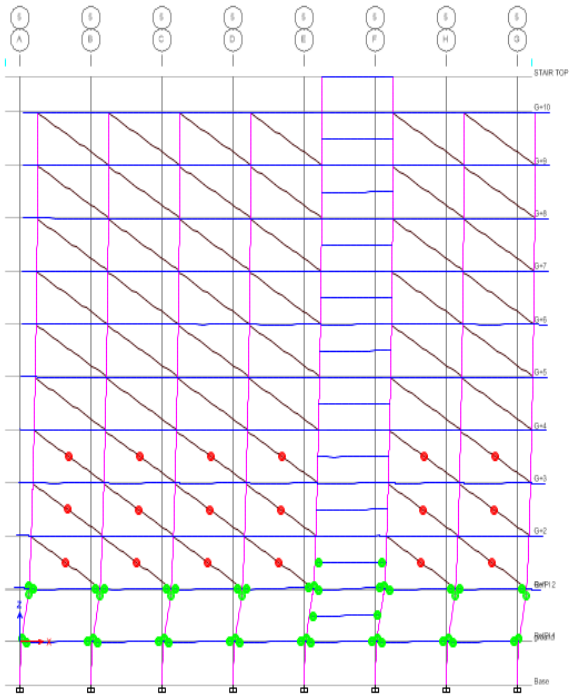

a. soft storey at ground storey

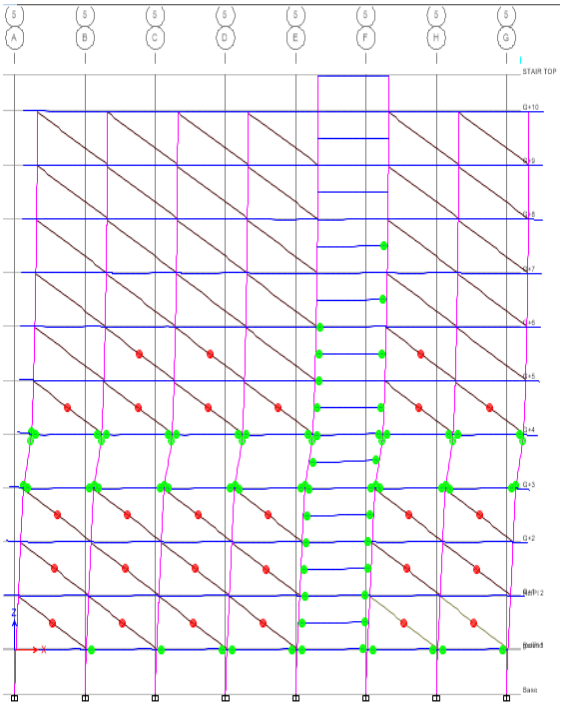

b. soft storey at 3rd storey

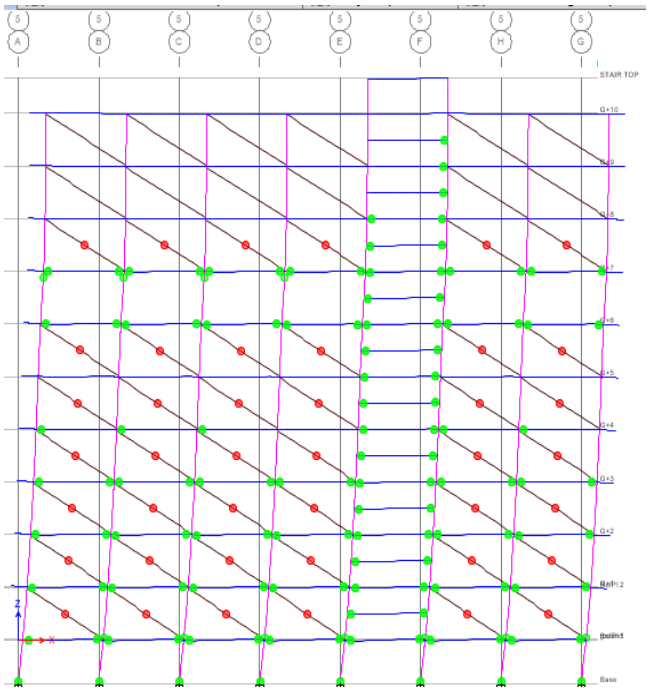

c. Soft storey at 7th storey

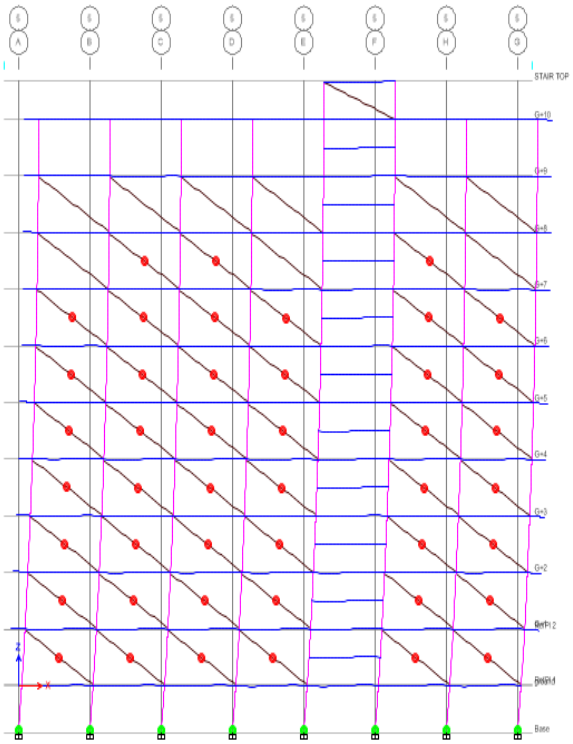

d. Soft storey at 10th storey

Figure4. 17 Typical failure modes observed for (G+10) plan irregular building models

Table4.3 Number of hinges in each state of soft storey location for (G+7) plan regular building.

Step	Displacement (mm)	Base Force(KN)	A-B	B-C	C-D	D-E	>E	A-IO	IO-LS	LS-CP	>CP	Total
0	0	0	2848	0	0	0	0	2848	0	0	0	2848
1	17.387	2108.7056	2846	2	0	0	0	2848	0	0	0	2848
2	38.428	4649.2883	2836	12	0	0	0	2824	18	6	0	2848
3	60.204	7150.395	2686	144	0	0	18	2794	34	2	18	2848
4	83.269	9389.5171	2634	190	0	0	24	2786	25	13	24	2848
5	98.399	10752.0492	2578	234	0	0	36	2776	21	15	36	2848
6	102.319	10962.2811	2566	246	0	0	36	2774	18	18	38	2848
7	103.41	10994.891	2562	250	0	0	36	2774	18	18	38	2848
8	118.455	11229.1029	2558	254	0	0	36	2766	18	18	46	2848
9	124.855	11389.5319	2554	258	0	0	36	2764	20	18	46	2848
10	142.204	11635.8211	2553	258	0	0	37	2764	20	17	47	2848
11	154.988	12014.2843	2544	266	0	0	38	2736	46	16	50	2848
12	157.176	12057.1802	2544	266	0	0	38	2710	72	16	50	2848
13	172.617	12169.852	2542	268	0	0	38	2640	142	16	50	2848
14	188.776	12625.369	2512	292	0	0	44	2638	144	10	56	2848
15	192.232	12683.358	2508	296	0	0	44	2634	148	10	56	2848
16	192.233	12683.3936	2508	296	0	0	44	2634	148	10	56	2848
17	192.235	12682.1174	2508	296	0	0	44	2634	148	10	56	2848
18	192.56	12690.098	2508	296	0	0	44	2634	148	10	56	2848
19	192.885	12694.1866	2508	296	0	0	44	2634	148	10	56	2848
20	195.757	12712.3598	2506	298	0	0	44	2634	146	12	56	2848
21	197.986	12744.1594	2500	304	0	0	44	2634	146	12	56	2848

22	200.452	12761.9922	2500	304	0	0	44	2630	146	16	56	2848
23	202.054	12787.1735	2498	306	0	0	44	2626	150	16	56	2848
24	202.933	12794.1756	2496	308	0	0	44	2622	150	18	58	2848
25	202.96	12796.5932	2496	308	0	0	44	2622	150	18	58	2848
26	203.225	12799.204	2496	308	0	0	44	2620	152	18	58	2848
27	206.825	12816.3781	2492	312	0	0	44	2604	160	26	58	2848
28	210	12847.7517	2484	320	0	0	44	2592	164	34	58	2848

a. Soft storey at ground floor**.**

Step	Displacement(mm)	Base Force(KN)	A-B	B-C	C-D	D-E	>E	A-IO	IO-LS	LS-CP	>CP	Total
0	0	0	2848	0	0	0	0	2848	0	0	0	2848
1	18.037	2291.865	2846	2	0	0	0	2848	0	0	0	2848
2	39.853	5057.6824	2834	14	0	0	0	2795	43	10	0	2848
3	62.474	7843.6761	2763	50	0	0	35	2794	1	18	35	2848
4	83.637	10038.061	2568	226	0	0	54	2779	15	0	54	2848
5	106.176	12228.832	2518	276	0	0	54	2776	18	0	54	2848
6	129.455	14447.291	2444	350	0	0	54	2776	14	4	54	2848
7	150.719	16202.633	2374	420	0	0	54	2768	7	15	58	2848
8	177.451	17709.059	2363	428	0	0	57	2757	9	15	67	2848
9	200.165	19009.053	2344	438	0	0	66	2735	21	6	86	2848
10	210	19567.779	2331	450	0	0	67	2711	43	5	89	2848

b. Soft storey at 3rd floor

Step	Displacement(mm)	Base Force(KN)	A-B	B-C	C-D	D-E	>E	A-IO	IO-LS	LS-CP	>CP	Total
0	0	0	2848	0	0	0	0	2848	0	0	0	2848
1	17.041	2481.7437	2846	2	0	0	0	2848	0	0	0	2848
2	38.366	5585.8183	2840	8	0	0	0	2781	57	10	0	2848
3	60.43	8770.9282	2772	40	0	0	36	2776	6	30	36	2848
4	82.073	11696.157	2562	214	0	0	72	2760	16	0	72	2848
5	103.745	14335.192	2408	368	0	0	72	2758	18	0	72	2848
6	123.021	16247.303	2314	462	0	0	72	2754	7	11	76	2848
7	145.669	17665.389	2260	516	0	0	72	2744	0	18	86	2848
8	167.821	19091.314	2213	556	0	0	79	2736	6	11	95	2848
9	192.844	20658.008	2182	576	0	0	90	2708	34	0	106	2848
10	210	21678.29	2172	586	0	0	90	2648	92	2	106	2848

c. Soft storey at 5th floor

Step	Displacement mm)	Base Force(KN)	A-B	B-C	C-D	D-E	>E	A-IO	IO-LS	LS-CP	>CP	Total
0	0	0	2848	0	0	0	0	2848	0	0	0	2848
1	21	3506.9274	2848	0	0	0	0	2837	11	0	0	2848
2	31.234	5217.2588	2846	2	0	0	0	2794	50	4	0	2848
3	52.482	8762.7066	2788	24	0	0	36	2775	19	18	36	2848
4	74.498	12337.959	2658	132	0	0	58	2758	18	14	58	2848
5	96.152	15573.654	2504	272	0	0	72	2753	10	13	72	2848
6	102.799	16261.929	2458	318	0	0	72	2746	10	16	76	2848
7	125.042	17875.731	2388	384	0	0	76	2727	13	14	94	2848
8	147.322	19487.974	2328	434	0	0	86	2704	32	4	108	2848
9	168.812	21015.22	2266	492	0	0	90	2680	56	0	112	2848
10	190.121	22478.093	2230	528	0	0	90	2608	117	11	112	2848
11	196.299	22883.496	2214	540	4	0	90	2608	112	14	114	2848
12	196.416	22875.389	2210	544	4	0	90	2608	112	12	116	2848
13	196.808	22905.444	2210	544	4	0	90	2608	112	12	116	2848
14	196.812	22905.445	2210	544	4	0	90	2608	112	12	116	2848
15	196.812	22905.447	2210	544	4	0	90	2608	112	12	116	2848

16	196.818	22905.962	2210	544	4	0	90	2608	112	12	116	2848
17	196.821	22905.818	2210	544	4	0	90	2608	112	12	116	2848
18	196.927	22914.539	2208	546	4	0	90	2608	112	12	116	2848
19	196.932	22914.431	2208	546	4	0	90	2608	112	12	116	2848
20	197.03	22921.332	2208	546	4	0	90	2608	112	12	116	2848
21	197.031	22921.16	2208	546	4	0	90	2608	112	12	116	2848

d. Soft storey at 7th floor

Figure 4.21 shows the state of hinges generated in color code and Table 4.3 shows the number of hinges generated in each state of performance levels .the number of hinges generated in collapse prevention state increase when the location of soft storey increase. Using ground soft storey building as a control group the number of hinges generated increased by 53 %, 83%, 100% for model 2, model 3 and model 4 respectively depending on the stiffness ratio used for soft storey.

Table4. 4 Number of hinges in each state of soft storey location for (G+10) plan regular building.

Step	Displacement mm)	Base Force(KN)	A-B	B-C	C-D	D-E	>E	A-IO	IO-LS	LS-CP	>CP	Total
0	0	0	3959	0	0	0	0	3959	0	0	0	3959
1	30	3004.7922	3959	0	0	0	0	3945	14	0	0	3959
2	40.252	4032.1788	3957	2	0	0	0	3936	23	0	0	3959
3	71.038	7102.8645	3909	32	0	0	18	3885	41	15	18	3959
4	101.051	9862.7363	3761	158	0	0	40	3862	32	25	40	3959
5	117.466	11055.134	3635	270	0	0	54	3851	36	18	54	3959
6	132.422	11500.8011	3607	296	0	0	56	3851	33	19	56	3959
7	134.358	11528.9747	3602	300	0	0	57	3837	47	18	57	3959
8	143.298	11580.832	3594	308	0	0	57	3803	81	18	57	3959
9	156.326	11618.7348	3584	318	0	0	57	3777	107	18	57	3959
10	167.531	11630.3479	3580	318	4	0	57	3755	85	62	57	3959
11	167.545	11630.9953	3580	318	4	0	57	3755	85	62	57	3959
12	167.2	10629.2108	3580	310	12	0	57	3755	85	50	69	3959

a. Soft storey at ground floor

Step	Displacement mm)	Base Force(KN)	A-B	B-C	C-D	D-E	>E	A-IO	IO-LS	LS-CP	>CP	Total
0	0	0	3959	0	0	0	0	3959	0	0	0	3959
1	30	3098.0238	3959	0	0	0	0	3959	0	0	0	3959
2	45.688	4719.4703	3957	2	0	0	0	3889	70	0	0	3959
3	77.799	8029.7039	3886	22	0	0	51	3869	18	21	51	3959
4	108.596	11153.833	3837	50	0	0	72	3851	33	3	72	3959
5	141.18	14237.654	3567	314	0	0	78	3844	25	12	78	3959
6	161.323	15608.126	3470	402	0	0	87	3839	24	9	87	3959
7	163.577	15692.041	3460	412	0	0	87	3838	24	10	87	3959
8	168.204	15782.936	3449	422	0	0	88	3835	26	10	88	3959
9	201.271	15960.41	3440	430	0	0	89	3740	94	36	89	3959
10	207.917	15993.35	3434	426	10	0	89	3738	94	38	89	3959
11	207.927	15993.845	3434	426	10	0	89	3738	94	38	89	3959
12	206.94	15086.638	3434	426	10	0	89	3738	94	30	97	3959

b. Soft storey at 4th floor

Step	Displacement mm)	Base Force(KN)	A-B	B-C	C-D	D-E	>E	A-IO	IO-LS	LS-CP	>CP	Total
0	0	0	3959	0	0	0	0	3959	0	0	0	3959
1	30	3387.7919	3959	0	0	0	0	3957	2	0	0	3959

2	48.814	5514.2878	3957	2	0	0	0	3886	71	2	0	3959
3	79.593	8992.8572	3897	12	0	0	50	3851	34	24	50	3959
4	110.72	12470.913	3769	92	0	0	98	3833	18	10	98	3959
5	141.249	15778.912	3653	198	0	0	108	3833	11	7	108	3959
6	172.64	18811.611	3416	428	0	0	115	3833	0	11	115	3959
7	207.224	21186.73	3301	532	0	0	126	3830	3	0	126	3959
8	239.723	23340.803	3219	614	0	0	126	3824	9	0	126	3959
9	273.419	25546.762	3089	744	0	0	126	3778	55	0	126	3959
10	284.555	26266.043	3055	778	0	0	126	3776	57	0	126	3959
11	284.558	26240.778	3045	788	0	0	126	3776	57	0	126	3959
12	300	27206.466	3013	820	0	0	126	3739	94	0	126	3959

c. Soft storey at 7th floor

Step	Displacement mm)	Base Force(KN)	A-B	B-C	C-D	D-E	>E	A-IO	IO-LS	LS-CP	>CP	Total
0	0	0	3959	0	0	0	0	3959	0	0	0	3959
1	30	3685.9641	3959	0	0	0	0	3943	16	0	0	3959
2	60	7376.3058	3945	0	0	0	14	3863	42	40	14	3959
3	66.091	8126.1341	3922	2	0	0	35	3851	44	29	35	3959
4	98.219	12069.532	3822	56	0	0	81	3833	28	17	81	3959
5	129.522	15800.259	3684	170	0	0	105	3820	24	10	105	3959
6	160.426	19077.427	3535	310	0	0	114	3815	18	12	114	3959
7	190.906	21353.133	3446	388	0	0	125	3811	18	5	125	3959
8	221.959	23618.635	3359	474	0	0	126	3800	26	7	126	3959
9	255.104	26013.208	3253	578	0	0	128	3756	60	15	128	3959
10	280.611	27683.615	3155	672	0	0	132	3693	122	12	132	3959
11	296.752	28105.022	3136	688	2	0	133	3670	107	49	133	3959
12	297.33	28057.062	3136	686	4	0	133	3670	101	53	135	3959
13	297.344	28058.561	3136	686	4	0	133	3670	101	53	135	3959
14	297.347	28058.669	3136	686	4	0	133	3670	101	51	137	3959
15	297.367	28060.047	3136	686	4	0	133	3670	101	51	137	3959
16	297.378	28060.417	3136	686	4	0	133	3670	101	51	137	3959
17	297.383	28060.983	3136	686	4	0	133	3670	101	51	137	3959
18	297.388	28061.065	3136	686	4	0	133	3670	101	51	137	3959
19	297.388	28061.068	3136	686	4	0	133	3670	101	51	137	3959
20	297.391	28061.355	3136	686	4	0	133	3670	101	51	137	3959
21	297.393	28061.482	3136	686	4	0	133	3670	101	51	137	3959
22	297.393	28061.482	3136	686	4	0	133	3670	101	51	137	3959
23	297.393	28061.5	3136	686	4	0	133	3670	101	51	137	3959
24	297.394	28061.504	3136	686	4	0	133	3670	101	51	137	3959

d. Soft storey at 10th floor

Figure 4.22 shows the state of hinges generated in color code and Table 4.4 shows the number of hinges generated in each state of performance levels .the number of hinges generated in collapse prevention state increase when the location of soft storey increase. Using ground soft storey building as a control group the number of hinges generated increased by 40.6%, 82.6%, 98% for model 6, model 7 and model 8 respectively depending on stiffness ratio used for the soft storey.

Table4. 5 Number of hinges in each state of soft storey location for (G+7) plan irregular building**.**

Step	Displacement mm)	Base Force(KN)	A-B	B-C	C-D	D-E	>E	A-IO	IO-LS	LS-CP	>CP	Total
0	0	0	3539	0	0	0	0	3539	0	0	0	3539

1	21	3170.1508	3539	0	0	0	0	3529	10	0	0	3539
2	27.304	4122.0866	3529	10	0	0	0	3518	18	3	0	3539
3	48.393	7170.4857	3473	56	0	0	10	3485	26	18	10	3539
4	70.409	10121.4638	3369	138	0	0	32	3463	30	14	32	3539
5	90.424	12399.1316	3291	204	0	0	44	3452	30	13	44	3539
6	95.803	12665.4613	3259	234	0	0	46	3452	27	14	46	3539
7	105.117	12905.4819	3218	272	0	0	49	3422	53	15	49	3539
8	113.395	13005.6878	3199	290	0	0	50	3408	67	14	50	3539
9	132.058	13102.5155	3175	310	4	0	50	3357	86	46	50	3539
10	132.134	13103.9009	3175	310	4	0	50	3357	86	46	50	3539
11	132.14	13102.823	3175	310	4	0	50	3357	86	44	52	3539
12	132.142	13101.2396	3175	310	4	0	50	3357	86	42	54	3539
13	132.148	13101.3684	3175	310	4	0	50	3357	86	42	54	3539
14	132.148	13101.3689	3175	310	4	0	50	3357	86	42	54	3539

a. Soft storey at ground floor

Step	Displacement mm)	Base Force(KN)	A-B	B-C	C-D	D-E	>E	A-IO	IO-LS	LS-CP	>CP	Total
0	0	0	3539	0	0	0	0	3539	0	0	0	3539
1	21	3350.8068	3539	0	0	0	0	3520	19	0	0	3539
2	26.024	4152.9522	3537	2	0	0	0	3507	32	0	0	3539
3	47.038	7489.8095	3480	38	0	0	21	3472	20	26	21	3539
4	66.404	10220.533	3333	154	0	0	52	3463	10	14	52	3539
5	71.131	10561.271	3285	200	0	0	54	3463	10	12	54	3539
6	75.241	10690.301	3265	220	0	0	54	3463	10	12	54	3539
7	75.696	10698.341	3263	222	0	0	54	3463	10	12	54	3539
8	76.383	10704.674	3255	228	0	0	56	3463	10	10	56	3539
9	89.706	10774.482	3238	244	0	0	57	3436	37	9	57	3539
10	91.947	10781.768	3235	246	0	0	58	3414	59	8	58	3539
11	113.604	10769.188	3225	256	0	0	58	3349	104	28	58	3539
12	119.751	10764.532	3219	256	6	0	58	3341	56	84	58	3539
13	119.752	10764.549	3219	256	6	0	58	3341	56	83	59	3539
14	120.876	9360.8992	3219	242	19	0	59	3341	56	70	72	3539

b. Soft storey at 3rd floor

Step	Displacement mm)	Base Force(KN)	A-B	B-C	C-D	D-E	>E	A-IO	IO-LS	LS-CP	>CP	Total
0	0	0	3539	0	0	0	0	3539	0	0	0	3539
1	21	3839.0143	3539	0	0	0	0	3519	20	0	0	3539
2	26.594	4862.2057	3537	2	0	0	0	3490	43	6	0	3539
3	48.862	8912.0847	3454	54	0	0	31	3445	30	33	31	3539
4	70.667	12796.642	3368	104	0	0	67	3438	13	21	67	3539
5	92.748	16496.683	3157	292	0	0	90	3429	12	8	90	3539
6	111.061	19014.945	3005	436	0	0	98	3429	7	5	98	3539
7	120.428	19610.848	2973	468	0	0	98	3429	3	9	98	3539
8	143.748	20095.43	2943	498	0	0	98	3349	81	11	98	3539
9	168.871	20390.315	2931	506	4	0	98	3317	46	78	98	3539
10	169.159	20406.805	2931	506	4	0	98	3317	46	78	98	3539
11	169.18	20410.562	2931	506	4	0	98	3317	46	78	98	3539
12	169.182	20412.638	2931	506	4	0	98	3317	46	78	98	3539
13	169.223	20414.331	2931	506	4	0	98	3317	46	76	100	3539
14	169.223	20414.349	2931	506	4	0	98	3317	46	76	100	3539
15	169.264	20417.085	2931	506	4	0	98	3317	46	76	100	3539
16	169.264	20417.119	2931	506	4	0	98	3317	46	76	100	3539
17	169.285	20418.32	2931	506	4	0	98	3317	46	76	100	3539
18	169.287	20418.584	2931	506	4	0	98	3317	46	76	100	3539

c. Soft storey at 5th floor

Step	Displacement mm)	Base Force(KN)	A-B	B-C	C-D	D-E	>E	A-IO	IO-LS	LS-CP	>CP	Total
0	0	0	3539	0	0	0	0	3539	0	0	0	3539
1	21	4400.6352	3539	0	0	0	0	3510	29	0	0	3539
2	32.876	6891.338	3525	2	0	0	12	3464	50	13	12	3539
3	55.413	11542.592	3421	56	0	0	62	3436	27	14	62	3539
4	76.738	15886.595	3318	142	0	0	79	3419	22	19	79	3539
5	98.232	20025.358	3233	208	0	0	98	3409	17	15	98	3539
6	122.411	23057.277	3139	296	0	0	104	3407	12	16	104	3539
7	147.043	25520.137	3055	370	0	0	114	3403	16	6	114	3539
8	170.047	27792.958	2957	462	0	0	120	3325	90	4	120	3539
9	194.528	30074.032	2853	566	0	0	120	3251	155	13	120	3539
10	206.915	31043.892	2787	630	2	0	120	3247	138	34	120	3539
11	207.361	31044.789	2785	630	4	0	120	3247	138	32	122	3539
12	207.362	31044.903	2785	630	4	0	120	3247	138	30	124	3539
13	207.362	31044.893	2785	630	4	0	120	3247	138	30	124	3539
14	207.258	30915.327	2783	628	8	0	120	3247	138	28	126	3539

d. Soft storey at 7th floor

Figure 4.23 shows the state of hinges generated in color code and Table 4.5 shows the number of hinges generated in each state of performance levels .The number of hinges generated in collapse prevention state increase when the location of soft storey increase. Using ground soft storey building as a control group the number of hinges generated increased by 33 %, 85%, 133% for model 10, model 11 and model 12 respectively depending on stiffness ratio used for soft storey.

Table4. 6 Number of hinges in each state of soft storey location for (G+10) plan irregular building.

Step	Displacement mm)	Base Force(KN)	A-B	B-C	C-D	D-E	>E	A-IO	IO-LS	LS-CP	>CP	Total
0	0	0	4918	0	0	0	0	4918	0	0	0	4918
1	30	3917.5708	4918	0	0	0	0	4900	18	0	0	4918
2	54.464	7114.5803	4906	2	0	0	10	4844	46	18	10	4918
3	84.659	10998.7446	4804	71	0	0	43	4802	46	27	43	4918
4	115.567	14213.917	4613	232	0	0	73	4787	33	25	73	4918
5	119.975	14513.0455	4587	256	0	0	75	4787	33	23	75	4918
6	137.204	15130.7047	4539	299	0	0	80	4751	61	26	80	4918
7	140.133	15185.8986	4532	304	1	0	81	4742	66	28	82	4918
8	140.806	12926.7081	4531	302	1	0	84	4742	66	26	84	4918

a. Soft storey at ground floor

Step	Displacement mm)	Base Force(KN)	A-B	B-C	C-D	D-E	>E	A-IO	IO-LS	LS-CP	>CP	Total
0	0	0	4918	0	0	0	0	4918	0	0	0	4918
1	30	4071.2009	4918	0	0	0	0	4886	32	0	0	4918
2	60	8147.0707	4887	0	0	0	31	4821	36	30	31	4918
3	61.266	8319.3091	4884	2	0	0	32	4821	27	38	32	4918
4	92.558	12556.844	4812	20	0	0	86	4795	28	9	86	4918
5	122.987	16626.39	4748	72	0	0	98	4779	29	12	98	4918
6	150.946	19902.538	4474	338	0	0	106	4770	26	16	106	4918
7	154.229	20144.798	4445	366	0	0	107	4770	25	16	107	4918
8	178.675	20841.91	4369	436	2	0	111	4720	62	25	111	4918
9	178.6	18126.241	4369	434	1	0	114	4716	65	23	114	4918

b. Soft storey at 4th floor

Step	Displacement mm)	Base Force(KN)	A-B	B-C	C-D	D-E	>E	A-IO	IO-LS	LS-CP	>CP	Total
0	0	0	4918	0	0	0	0	4918	0	0	0	4918
1	30	4460.1955	4918	0	0	0	0	4893	25	0	0	4918
2	60	8925.2346	4894	0	0	0	24	4788	67	39	24	4918
3	70.49	10487.635	4867	2	0	0	49	4780	44	45	49	4918
4	102.394	15234.577	4786	24	0	0	108	4765	21	24	108	4918
5	132.945	19676.267	4629	155	0	0	134	4764	12	8	134	4918
6	163.891	23760.284	4516	260	0	0	142	4762	3	11	142	4918
7	195.79	27065.839	4271	497	0	0	150	4761	3	4	150	4918
8	226.202	29846.974	4196	568	0	0	154	4737	27	0	154	4918
9	257.599	32665.785	4084	680	0	0	154	4708	56	0	154	4918
10	287.755	34910.979	3997	767	0	0	154	4654	93	17	154	4918
11	292.512	35185.972	3978	785	1	0	154	4641	96	27	154	4918
12	290.228	34820.151	3976	787	1	0	154	4637	100	26	155	4918

c. Soft storey at 7^{th} floor

Step	Displacement mm)	Base Force(KN)	A-B	B-C	C-D	D-E	>E	A-IO	IO-LS	LS-CP	>CP	Total
0	0	0	2546	0	0	0	0	2546	0	0	0	2546
1	30	4857.63	2546	0	0	0	0	2511	35	0	0	2546
2	60	9720.7013	2515	0	0	0	31	2421	51	43	31	2546
3	90	14589.217	2449	0	0	0	97	2393	33	23	97	2546
4	108.684	17624.008	2426	2	0	0	118	2380	28	20	118	2546
5	148.563	23825.564	2377	27	0	0	142	2368	23	13	142	2546
6	183.373	28352.021	2347	46	0	0	153	2362	18	13	153	2546
7	223.159	33106.668	2334	51	0	0	161	2329	45	11	161	2546
8	273.217	39051.399	2316	60	0	0	170	2303	59	14	170	2546
9	291.92	41154.559	2300	73	1	0	172	2303	43	27	173	2546
10	291.923	41154.902	2300	73	1	0	172	2303	43	27	173	2546
11	294.1	41378.613	2297	76	1	0	172	2302	44	27	173	2546

d. Soft storey at 10^{th} floor

Figure 4.24 shows the state of hinges generated in color code and Table 4.6 shows the number of hinges generated in each state of performance levels .the number of hinges generated in collapse prevention state increase when the location of soft storey increase. Using ground soft storey building as a control group the number of hinges generated increased by 36%, 84.5%, 105.9% for model 14, model 15and model 16 respectively depending on stiffness ratio used for soft storey.

Figure 4.21- 4.24 show the state of hinges generated in color code and Table 4.3-4.6 states the number of hinges generated from pushover analysis. In the state of collapse prevention, the number of hinges generated increases when the location of soft storey changes from lower level to higher level of the building. The number of hinges generated in collapse prevention increase by 98% and above for soft storey location changes from bottom to top of the building based on the values of stiffness ratios considered in this study. But the hinges generated in state of collapse prevention are on the strut part of the model for soft storey building at the top than bottom. Therefore the performance of the building relatively increases when soft storey changes from bottom to above levels.

4.2.7 Strengthening of Soft Storey

After the strengthening of soft storey comparisons of storey displacement, storey drift and target displacement have determined from pushover analysis results.

4.2.7.1 Storey Drift

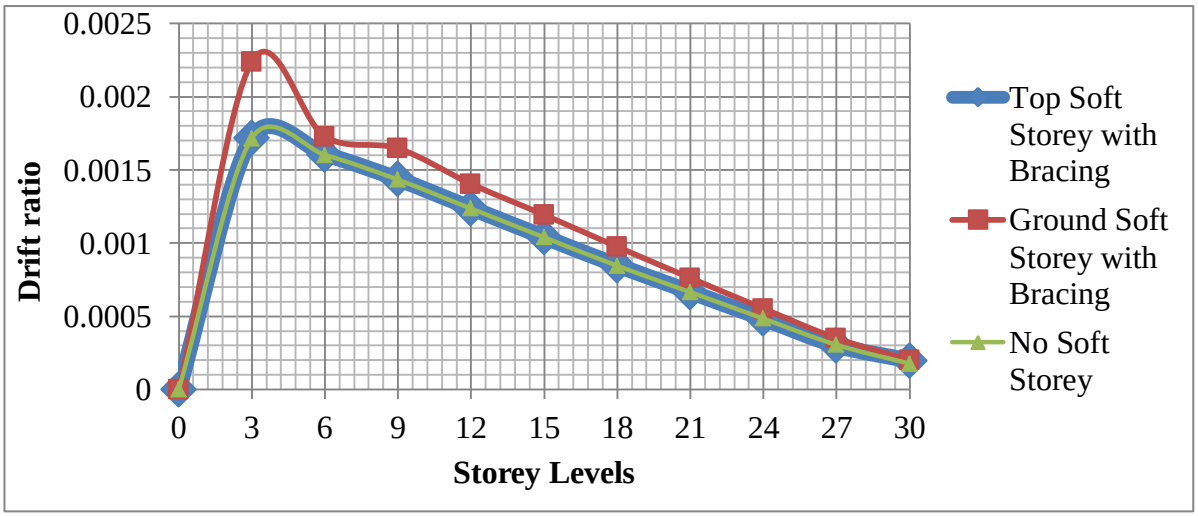

Figure 4.18 Comparison of drift ratio for (G+10) braced soft storey and without soft storey building models for push **X-** load.

Figure 4.18 shows the maximum drift ratio of soft storey at ground floor strengthen by bracing, soft storey at top strengthen by bracing and building without soft storey. As the graph shows that the maximum drift ratio of top soft storey building strengthens by X-steel bracing and building without soft storey have the same value. But building soft storey at ground floor strengthen by the same dimension of X-steel bracing have a larger maximum drift ratio and not coincide with maximum drift ratio of building without soft storey. Then to minimize this maximum drift ratio and to strengthen soft storey at ground floor additional bracing is required. The maximum drift ratio of building soft storey at the ground floor and strengthen by X-steel bracing is 29% greater than building soft storey at the top level and strengthen by X- steel bracing.

4.2.7 .2 Storey Displacement

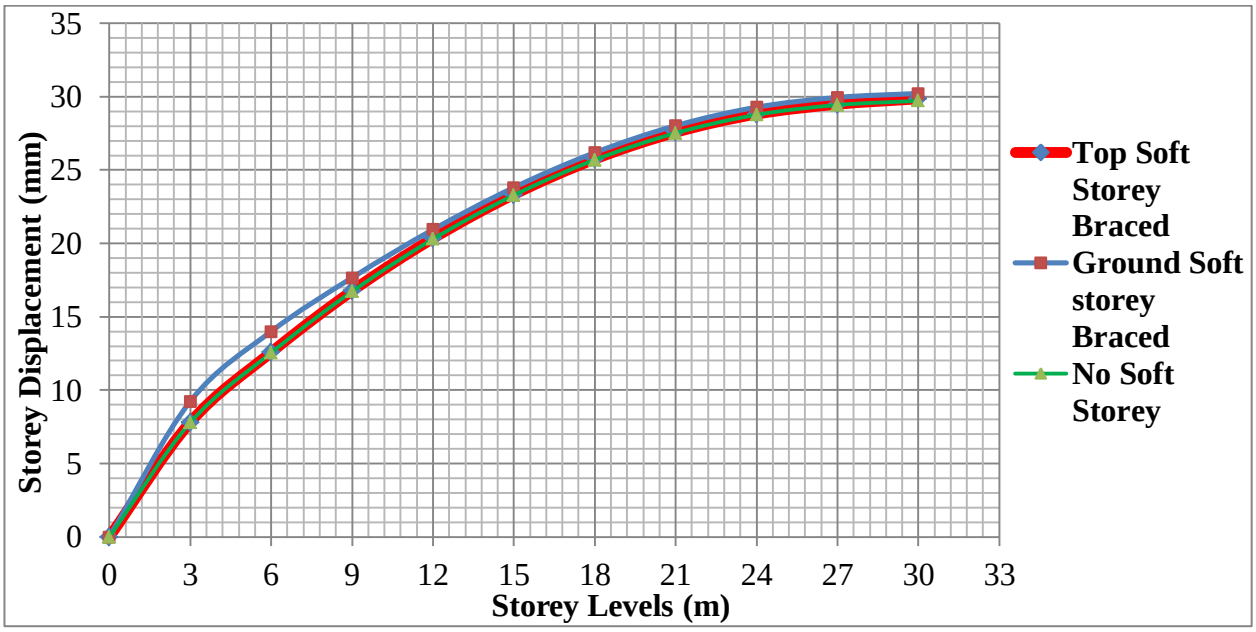

Figure 4.19 Comparison of Storey displacements for (G+10) braced soft storey and without soft storey building models for push **X-** load.

Figure 4.19 shows the Storey displacement of soft storey at ground floor strengthen by bracing, soft storey at top strengthen by bracing and building without the soft storey. As the graph shows that the storey displacement of top soft storey building strengthens by X-steel bracing and building without soft storey have the same value. But building soft storey at ground floor level strengthen by the same dimension of X-steel bracing have larger storey displacement and not coincide with storey displacement of building without soft storey. Then to minimize the storey displacement and to strengthen soft storey at ground floor additional bracing is required. The table in appendix G 1.2 shows that the roof and ground storey displacement of building soft storey at the ground floor level strengthen by X-steel bracing is increased by 1.3% and 30% respectively than building soft storey at the top level strengthen by X- steel bracing.

4.2.7.3 Target Displacement

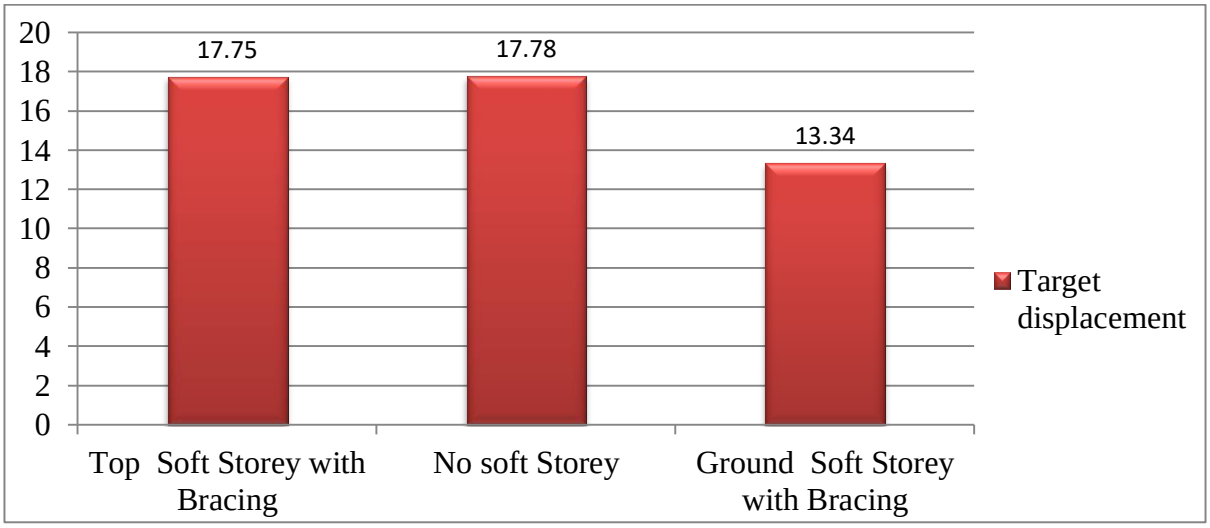

Figure 4.20 Comparison of target displacement for (G+10) braced soft storey and without soft storey building models for push **X-** loads.

Figure 4.20 shows the target displacement of soft storey at ground floor level strengthen by bracing, soft storey at top-level strengthen by bracing and building without soft storey. As the graph shows that the target displacements of top soft storey building strengthen by X-steel bracing and building without soft storey have the same value. But building soft storey at ground floor level strengthen by the same dimension of X-steel bracing has small target displacement and not coincide with target displacement of building without soft storey. This means that building soft storey at ground floor level strengthen by X-steel bracing yield first than building soft storey at top-level strengthen by the same dimension of X- steel bracing.

Then to strength soft storey more bracing is required for building soft storey at ground level than building soft storey at the top level.

CHAPTER FIVE

CONCLUSIONS AND RECOMMENDATIONS

5.1 Conclusions

This study focuses on the effect of soft storey location on the seismic performance of the reinforced concrete buildings. Soft stories are modeled by considering the effect of infill wall (HCB) on the seismic performance of RC building. Infill panels are modeled by nonlinear diagonal strut elements, which only have compressive strength.

- Single diagonal equivalent struts for masonry wall modeling were used for this study. The equivalent strut width was estimated using equations derived by Smith and Carter, FEMA 306.

Nonlinear models of the frame system with different locations of soft storey are subjected to a series of modal lateral load pattern in the X- direction in order to assess the effect of soft storey location on seismic performance of RC building. Followings are the salient conclusions obtained from the present study:

1. A building with soft storey is more affected by earthquake load and more number of hinges is developed at the soft storey location due to weakness of stiffness.
2. Nonlinear static (pushover) analysis shows that the location of soft storey (irregular distribution of infill wall) has an effect on seismic demand and performance of RC buildings.
3. The base shear resistance of the building increases when the location of soft storey changes from bottom to other location. The base shear resistance increase by (23-39) % when soft storey changes from bottom to the top level of the building depending on the value of stiffness ratios for the soft storey.
4. The roof displacement of the building is the maximum displacement for the exciting earthquake. The displacement of the top storey (roof) converges at one point as shown in the above graphs. Therefore the location of soft storey does not affect the roof (maximum) displacement of the building.
5. The storey shear resistances of the buildings increase when the location of soft storey shifts from bottom to the above location. The storey shear force on the storey increases by (21-68) % when soft storey located at top storey than bottom storey based on the value of stiffness ratio considered.

6. Buildings with soft storey at the ground floor have a higher maximum drift ratio than the other. Relatively the maximum drift ratio decreases when the location of soft storey shifts from ground floor to the above floor levels. When the soft storey located near the top floor has less maximum drift ratio than buildings with soft storey at the ground floor and the maximum drift ratio decrease by (43-51) % soft storey located near the top than bottom based on the value of stiffness ratio considered.
7. The location of soft storey has an effect on target displacement and base shear at performance point according to EC8 computation results. Buildings with the soft storey at top have maximum base shear at performance point than other location. The base shear resistance of buildings at performance point with soft storey at the top floor level is maximum. But the target displacement of the buildings with soft storey located at the top is decreased by (17-36) % than buildings soft storey located on the ground floor. Then based on the earthquake demand of reinforced concrete building at performance point providing soft storey at the top floor is good in case of displacement reduction and increment of base shear.
8. The number of hinges generated in the state of collapse prevention increases when the location of soft storey changes from lower level to higher level of the building. The number of hinges generated in collapse prevention state increase by 98% and above based on the stiffness ratio considered but most of the hinges generated in collapse prevention for soft storey at top are on the strut part than soft storey at ground. Then according to performance evaluation results from pushover analysis of reinforced concrete building provision of soft storey at the top-level increases the plastic resistance of the building.
9. Number of X- steel bracing required to strengthen building soft storey at the ground floor level larger than building soft storey at the top level. Then providing soft storey at the top level is batter to minimize the requirement of the number of X-steel bracing.

5.2 Recommendation

i. The macro modeling approach used here takes into account only the equivalent global behavior of the infill in the analysis. As a result, the approach does not permit study of local effects such as frame-infill interaction within the individual infilled frame subassemblies. More detailed finite element modeling approaches need to be used to capture the local conditions within the infill to know the effect of soft storey location on seismic performance of RC building.

ii. This study was carried out using nonlinear static (pushover) analysis method for the seismic analysis. This can be validated by an interested body using a nonlinear dynamic (time history) analysis method.

iii. In ES EN-2015 manual the effect of infill wall performance on lateral load is not included; so the design and analysis principles for lateral load effect of infill wall should be incorporated by considering performance-based design.

References

American Concrete Institute (ACI) (1995). Building Code requirements for structural Concrete.

Applied Technology Council (ATC-40) (1996). Seismic evaluation and retrofit of concrete buildings. Volume 1, Redwood City, California.

Arunkumar, S. And Devi, G. N. (2016). Seismic demand study of soft storey building and it ' s strengthening for seismic resistance. International Journal of Emerging Trends & Technology in Computer Science (IJETTCS), 5(2).

B. Stafford-Smith (1962. Lateral stiffness of infilled frames, Proceedings of the Institution of Civil Engineers; 88 (6), PP 183–199

BABU, N. J. (2015). A thesis on Pushover analysis of unsymmetrical framed structures on the sloping ground', (December).

Basavaraju, Y. K., & Babu, B. S. J. (2016). Seismic performance of multi-story RC frame buildings with soft storey from pushover analysis. International Journal of Engineering Science and Computing, 6(7).

Chopra, A. K. And Goel, R. K. (2002). 'A Modal pushover analysis procedure to estimating seismic demands for buildings: Theory and Preliminary Evaluation, PERR Report 2001/03, Pacific Earthquake Engineering Research Center, University of California, Berkeley.

Combescure, D. And Pegon, P. (2000). 'Application of the local-to-global approach to the study of infilled frame structures under seismic loading', Nuclear Engineering and Design, 196, pp. 17–40.

Dhanasekar, M. And Page, A. W. (1987).'The influence of brick masonry infill properties on the behavior of infilled frames', Preceding of the Institution of Civil Engineer, (February), pp. 593–605.

Dorji, J. (2009). 'A thesis on seismic performance of brick infilled RC frame structures in low and medium-rise Buildings in Bhutan', (June).

EN 1998-1(2005) Euro code 8. Design of structures for earthquake resistance.

ESEN1998 (2015). Design of Structures for Earthquake Resistance. Ethiopian Building Code Standard prepared by Ministry of Works and Urban Development. Addis Ababa, Ethiopia.

Federal Emergency Management Agency **(FEMA-356)**(2000). Prestandard and commentary for

the rehabilitation of Buildings.

G. Al-Chaar (2002). Evaluating strength and stiffness of unreinforced masonry infill structures. U.S. Army Corps of Engineers, Construction Engineering Research Laboratories.

Girma Zewdie (2017). A thesis on "seismic performance of reinforced concrete buildings with masonry infill." Addis Ababa University.

Gupta B. (1999). Dissertation on "Enhanced pushover procedure and inelastic demand estimation for performance-based seismic evaluation of buildings." University of Central Florida.

Habibullah, B. A. And Pyle, S. (1998). 'Practical three dimensional nonlinear static pushover analysis', Structure Magazine,USA. pp 1-2.

Homles, M. (1961). Steel frames with brickwork and concrete infilling. Proceedings of the Institution of Civil Engineers, (6501), 473–478.

Inel M. Et al (2003). The significance of lateral load pattern in pushover analysis. Istanbul Fifth National Conference on Earthquake Engineering, İstanbul Turkey.

Inel, M. And Ozmen, H. B. (2006). Effects of plastic hinge properties in nonlinear analysis of reinforced concrete buildings, (September). Doi: 10.1016/j.engstruct.2006.01.017.

J.Macgregor, and K. Wight. And J. (1997) 'Reinforced concrete mechanics and design. 3rd edition.' Prentice Hall, Inc.

Kirac, N., Dogan, M., & Ozbasaran, H. (2011). Failure of weak-storey during earthquakes. 18, 572–581. https://doi.org/10.1016/j.engfailanal.2010.09.021

Krawinkler, H. (1998). Pros and cons of a pushover analysis of seismic performance evaluation, Engineering Structures, 0296(97), pp. 452–464.

Kumar, J., Garg, V., & Sharma, A. (2014). Analytical identification of the most appropriate location of a soft storey in RC building. 2(6), PP (1322–1329).

M, C. J. And Jayalekshmi, B. R. (2013). Modeling of masonry infills. American Journal of Engineering Research (AJER)', pp. 59–63.

M.Selim Gunay. A practical Guide to Nonlinear static analysis of reinforced concrete buildings with masonry infill walls. University of California, Berkeley.

Mallick, D. (1971) ' Effect of openings on the lateral stiffness of infilled frames', Institute of Civil Engineering, (December), pp. 193–209.

Naphade, A. S. (2015). Pushover analysis of RC building with soft storey at different levels. Journal of Mechanical and Civil Engineering, pp(100–108).

Nassar A.A. and Krawinkler H. (1991).Seismic demands for SDOF and MDOF systems, report No.95. John A. Blume Earthquake Engineering Center, Stanford University.

Oguz, S. (2011) 'A thesis on "Evaluation of pushover analysis procedures for frame structures', (July).Thapar University

PATEL, S. (2012). A Thesis on Earthquake resistant design of low-rise open ground storey framed building, (May).

Patnala V. & Ramancharla P. (2014). Seismic behavior of RC frames with URM infill .International Journal of Education and Applied Research (IJEAR). Vol 4.

Pavithra, R., & Prakash, T. M. (2018). Study of behavior of the soft stories at different locations in the multi-story building. International Journal of Engineering Research & Technology (IJERT), 7(06), 53–59.

Pradhan, P. M.(2012).Equivalent strut width for partial infill frames. Journal of Civil Engineering Research; 2(5); pp 42-48.

Sasaki F. Et al. (1998). Multi-Mode Pushover Procedure (MMP) - A Method to identify the effect of higher modes in a pushover analysis. 6th U.S. National Conference on Earthquake Engineering, Seattle.

Siamak Sattar and Abbie b. liel (2010). 'Seismic performance of reinforced concrete frame structures with and without masonry infill walls'. University of Colorado.

Skafida, S., Koutas, L. And Bousias, S. N. (2014). 'Analytical modeling of Masonry Infilled RC Frames and Verification with Experimental Data', 2014.

Smith, B. S. And Carter, C. (1970). 'A method of analysis for infilled frames', Proceedings of the Institution of Civil Engineers, (February), pp. 31–48.

T. Paulay and M. Priestley (1992). Seismic design of reinforced concrete and masonry buildings. New York: Jhon Wiley & Sons.

Uruci, R. And Bilgin, H. (2016). 'Effects of soft storey irregularity on RC building response', 3rd

International Balkans Conference on Challenges of Civil Engineering, (May), pp. 19–21.

Yadunandan, C. And N, K. K. K. (2017). 'Study on behavior of Rc structure with infill walls due to seismic loads', International Research Journal of Engineering and Technology (IRJET), pp. 2494–2500.

Appendix- A: Behavior factor calculation for frame system

A. For plan regular building

For buildings that are irregular in elevation, the values of behavior factor q can be calculated as follows.

$$q = q_o K_w \geq 1.5$$

From the table 5.1 of ES EN1998-2015

$$q_o = 3\left(\frac{\alpha u}{\alpha 1}\right) \text{ for Ductility Class Medium (DCM)}$$

For multistory, multi-bay frames or frame-equivalent dual structures: αu/α1=1.3

And Kw = 1.00.

$$qo = 3 * 1.3 = 3.9$$

For buildings which are not regular in elevation, the value of q_o should be reduced by 20%

$$qo = 0.8 * 3.9 = 3.12$$

$$q = qoKw \geq 1.5$$

$$q = 3.12 * 1 = 3.12$$

B. For plan irregular building

For buildings which are not regular in plan the value of αu/α1 is equal to the average of the following things

1. Multistory, multi-bay frames or frame-equivalent dual structures: αu/α1=1.3.
2. Wall-equivalent dual, or coupled wall systems: αu/α1=1.2

$$\alpha u/\alpha 1 = \frac{1.3+1.2}{2} = 1.25$$

And $q_o = 3 * 1.25 = 3.75$

$$qo = 0.8 * 3.75 = 3$$

$$q = qoKw \geq 1.5, \quad q = 3 * 1 = 3$$

Appendix- B: Modeling of the Frame

This illustration details the procedure for estimating the equivalent width of masonry wall and strut capacity for modeling in a structural analysis program (ETABS) push-over

Table B1.1 Physical properties of the frame and infill panel

Frame	**Infill wall**	**Openings**
E_c = 31000MPa	Em = 2250MPa	h_{door} = 200cm
f_c = 25Mpa	Fm = 3Mpa	b_{door} = 100cm
	H = 300cm	
G+7 model		
h_c = 50cm	h = 265cm	
b_c = 50cm	Lp (G+) = 450cm	
I_c = 520833cm^4	text = 20cm	h_{window} = 100cm
h_b = 35cm	tint = 15cm	b_{window} = 200cm
b_b = 35cm	D = 583cm	
I_b = 125052cm^4	Ɵ = 31^o	
G+10 model		A_{opning} = 40000cm2
h_c = 70cm		$A_{panel(G+7)}$ =119250cm2
b_c = 70cm	Lp (G+) = 430cm	$A_{panel(G+10)}$ =113950 cm2
I_c = 2*10^{6}cm^4		

The first step is to model the bare frame according to its proper dimensions and physical properties as listed in Table B1.1. The frame should be modeled according to standard modeling procedures for R/C frames. After modeling the bare frame, the equivalent diagonal struts are added to represent the masonry infill the remove the diagonal region in different locations to model soft storey. Since most of the panels are fully infilled, the struts should, at first, be designed to represent full infill panels, and then multiplied by a proper reduction factor to account for any openings in the infill panel.

The equivalent strut width is evaluated by first using Equation 2.4 to calculate the parameter λ_1, as shown in Equation B1. λ_1 is then inserted into Equation 2.5 to determine the equivalent strut width

(w) as illustrated in Equation **B2**. Since the infill panels are assumed to be undamaged, *R2* is taken to be 1.0.

$$\lambda 1 = \sqrt[4]{\frac{Emtsin2\theta}{4EcIcolh}} \quad \text{---------- (B1)}$$

$$w = 0.175D\,(\lambda_1 H)^{-0.4} \quad \text{---------- (B2)}$$

For G+7 building Models

$$\lambda_{1\,(\text{external struts})} = \sqrt[4]{\frac{2250*20\,\sin(62)}{4*31000*520833*265}} = 0.0069$$

$$\lambda_{1\,(\text{internal struts})} = \sqrt[4]{\frac{2250*15\,\sin(62)}{4*31000*520833*265}} = 0.0067$$

$$w\,(_{\text{external strut}}) = 0.175*583*(0.0069*300)^{-0.4} = 75.5\text{cm}$$

$$w\,(_{\text{internal strut}}) = 0.175*583*(0.0067*300)^{-0.4} = 764.5\text{cm}$$

For G+10 building Models

$$\lambda_{1\,(\text{external struts})} = \sqrt[4]{\frac{2250*20\,\sin(62)}{4*31000*2000000*265}} = 0.00495$$

$$\lambda_{1\,(\text{internal struts})} = \sqrt[4]{\frac{2250*15\,\sin(62)}{4*31000*2000000*265}} = 0.0046$$

$$w\,(_{\text{external strut}}) = 0.175*583*(0.00495*300)^{-0.4} = 86.6\text{cm}$$

$$w\,(_{\text{internal strut}}) = 0.175*583*(0.0046*300)^{-0.4} = 88.7\text{cm}$$

Opening correction (R_1)

$$R_1 = 0.6\left(\frac{Aopen}{Apanel}\right)^2 - 1.6\left(\frac{Aopen}{Apanel}\right) + 1 \quad \text{---------- (B3)}$$

$$= 0.6\left(\frac{20000}{119250}\right)^2 - 1.6\left(\frac{20000}{119250}\right) + 1 = 0.75$$

Width required will be

$$W_{red} = w * R_1 * R2 \text{ ---------- (B4)}$$

$$w\ (_{external\ strut}) = 75.5*0.75*1.0\ cm = 56.6cm$$

$$w\ (_{internal\ strut}) = 76.45*0.75*1.0\ cm = 57.33$$

$$w\ (_{external\ strut}) = 86.6*0.75*1.0\ cm = 65cm$$

$$w\ (_{external\ strut}) = 88.7*0.75*1.0\ cm = 66.5cm$$

Upon width of the strut determined, the capacity of the strut hinges (R_{strut}) should be computed. The compressive strength (R_{strut}) should be calculated using Equations 2.12 as illustrated in Equations B5

Crushing strength (compressive resistance)

$$A_{cr} = w_{red}\, t_{eff}\, f_c \text{ ---------- (B5)}$$

For G+7 building models

$$A_{cr\ (ex)} = 56.6cm*\ 20cm*\ 3MPa = 340KN$$

$$A_{cr\ (in)} = 57.3cm*\ 15cm*\ 3MPa = 257KN$$

For G+10 building models

$$A_{cr\ (ex)} = 65cm*\ 20cm*\ 3MPa = 390KN$$

$$A_{cr\ (in)} = 66.5cm*\ 15cm*\ 3MPa = 300KN$$

Appendix C: Tabulated Results

Table C1.1 Monitored displacement and base shear for (G+7) regular plan building.

	Model 1		**Model 2**		**Model 3**		**Model 4**	
Step	Disp. (mm)	Base Shear(KN)	Disp. (mm)	Base Shear(KN)	Disp. (mm)	Base Shear(KN)	Disp. (mm)	Base Shear(KN)
0	0	0	0	0	0	0	0	0
1	17.387	2108.7056	18.037	2291.865	17.041	2481.744	21	3506.927
2	38.428	4649.2883	39.853	5057.682	38.366	5585.818	31.234	5217.259
3	60.204	7150.395	62.474	7843.676	60.43	8770.928	52.482	8762.707
4	83.269	9389.5171	83.637	10038.06	82.073	11696.16	74.498	12337.96

5	98.399	10752.0492	106.176	12228.83	103.745	14335.19	96.152	15573.65
6	102.319	10962.2811	129.455	14447.29	123.021	16247.3	102.799	16261.93
7	103.41	10994.891	150.719	16202.63	145.669	17665.39	125.042	17875.73
8	118.455	11229.1029	177.451	17709.06	167.821	19091.31	147.322	19487.97
9	124.855	11389.5319	200.165	19009.05	192.844	20658.01	168.812	21015.22
10	142.204	11635.8211	210	19567.78	210	21678.29	190.121	22478.09
11	154.988	12014.2843					196.299	22883.5
12	157.176	12057.1802					196.416	22875.39
13	172.617	12169.852					196.808	22905.44
14	188.776	12625.369					196.812	22905.45
15	192.232	12683.358					196.812	22905.45
16	192.233	12683.3936					196.818	22905.96
17	192.235	12682.1174					196.821	22905.82
18	192.56	12690.098					196.927	22914.54
19	192.885	12694.1866					196.932	22914.43
20	195.757	12712.3598					197.03	22921.33
21	197.986	12744.1594					197.031	22921.16
22	200.452	12761.9922						
23	202.054	12787.1735						
24	202.933	12794.1756						
25	202.96	12796.5932						
26	203.225	12799.204						
27	206.825	12816.3781						
28	210	12847.7517						

Table C1.2 Monitored displacement and base shear for (G+10) regular plan building.

	Model 5		**Model 6**		**Model 7**		**Model 8**	
Step	Disp. (mm)	Base shear(KN)	Disp. (mm)	Base shear(KN)	Disp. (mm)	Base shear(KN)	Disp. (mm)	Base shear(KN)
0	0	0	0	0	0	0	0	0
1	30	3004.7922	30	3098.024	30	3387.792	30	3685.964
2	40.252	4032.1788	45.688	4719.47	48.814	5514.288	60	7376.306
3	71.038	7102.8645	77.799	8029.704	79.593	8992.857	66.091	8126.134
4	101.051	9862.7363	108.596	11153.83	110.72	12470.91	98.219	12069.53
5	117.466	11055.134	141.18	14237.65	141.249	15778.91	129.522	15800.26
6	132.422	11500.8011	161.323	15608.13	172.64	18811.61	160.426	19077.43

7	134.358	11528.9747	163.577	15692.04	207.224	21186.73	190.906	21353.13
8	143.298	11580.832	168.204	15782.94	239.723	23340.8	221.959	23618.63
9	156.326	11618.7348	201.271	15960.41	273.419	25546.76	255.104	26013.21
10	167.531	11630.3479	207.917	15993.35	284.555	26266.04	280.611	27683.61
11	167.545	11630.9953	207.927	15993.85	284.558	26240.78	296.752	28105.02
12	167.2	10629.2108	206.94	15086.64	300	27206.47	297.33	28057.06
13							297.344	28058.56
14							297.347	28058.67
15							297.367	28060.05
16							297.378	28060.42
17							297.383	28060.98
18							297.388	28061.07
19							297.388	28061.07
20							297.391	28061.35
21							297.393	28061.48
22							297.393	28061.48
23							297.393	28061.5
24							297.394	28061.5

TableC1.3 Monitored displacement and base shear for (G+7) irregular plan building.

	Model 9		**Model 10**		**Model 11**		**Model 12**	
Step	Disp. (mm)	Base shear(KN)	Disp. (mm)	Base shear(KN)	Disp. (mm)	Base shear(KN)	Disp. (mm)	Base shear(KN)
0	0	0	0	0	0	0	0	0
1	21	3170.1508	21	3350.807	21	3839.014	21	4400.635
2	27.304	4122.0866	26.024	4152.952	26.594	4862.206	32.876	6891.338
3	48.393	7170.4857	47.038	7489.81	48.862	8912.085	55.413	11542.59
4	70.409	10121.4638	66.404	10220.53	70.667	12796.64	76.738	15886.59
5	90.424	12399.1316	71.131	10561.27	92.748	16496.68	98.232	20025.36
6	95.803	12665.4613	75.241	10690.3	111.061	19014.95	122.411	23057.28
7	105.117	12905.4819	75.696	10698.34	120.428	19610.85	147.043	25520.14
8	113.395	13005.6878	76.383	10704.67	143.748	20095.43	170.047	27792.96
9	132.058	13102.5155	89.706	10774.48	168.871	20390.31	194.528	30074.03
10	132.134	13103.9009	91.947	10781.77	169.159	20406.81	206.915	31043.89
11	132.14	13102.823	113.604	10769.19	169.18	20410.56	207.361	31044.79
12	132.142	13101.2396	119.751	10764.53	169.182	20412.64	207.362	31044.9

13	132.148	13101.3684	119.752	10764.55	169.223	20414.33	207.362	31044.89
14	132.148	13101.3689	120.876	9360.899	169.223	20414.35	207.258	30915.33
15					169.264	20417.08		
16					169.264	20417.12		
17					169.285	20418.32		
18					169.287	20418.58		

Table C1. 4 Monitored displacement and base shear for (G+10) irregular plan building.

	Model 13		**Model 14**		**Model 15**		**Model 16**	
Step	Disp. (mm)	Base shear(KN)	Disp. (mm)	Base shear(KN)	Disp. (mm)	Base shear(KN)	Disp. (mm)	Base shear(KN)
0	0	0	0	0	0	0	0	0
1	30	3917.5708	30	4071.201	30	4460.196	30	4857.63
2	54.464	7114.5803	60	8147.071	60	8925.235	60	9720.701
3	84.659	10998.7446	61.266	8319.309	70.49	10487.64	90	14589.22
4	115.567	14213.917	92.558	12556.84	102.394	15234.58	108.684	17624.01
5	119.975	14513.0455	122.987	16626.39	132.945	19676.27	148.563	23825.56
6	137.204	15130.7047	150.946	19902.54	163.891	23760.28	183.373	28352.02
7	140.133	15185.8986	154.229	20144.8	195.79	27065.84	223.159	33106.67
8	140.806	12926.7081	178.675	20841.91	226.202	29846.97	273.217	39051.4
9			178.6	18126.24	257.599	32665.78	291.92	41154.56
10					287.755	34910.98	291.923	41154.9
11					292.512	35185.97	294.1	41378.61
12					290.228	34820.15		

Table C1.5 Storey displacement for (G+7, G+10) regular plan building

Table : Storey displacement(mm)											
G+7						**G+10**					
Storey	Elev. (m)	Mod.1	Mod.2	Mod.3	Mode.4	Storey	Elev. (m)	Mod.5	Mod.6	Mod.7	Mod.8
G+7	21	17.442	18.036	18.093	17.031	G+10	30	29.721	29.592	29.611	29.509
G+6	18	17.311	17.898	17.89	16.888	G+9	27	29.481	29.347	29.345	29.041
G+5	15	16.819	17.364	17.734	15.881	G+8	24	28.955	28.804	28.696	28.341
G+4	12	15.817	16.273	17.01	12.922	G+7	21	27.966	27.781	27.008	27.106
G+3	9	14.302	13.841	15.419	10.789	G+6	18	26.513	26.278	23.71	25.301

G+2	6	12.262	8.346	11.945	8.362	G+5	15	24.599	24.21	21.09	22.928
G+1	3	8.856	4.901	7.534	5.291	G+4	12	22.221	20.71	18.339	19.984
ground	0	0	0	0	0	G+3	9	19.373	14.741	15.099	16.463
						G+2	6	15.935	10.471	11.331	12.354
						G+1	3	11.055	6.439	7.036	7.669
						ground	0	0	0	0	0

Table C1.6 Storey displacement for (G+7, G+10) irregular plan building

Table : storey displacement(mm)											
G+7						**G+10**					
Storey	**Elev. (m)**	**Mod.9**	**Mod.10**	**Mod.11**	**Mod.12**	**Storey**	**Elev. (m)**	**Mod.13**	**Mod.14**	**Mod.15**	**Mod.16**
G+7	21	21.011	21.075	21.115	21.125	G+10	30	30.119	30.395	30.444	30.573
G+6	18	20.664	20.707	20.704	19.806	G+9	27	29.765	29.932	29.932	29.599
G+5	15	19.876	19.873	19.204	18.56	G+8	24	29.083	29.16	29.058	28.661
G+4	12	18.597	18.55	14.918	16.723	G+7	21	27.984	28.014	27.231	27.26
G+3	9	16.818	15.783	12.258	14.167	G+6	18	26.456	26.416	23.654	25.324
G+2	6	14.585	8.889	9.437	10.897	G+5	15	24.501	24.306	20.911	22.848
G+1	3	10.797	5.219	6.06	6.99	G+4	12	22.119	20.778	18.105	19.829
ground	0	0	0	0	0	G+3	9	19.312	14.487	14.85	16.268
						G+2	6	16.022	10.191	11.11	12.167
						G+1	3	11.217	6.364	6.99	7.649
						ground	0	0	0	0	0

Table C1. 7 Storey shear for (G+7) regular plan building

Table : Storey Shear (KN)						
Storey	**Elevation(m)**	**Location**	**Model 1**	**Model 2**	**Model 3**	**Model 4**
G+7	21	Top	45.901	49.8876	54.0207	76.3362
	18	Bottom	46.663	50.7165	54.9183	77.6045
G+6	18	Top	339.208	368.6716	399.2156	564.1275
	15	Bottom	339.972	369.501	400.1143	565.3963
G+5	15	Top	635.340	690.5245	747.7346	1056.614
	12	Bottom	636.104	691.3549	748.6337	1057.884
G+4	12	Top	931.473	1012.379	1096.254	1549.103

	9	Bottom	932.239	1013.215	1097.154	1550.374
G+3	9	Top	1227.608	1334.242	1444.775	2041.593
	6	Bottom	1228.376	1335.075	1445.678	2042.866
G+2	6	Top	1523.746	1656.101	1793.3	2534.087
	3	Bottom	1524.511	1656.931	1794.204	2535.361
G+1	3	Top	1819.883	1977.958	2141.827	3026.582
	0	Bottom	1820.629	1978.769	2142.707	3027.833
ground	0	Top	2106.647	2289.63	2479.322	3503.501

Table C1. 8 Storey shear for (G+10) regular plan building

Table: Storey Shear (KN)						
Storey	**Elevation (m)**	**Location**	**Model 5**	**Model 6**	**Model 7**	**Model 8**
G+10	30	Top	52.4716	54.0996	59.1597	64.3667
	27	Bottom	52.4817	54.1101	59.1712	64.3791
G+9	27	Top	360.9551	372.1547	406.9635	442.7819
	24	Bottom	360.9656	372.1655	406.9753	442.7946
G+8	24	Top	669.4392	690.2103	754.7678	821.1976
	21	Bottom	669.4505	690.2219	754.7816	821.2111
G+7	21	Top	977.9244	1008.267	1102.575	1199.614
	18	Bottom	977.9368	1008.28	1102.589	1199.629
G+6	18	Top	1286.4113	1326.325	1450.383	1578.033
	15	Bottom	1286.4251	1326.34	1450.396	1578.049
G+5	15	Top	1594.9004	1644.387	1798.19	1956.454
	12	Bottom	1594.916	1644.411	1798.206	1956.471
G+4	12	Top	1903.3921	1962.461	2146.001	2334.877
	9	Bottom	1903.4095	1962.479	2146.02	2334.897
G+3	9	Top	2211.8866	2280.528	2493.816	2713.303
	6	Bottom	2211.9045	2280.536	2493.836	2713.324
G+2	6	Top	2520.3827	2598.585	2841.633	3091.732
	3	Bottom	2520.3908	2598.597	2841.647	3091.746
G+1	3	Top	2828.8641	2916.641	3189.438	3470.147
	0	Bottom	2828.8509	2916.625	3189.424	3470.134
ground	0	Top	3004.8158	3098.051	3387.819	3685.991

Table C1. 9 Storey shear for (G+7) irregular plan building

Table: Storey Shear (KN)						
Storey	**Elevation (m)**	**Location**	**Model 9**	**Model 10**	**Model 11**	**Model 12**
G+7	21	Top	172.3486	182.1702	208.7121	239.2452
	18	Bottom	172.3599	182.1821	208.7257	239.2608
G+6	18	Top	599.5128	633.677	726.0026	832.2117
	15	Bottom	599.5247	633.6895	726.0178	832.2279
G+5	15	Top	1029.8699	1088.559	1247.161	1429.61
	12	Bottom	1029.8831	1088.572	1247.177	1429.627
G+4	12	Top	1460.229	1543.442	1768.32	2027.01
	9	Bottom	1460.2438	1543.464	1768.336	2027.029
G+3	9	Top	1890.5907	1998.337	2289.48	2624.413
	6	Bottom	1890.6084	1998.354	2289.5	2624.435
G+2	6	Top	2320.9567	2453.227	2810.645	3221.82
	3	Bottom	2320.9695	2453.239	2810.667	3221.843
G+1	3	Top	2751.3194	2908.113	3331.814	3819.23
	0	Bottom	2751.3121	2908.101	3331.805	3819.223
ground	0	Top	3170.1614	3350.821	3839.028	4400.648

Table C1. 10 Storey shear for (G+10) irregular plan building

Table: Storey Shear (KN)						
Storey	**Elevation (m)**	**Location**	**Model 5**	**Model 6**	**Model 7**	**Model 8**
G+10	30	Top	61.9117	64.3396	70.4871	76.1648
	27	Bottom	62.7419	65.2024	71.4323	77.1869
G+9	27	Top	445.7858	463.2676	507.5317	552.1905
	24	Bottom	446.6165	464.1308	508.4774	553.213
G+8	24	Top	832.5229	865.1708	947.8359	1031.772
	21	Bottom	833.3546	866.035	948.7842	1032.795
G+7	21	Top	1219.2616	1267.076	1388.144	1511.354
	18	Bottom	1220.0946	1267.941	1389.092	1512.379
G+6	18	Top	1606.0022	1668.982	1828.452	1990.938
	15	Bottom	1606.837	1669.85	1829.399	1991.965
G+5	15	Top	1992.7455	2070.892	2268.76	2470.525
	12	Bottom	1993.5824	2071.774	2269.712	2471.553
G+4	12	Top	2379.4921	2472.82	2709.073	2950.115

	9	Bottom	2380.3312	2473.692	2710.027	2951.145
G+3	9	Top	2766.2421	2874.737	3149.39	3429.708
	6	Bottom	2767.0827	2875.596	3150.346	3430.74
G+2	6	Top	3152.9951	3276.642	3589.711	3909.305
	3	Bottom	3153.8235	3277.507	3590.659	3910.329
G+1	3	Top	3539.7284	3678.544	4030.014	4388.89
	0	Bottom	3540.6829	3679.534	4031.101	4390.072
ground	0	Top	3916.2961	4069.879	4458.743	4856.039

Table C1. 11 Storey drift for (G+7, G+10) regular plan building

Table: Storey drift ratio										
G+7							**G+10**			
Storey	**Elev.(mm)**	**Loc.**	**Mod.1**	**Mod. 2**	**Mod.3**	**Mod. 4**	**Mod.5**	**Mod.6**	**Mod.7**	**Mod.8**
G+10	30	Top					0.00015	0.00015	0.00016	0.00029
G+9	27	Top					0.00024	0.00025	0.00029	0.00033
G+8	24	Top					0.00038	0.00040	0.00058	0.00048
G+7	21	Top	0.00011	0.00011	0.00012	0.00036	0.00053	0.00055	0.00121	0.00065
G+6	18	Top	0.00022	0.00024	0.00037	0.00041	0.00067	0.00073	0.00095	0.00083
G+5	15	Top	0.00037	0.00041	0.00110	0.00063	0.00083	0.00117	0.00096	0.00102
G+4	12	Top	0.00054	0.00081	0.00078	0.00092	0.00100	0.00209	0.00112	0.00122
G+3	9	Top	0.00072	0.00191	0.00085	0.00121	0.00119	0.00153	0.00129	0.00141
G+2	6	Top	0.00118	0.00123	0.00105	0.00150	0.00172	0.00135	0.00145	0.00158
G+1	3	Top	0.00225	0.00110	0.00119	0.00170	0.00264	0.00142	0.00155	0.00169
Ground	0	Top	0	0	0	0	0	0	0	0

Table C1. 12 Storey drift for (G+7, G+10) irregular plan building

Table: Storey drift ratio										
G+7							**G+10**			
Storey	**Elev.(mm)**	**Loc.**	**Mod. 9**	**Mod.10**	**Mod.11**	**Mod.12**	**Mod. 13**	**Mod.14**	**Mod. 15**	**Mod.16**
G+10	30	Top					0.00016	0.00017	0.00019	0.00034
G+9	27	Top					0.00027	0.00028	0.00033	0.00037
G+8	24	Top					0.00041	0.00042	0.00064	0.00051

G+7	21	Top	0.00016	0.00017	0.00019	0.00054	0.00055	0.00057	0.00123	0.00069
G+6	18	Top	0.00028	0.00030	0.00051	0.00045	0.00069	0.00075	0.00098	0.00086
G+5	15	Top	0.00046	0.00049	0.00147	0.00064	0.00084	0.00119	0.00096	0.00104
G+4	12	Top	0.00064	0.00095	0.00095	0.00089	0.00098	0.00212	0.00111	0.00121
G+3	9	Top	0.00082	0.00232	0.00098	0.00113	0.00116	0.00149	0.00126	0.00139
G+2	6	Top	0.00132	0.00132	0.00118	0.00136	0.00166	0.00131	0.00142	0.00155
G+1	3	Top	0.00276	0.00114	0.00131	0.00151	0.00270	0.00136	0.00150	0.00164
ground	0	Top	0	0	0	0	0	0	0	0

Appendix D. ETABS output of target displacement and base shear at performance point.

Model 1

Plot Definition	
Plot Type	EC 8 2004 Target Displ
Load Case	PUSH X
Legend Type	Integrated
Demand Spectrum	
Spectrum Source	EC 8 2004 Horiz
Country	CEN Default
Ground Accel, ag/g	0.15
Spectrum Type	1
Ground Type	C
Behavior Factor, q	3.12
Damping Parameters	
Damping Ratio	0.05
Capacity Curve	
Bilinear Force-Displacement Curve	
Visible	No
Demand Curve	
Period Lines	
Target Displacement Results	
Displacement, dt (mm)	16.506
Shear at dt (kN)	2001.9112
Calculated Parameters	
Target Displ Found	Yes
Fy*, g	0.138
Em* (mm)	0.794
dy* (mm)	11.493
T* (sec)	0.579
Se(T*), g	0.138
det* (mm)	11.493
Tc (sec)	0.6
dt* (mm)	11.493
Gamma	1.436229

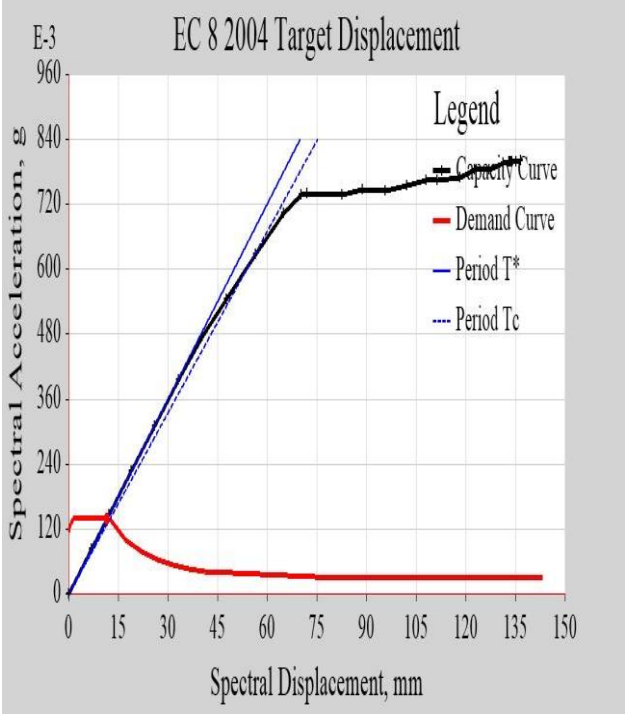

Model 2

Plot Definition	
Plot Type	EC 8 2004 Target Displ
Load Case	PUSH X
Legend Type	Integrated
Demand Spectrum	
Spectrum Source	EC 8 2004 Horiz
Country	CEN Default
Ground Accel, ag/g	0.15
Spectrum Type	1
Ground Type	C
Behavior Factor, q	3.12
Damping Parameters	
Damping Ratio	0.05
Capacity Curve	
Bilinear Force-Displacement Curve	
Visible	No
Demand Curve	
Period Lines	
Target Displacement Results	
Displacement, dt (mm)	11.913
Shear at dt (kN)	1513.5659
Calculated Parameters	
Target Displ Found	Yes
Fy*, g	0.138
Em* (mm)	0.55
dy* (mm)	7.962
T* (sec)	0.482
Se(T*), g	0.138
det* (mm)	7.962
Tc (sec)	0.6
dt* (mm)	7.962
Gamma	1.496283

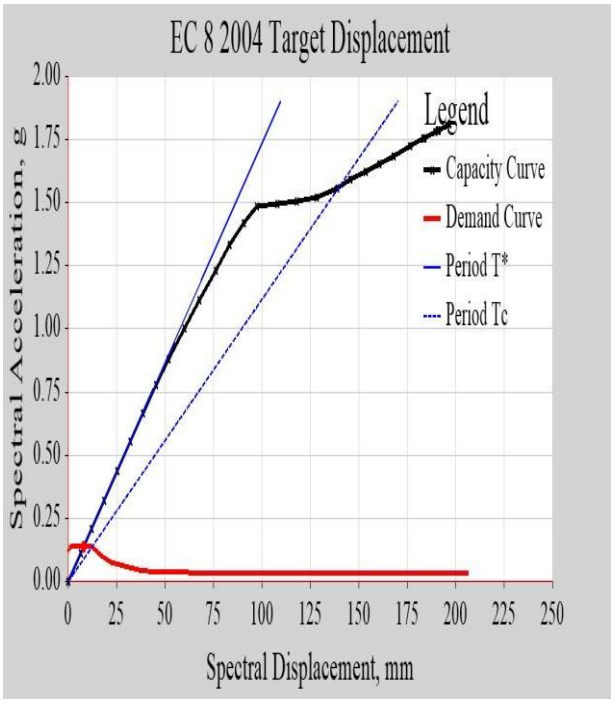

Model 3

Plot Definition	
Plot Type	EC 8 2004 Target Displ
Load Case	PUSH X
Legend Type	Integrated
Demand Spectrum	
Spectrum Source	EC 8 2004 Horiz
Country	CEN Default
Ground Accel. ag/g	0.15
Spectrum Type	1
Ground Type	C
Behavior Factor, q	3.12
Damping Parameters	
Damping Ratio	0.05
Capacity Curve	
Bilinear Force-Displacement Curve	
Visible	No
Demand Curve	
Period Lines	
Target Displacement Results	
Displacement, dt (mm)	11.321
Shear at dt (kN)	1648.5276
Calculated Parameters	
Target Displ Found	Yes
Fy*, g	0.138
Em* (mm)	0.481
dy* (mm)	6.963
T* (sec)	0.45
Se(T*), g	0.138
det* (mm)	6.963
Tc (sec)	0.6
dt* (mm)	6.963
Gamma	1.625769

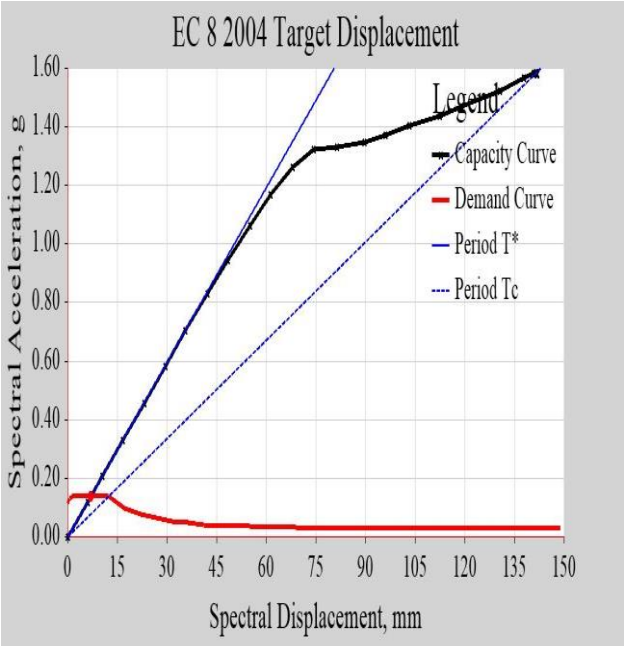

Model 4

Name	
Plot Definition	
Plot Type	EC 8 2004 Target Displ
Load Case	PUSH X
Legend Type	Integrated
Demand Spectrum	
Spectrum Source	EC 8 2004 Horiz
Country	CEN Default
Ground Accel. ag/g	0.15
Spectrum Type	1
Ground Type	C
Behavior Factor, q	3.12
Damping Parameters	
Damping Ratio	0.05
Capacity Curve	
Bilinear Force-Displacement Curve	
Visible	No
Demand Curve	
Period Lines	
Target Displacement Results	
Displacement, dt (mm)	10.457
Shear at dt (kN)	1746.2622
Calculated Parameters	
Target Displ Found	Yes
Fy*, g	0.138
Em* (mm)	0.457
dy* (mm)	6.612
T* (sec)	0.439
Se(T*), g	0.138
det* (mm)	6.612
Tc (sec)	0.6
dt* (mm)	6.612
Gamma	1.581603

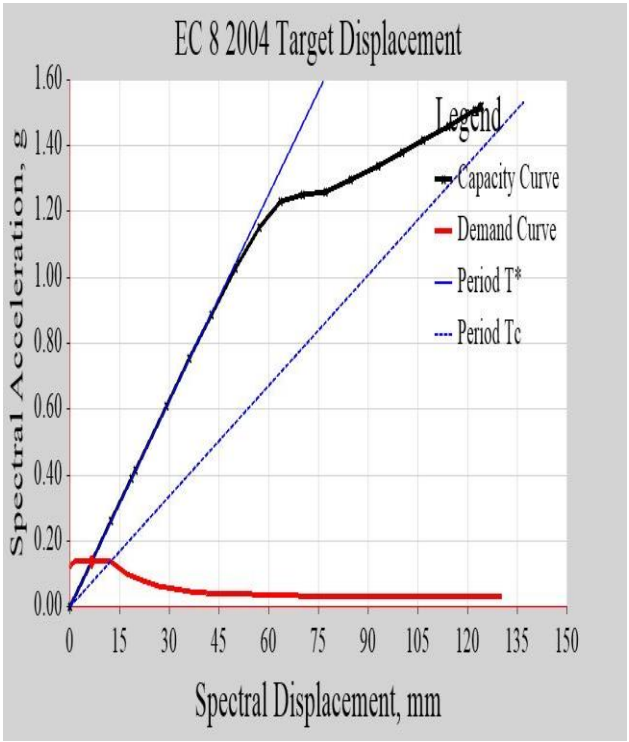

Figure D1. 1Results of target displacement & base shear for (G+7) regular plan building models

Model 5

Name	
Plot Definition	
Plot Type	EC 8 2004 Target Displ
Load Case	PUSH X
Legend Type	Integrated
Demand Spectrum	
Spectrum Source	EC 8 2004 Horiz
Country	CEN Default
Ground Accel. ag/g	0.15
Spectrum Type	1
Ground Type	C
Behavior Factor, q	3.12
Damping Parameters	
Damping Ratio	0.05
Capacity Curve	
Bilinear Force-Displacement Curve	
Visible	No
Demand Curve	
Period Lines	
Target Displacement Results	
Displacement, dt (mm)	22.421
Shear at dt (kN)	2245.5532
Calculated Parameters	
Target Displ Found	Yes
Fy*, g	0.12
Em* (mm)	0.901
dy* (mm)	14.962
T* (sec)	0.707
Se(T*), g	0.12
det* (mm)	14.961
Tc (sec)	0.6
dt* (mm)	14.961
Gamma	1.498685

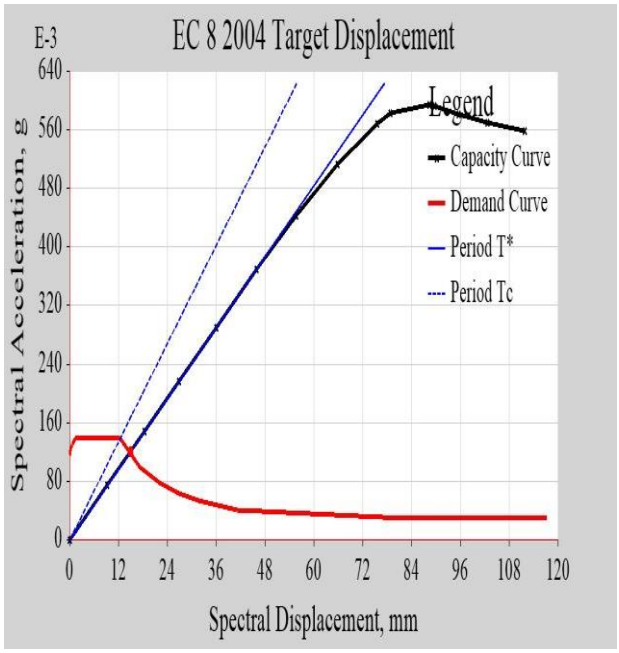

Model 6

Name	
Name	Pushover1
Plot Definition	
Plot Type	EC 8 2004 Target Displ
Load Case	PUSH X
Legend Type	Integrated
Demand Spectrum	
Spectrum Source	EC 8 2004 Horiz
Country	CEN Default
Ground Accel. ag/g	0.15
Spectrum Type	1
Ground Type	C
Behavior Factor, q	3.12
Damping Parameters	
Damping Ratio	0.05
Capacity Curve	
Bilinear Force-Displacement Curve	
Demand Curve	
Period Lines	
Target Displacement Results	
Displacement, dt (mm)	19.165
Shear at dt (kN)	1978.7818
Calculated Parameters	
Target Displ Found	Yes
Fy*, g	0.134
Em* (mm)	0.871
dy* (mm)	12.979
T* (sec)	0.624
Se(T*), g	0.134
det* (mm)	12.978
Tc (sec)	0.6
dt* (mm)	12.978
Gamma	1.476756

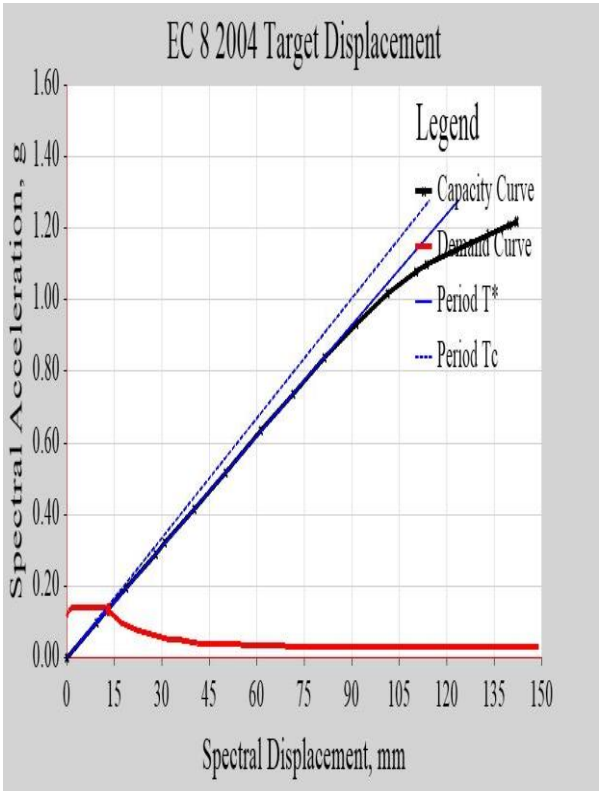

Model 7

Name	
Plot Definition	
Plot Type	EC 8 2004 Target Displ
Load Case	PUSH X
Legend Type	Integrated
Demand Spectrum	
Spectrum Source	EC 8 2004 Horiz
Country	CEN Default
Ground Accel. ag/g	0.15
Spectrum Type	1
Ground Type	C
Behavior Factor, q	3.12
Damping Parameters	
Damping Ratio	0.05
Capacity Curve	
Bilinear Force-Displacement Curve	
Visible	No
Demand Curve	
Period Lines	
Target Displacement Results	
Displacement, dt (mm)	18.963
Shear at dt (kN)	2141.118
Calculated Parameters	
Target Displ Found	Yes
Fy*, g	0.138
Em* (mm)	0.837
dy* (mm)	12.112
T* (sec)	0.594
Se(T*), g	0.138
det* (mm)	12.111
Tc (sec)	0.6
dt* (mm)	12.111
Gamma	1.565817

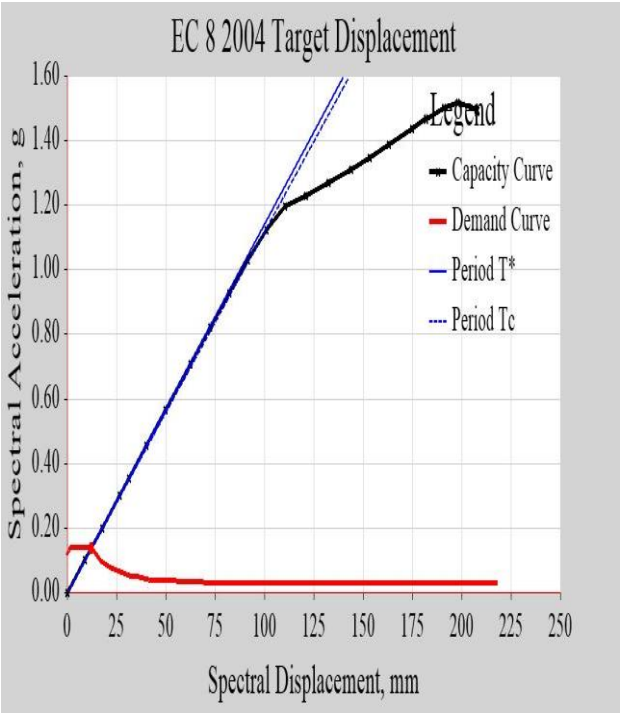

Model 8

Name	
Plot Definition	
Plot Type	EC 8 2004 Target Displ
Load Case	PUSH X
Legend Type	Integrated
Demand Spectrum	
Spectrum Source	EC 8 2004 Horiz
Country	CEN Default
Ground Accel. ag/g	0.15
Spectrum Type	1
Ground Type	C
Behavior Factor, q	3.12
Damping Parameters	
Damping Ratio	0.05
Capacity Curve	
Bilinear Force-Displacement Curve	
Demand Curve	
Period Lines	
Target Displacement Results	
Displacement, dt (mm)	18.051
Shear at dt (kN)	2217.3925
Calculated Parameters	
Target Displ Found	Yes
Fy*, g	0.138
Em* (mm)	0.808
dy* (mm)	11.687
T* (sec)	0.583
Se(T*), g	0.138
det* (mm)	11.686
Tc (sec)	0.6
dt* (mm)	11.686
Gamma	1.544673

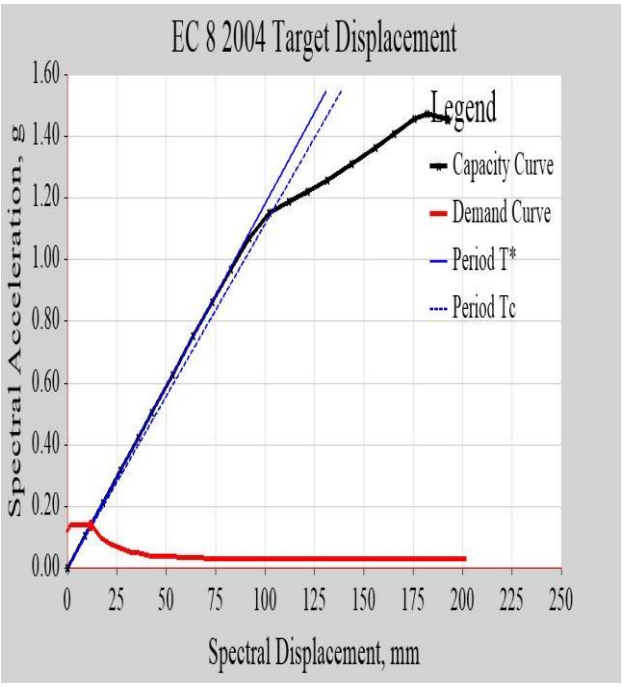

Figure D1. 2 Results of target displacement & base shear for (G+10) regular plan building models

Model 9

Name	
Plot Definition	
Plot Type	EC 8 2004 Target Displ
Load Case	PUSH X
Legend Type	Integrated
Demand Spectrum	
Spectrum Source	EC 8 2004 Horiz
Country	CEN Default
Ground Accel. ag/g	0.15
Spectrum Type	1
Ground Type	C
Behavior Factor, q	3.12
Damping Parameters	
Damping Ratio	0.05
Capacity Curve	
Bilinear Force-Displacement Curve	
Visible	No
Demand Curve	
Period Lines	
Target Displacement Results	
Displacement, dt (mm)	17.761
Shear at dt (kN)	2681.0726
Calculated Parameters	
Target Displ Found	Yes
Fy*, g	0.138
Em* (mm)	0.847
dy* (mm)	12.253
T* (sec)	0.597
Se(T*), g	0.138
det* (mm)	12.253
Tc (sec)	0.6
dt* (mm)	12.253
Gamma	1.449564

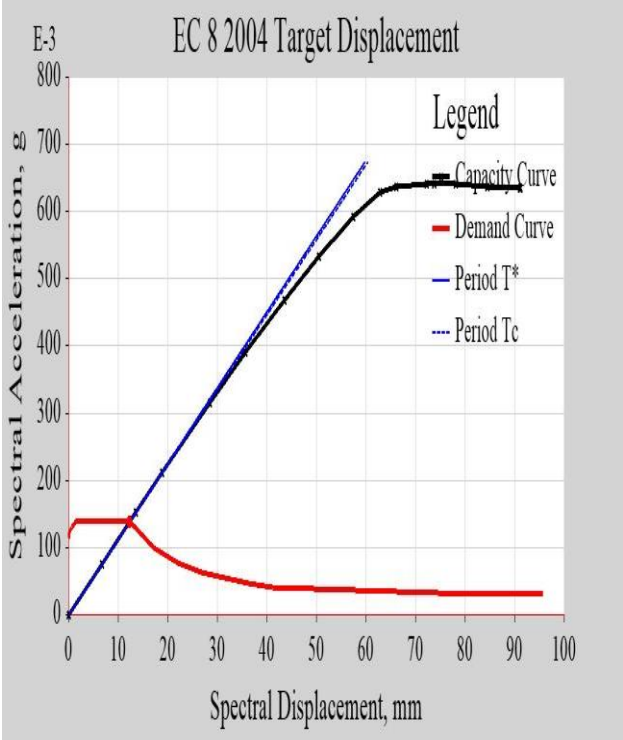

Model 10

Name	
Plot Definition	
Plot Type	EC 8 2004 Target Displ
Load Case	PUSH X
Legend Type	Integrated
Demand Spectrum	
Spectrum Source	EC 8 2004 Horiz
Country	CEN Default
Ground Accel. ag/g	0.15
Spectrum Type	1
Ground Type	C
Behavior Factor, q	3
Damping Parameters	
Damping Ratio	0.05
Capacity Curve	
Bilinear Force-Displacement Curve	
Visible	No
Demand Curve	
Period Lines	
Target Displacement Results	
Displacement, dt (mm)	13.052
Shear at dt (kN)	2082.3209
Calculated Parameters	
Target Displ Found	Yes
Fy*, g	0.144
Em* (mm)	0.619
dy* (mm)	8.619
T* (sec)	0.491
Se(T*), g	0.144
det* (mm)	8.618
Tc (sec)	0.6
dt* (mm)	8.618
Gamma	1.514454

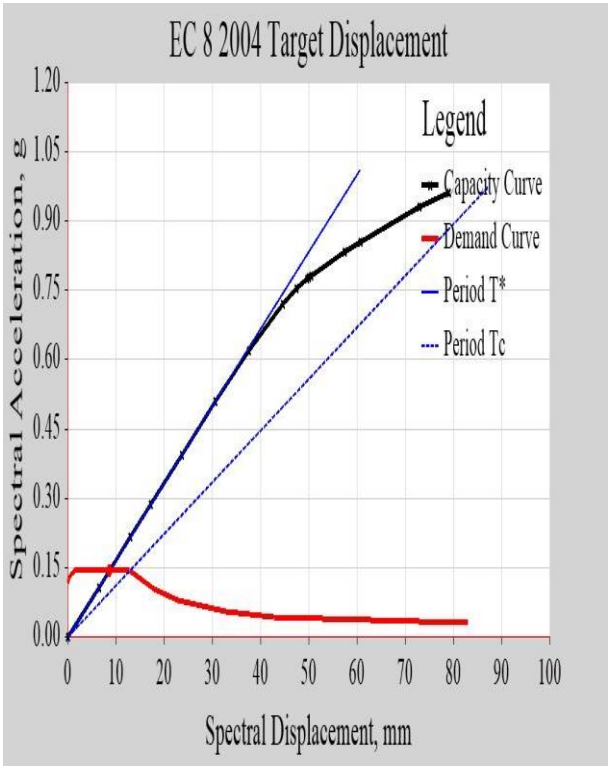

Model 11

Name	
Plot Definition	
Plot Type	EC 8 2004 Target Displ
Load Case	PUSH X
Legend Type	Integrated
Demand Spectrum	
Spectrum Source	EC 8 2004 Horiz
Country	CEN Default
Ground Accel. ag/g	0.15
Spectrum Type	1
Ground Type	C
Behavior Factor, q	3
Damping Parameters	
Damping Ratio	0.05
Capacity Curve	
Bilinear Force-Displacement Curve	
Visible	No
Demand Curve	
Period Lines	
Target Displacement Results	
Displacement, dt (mm)	12.387
Shear at dt (kN)	2264.1287
Calculated Parameters	
Target Displ Found	Yes
Fy*, g	0.144
Em* (mm)	0.539
dy* (mm)	7.496
T* (sec)	0.458
Se(T*), g	0.144
det* (mm)	7.495
Tc (sec)	0.6
dt* (mm)	7.495
Gamma	1.652674

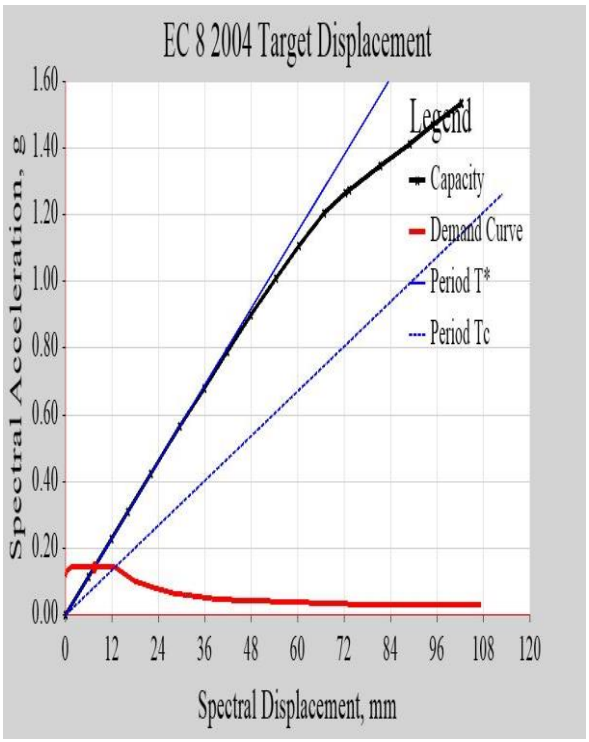

Model 12

Name	
Plot Definition	
Plot Type	EC 8 2004 Target Displ
Load Case	PUSH X
Legend Type	Integrated
Demand Spectrum	
Spectrum Source	EC 8 2004 Horiz
Country	CEN Default
Ground Accel. ag/g	0.15
Spectrum Type	1
Ground Type	C
Behavior Factor, q	3
Damping Parameters	
Damping Ratio	0.05
Capacity Curve	
Bilinear Force-Displacement Curve	
Visible	No
Demand Curve	
Period Lines	
Target Displacement Results	
Displacement, dt (mm)	11.551
Shear at dt (kN)	2420.0518
Calculated Parameters	
Target Displ Found	Yes
Fy*, g	0.144
Em* (mm)	0.507
dy* (mm)	7.052
T* (sec)	0.444
Se(T*), g	0.144
det* (mm)	7.052
Tc (sec)	0.6
dt* (mm)	7.052
Gamma	1.638025

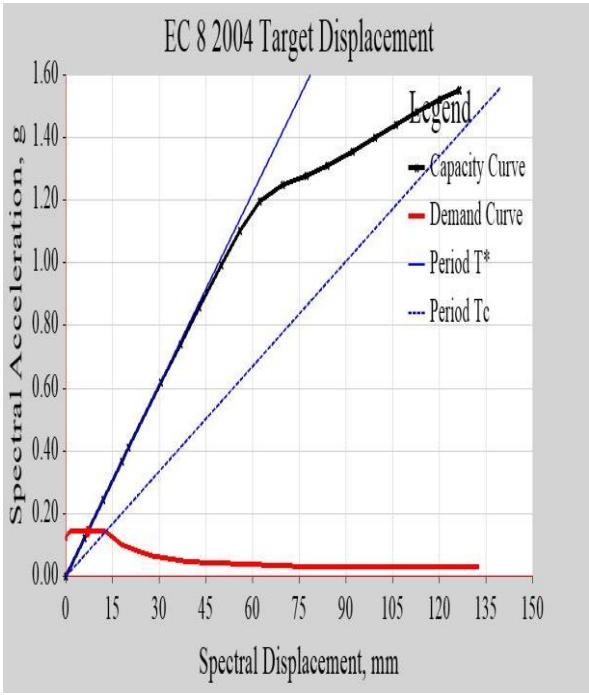

Figure D1. 3 Results of target displacement & base shear for (G+7) irregular plan building models

Model 13

Plot Definition	
Plot Type	EC 8 2004 Target Displ
Load Case	PUSH X
Legend Type	Integrated
Demand Spectrum	
Spectrum Source	EC 8 2004 Horiz
Country	CEN Default
Ground Accel. ag/g	0.15
Spectrum Type	1
Ground Type	C
Behavior Factor, q	3
Damping Parameters	
Damping Ratio	0.05
Capacity Curve	
Bilinear Force-Displacement Curve	
Visible	No
Demand Curve	
Period Lines	
Target Displacement Results	
Displacement, dt (mm)	23.653
Shear at dt (kN)	3088.7847
Calculated Parameters	
Target Displ Found	Yes
Fy*, g	0.126
Em* (mm)	0.974
dy* (mm)	15.47
T* (sec)	0.703
Se(T*), g	0.126
det* (mm)	15.47
Tc (sec)	0.6
dt* (mm)	15.47
Gamma	1.529007

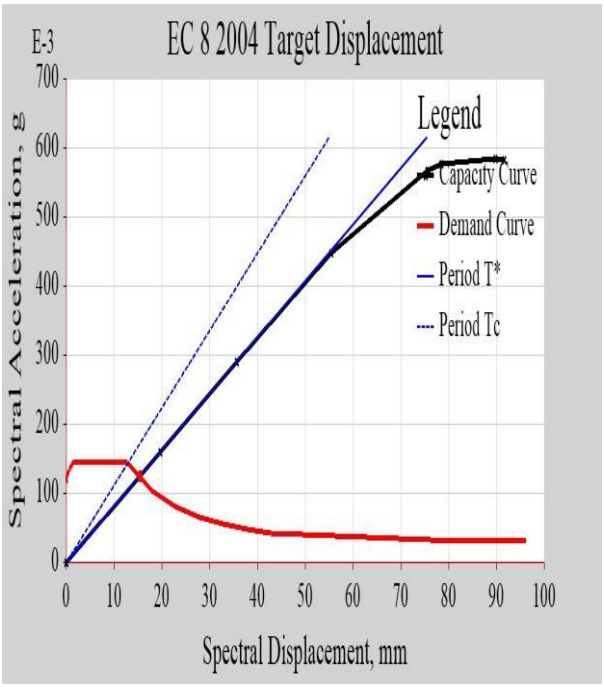

Model 14

Plot Definition	
Plot Type	EC 8 2004 Target Displ
Load Case	PUSH X
Legend Type	Integrated
Demand Spectrum	
Spectrum Source	EC 8 2004 Horiz
Country	CEN Default
Ground Accel. ag/g	0.15
Spectrum Type	1
Ground Type	C
Behavior Factor, q	3
Damping Parameters	
Damping Ratio	0.05
Capacity Curve	
Bilinear Force-Displacement Curve	
Visible	No
Demand Curve	
Period Lines	
Target Displacement Results	
Displacement, dt (mm)	19.995
Shear at dt (kN)	2713.4896
Calculated Parameters	
Target Displ Found	Yes
Fy*, g	0.141
Em* (mm)	0.935
dy* (mm)	13.22
T* (sec)	0.613
Se(T*), g	0.141
det* (mm)	13.22
Tc (sec)	0.6
dt* (mm)	13.22
Gamma	1.512525

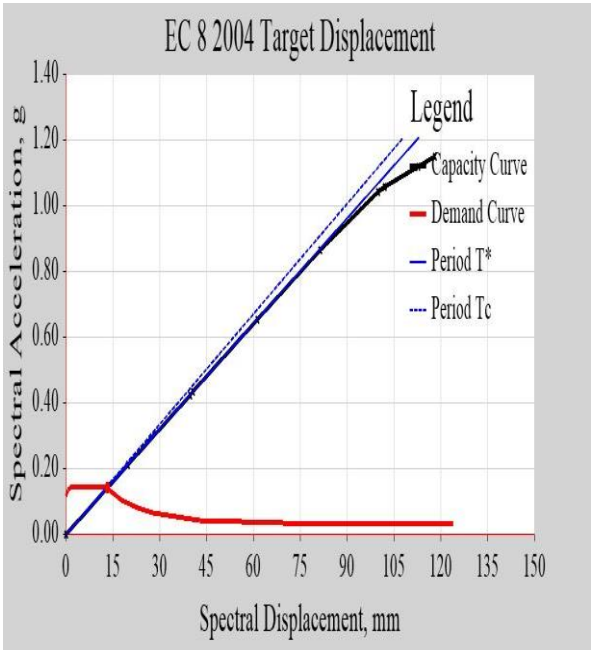

Model 15

Plot Definition	
Plot Type	EC 8 2004 Target Displ
Load Case	PUSH X
Legend Type	Integrated
Demand Spectrum	
Spectrum Source	EC 8 2004 Horiz
Country	CEN Default
Ground Accel, ag/g	0.15
Spectrum Type	1
Ground Type	C
Behavior Factor, q	3
Damping Parameters	
Damping Ratio	0.05
Capacity Curve	
Bilinear Force-Displacement Curve	
Visible	No
Demand Curve	
Period Lines	
Target Displacement Results	
Displacement, dt (mm)	19.573
Shear at dt (kN)	2909.9501
Calculated Parameters	
Target Displ Found	Yes
Fy*, g	0.144
Em* (mm)	0.875
dy* (mm)	12.168
T* (sec)	0.584
Se(T*), g	0.144
det* (mm)	12.168
Tc (sec)	0.6
dt* (mm)	12.168
Gamma	1.608599

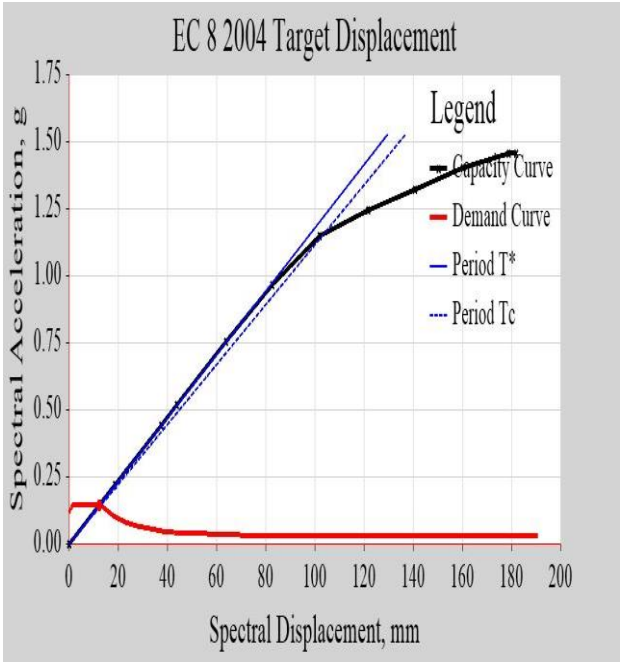

Model 16

Name	
Plot Definition	
Plot Type	EC 8 2004 Target Displ
Load Case	PUSH X
Legend Type	Integrated
Demand Spectrum	
Spectrum Source	EC 8 2004 Horiz
Country	CEN Default
Ground Accel, ag/g	0.15
Spectrum Type	1
Ground Type	C
Behavior Factor, q	3
Damping Parameters	
Damping Ratio	0.05
Capacity Curve	
Bilinear Force-Displacement Curve	
Demand Curve	
Period Lines	
Target Displacement Results	
Displacement, dt (mm)	18.622
Shear at dt (kN)	3015.289
Calculated Parameters	
Target Displ Found	Yes
Fy*, g	0.144
Em* (mm)	0.843
dy* (mm)	11.732
T* (sec)	0.573
Se(T*), g	0.144
det* (mm)	11.732
Tc (sec)	0.6
dt* (mm)	11.732
Gamma	1.587264

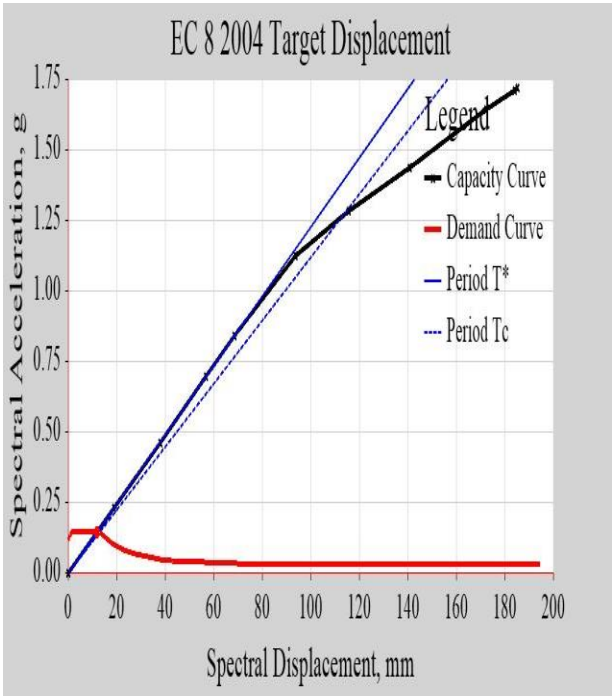

Figure D1. 4Results of target displacement & base shear for (G+10) irregular plan building models

Appendix E. 3-D design detail of building models

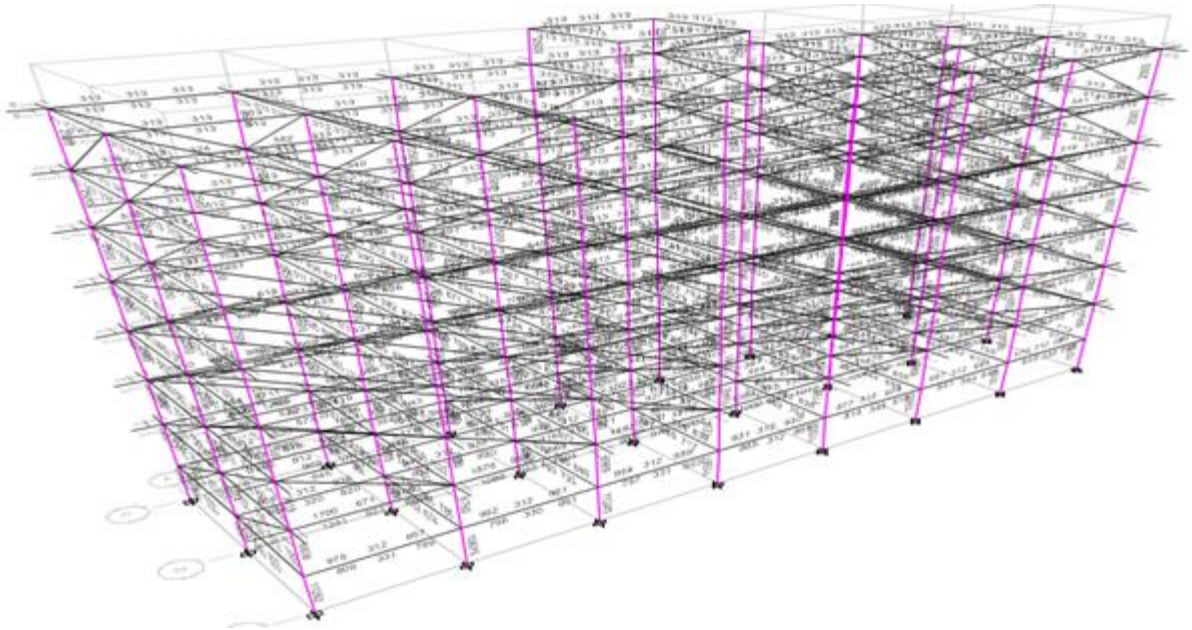

Figure E 1. 1 design of building for (G+7) plan regular building

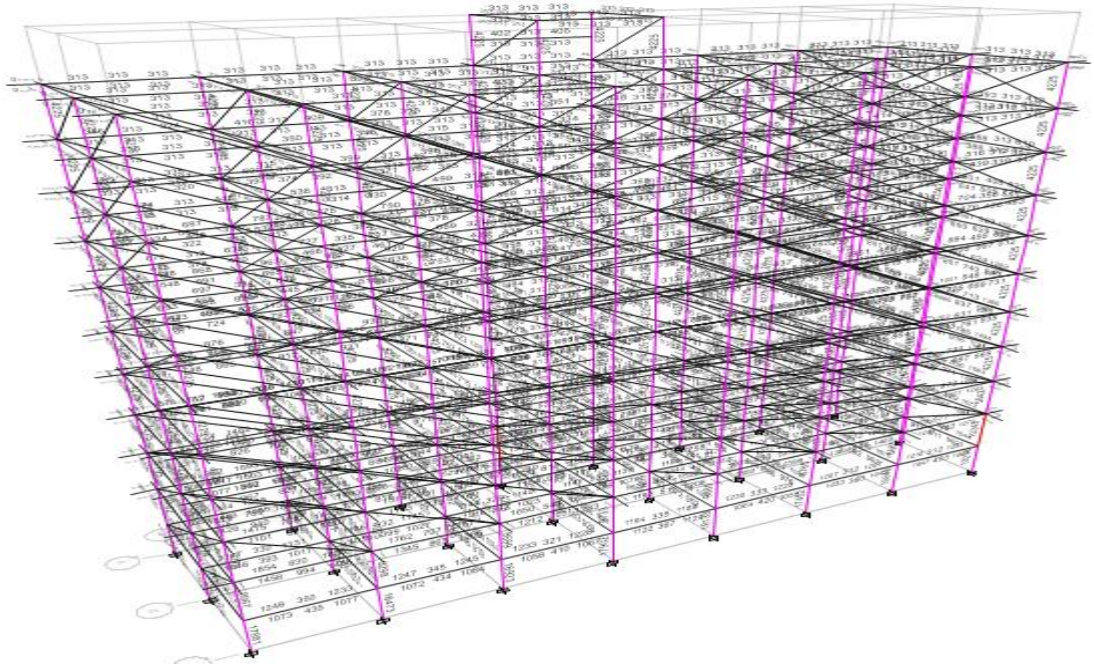

Figure E 1. 2 design of building for (G+10) plan regular model

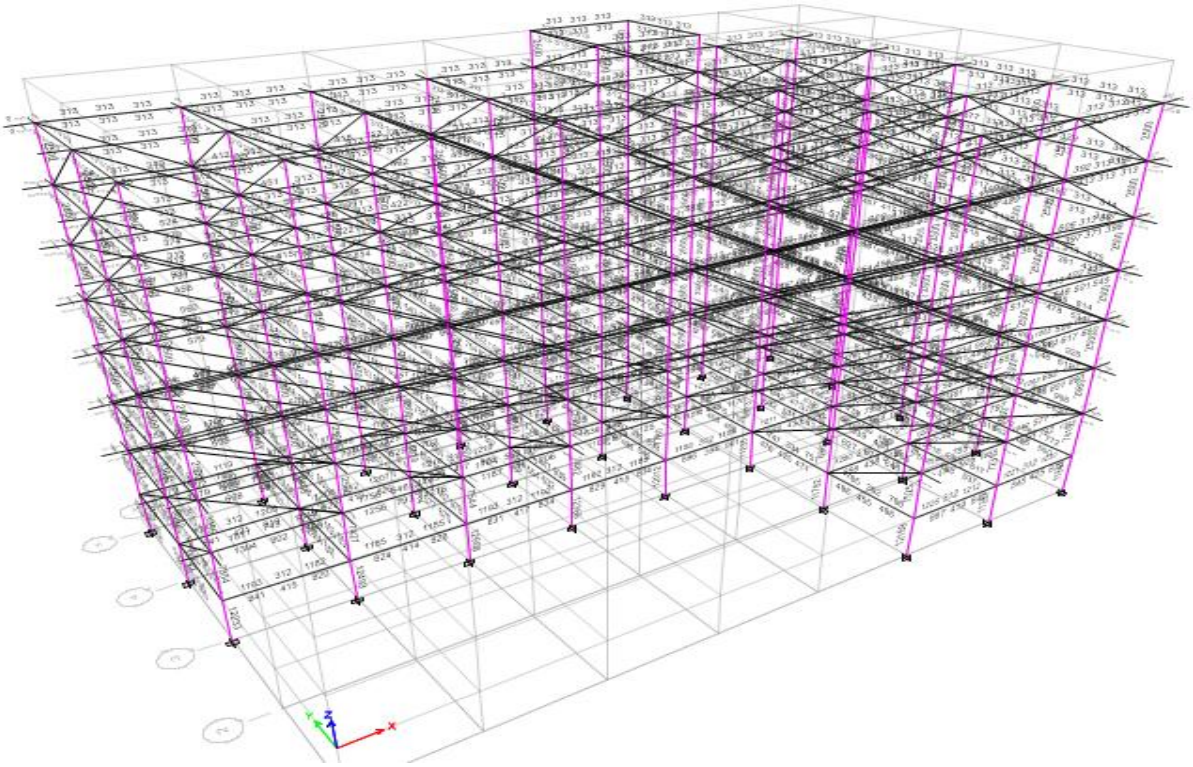

Figure E 1. 3design of building for (G+7) plan irregular model

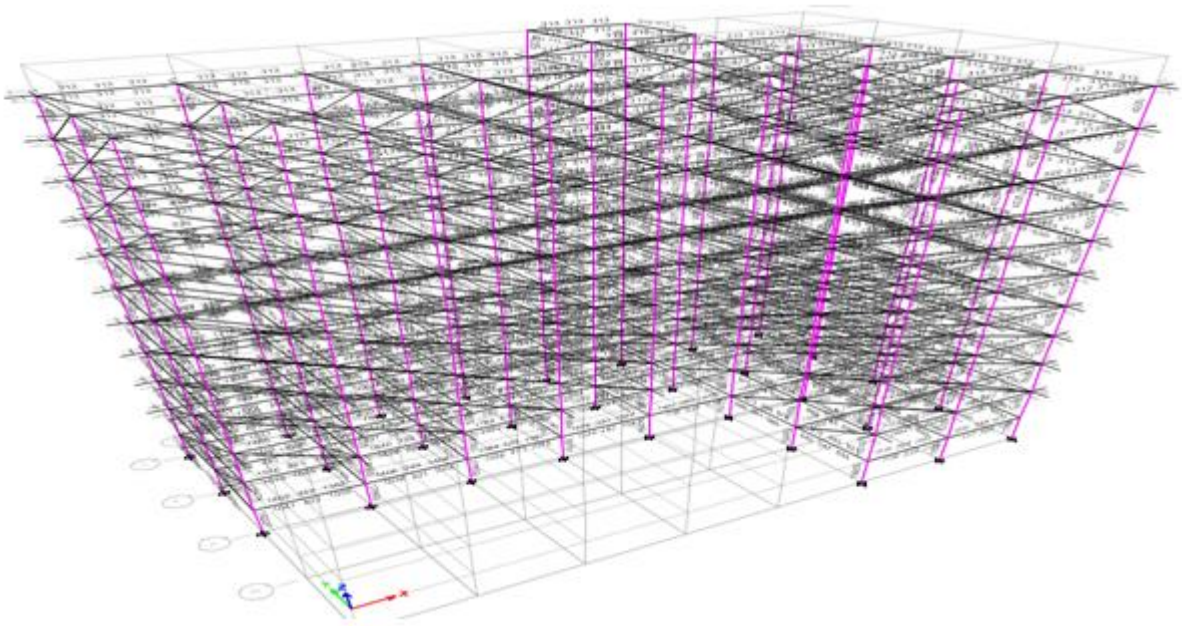

Figure E 1. 4 design of building for (G+10) plan irregular model

Appendix F. Stiffness of building models from response spectrum analysis and soft storey stiffness ratio computation.

Table F 1. 1 Stiffness of building models from response spectrum analysis

		plan regular (G+7) models	plan irregular (G+7) models			plan regular (G+10) models	plan irregular (G+10) models
Storey	Load Case	Stiffness X	Stiffness X	Storey	Load Case	Stiffness X	Stiffness X
		KN/m	KN/m			KN/m	KN/m
G+7	RS	188236.052	444296.218	G+10	RS	171209.088	182546.803
G+6	RS	491340.729	716322.561	G+9	RS	517647.876	647879.347
G+5	RS	551674.636	750479.571	G+8	RS	591293.318	734138.94
G+4	RS	584192.875	761588.816	G+7	RS	627717.393	765510.31
G+3	RS	578470.319	777167.214	G+6	RS	647684.361	782708.335
G+2	RS	377713.091	505618.758	G+5	RS	660511.105	793997.381
G+1	RS	**278530.701**	**346507.746**	G+4	RS	664348.998	800223.512
ground	RS	961836.029	1193086.153	G+3	RS	643584.569	782543.087
				G+2	RS	499353.94	645831.552
				G+1	RS	**429384.736**	**525228.037**
				ground	RS	1151911.363	1392274.855

If $\frac{\text{Ki}}{(\text{Ki}+1+\text{Ki}+2+\text{Ki}+3)/3} < 0.8$ called soft storey

Then by using the above equation and stiffness out puts from response spectrum analysis shown above the stiffness ratios in the X-direction for soft storey used in this study are.

1. For G+ 7 regular plans building

$$\frac{278530.701}{(377713.091+578470.319+584192.875)/3} = 0.54 < 0.8$$

2. For G+10 regular plans buildings

$$\frac{346507.746}{(505618.758+777167.214+761588.816)/3} = 0.71 < 0.8$$

3. For G+7 irregular plan buildings

$$\frac{429384.736}{(499353.94+643584.569+664348.998)/3} = 0.51 < 0.8$$

4. For G+10 irregular plan buildings
5. $$\frac{525228.037}{(645831.552+782543.087+800223.512)/3} = 0.71 < 0.8$$

Appendix G: Outputs after Soft storey Strengthening

Table G1. 1 Storey drift ratio after strengthening of soft storey and building without soft storey

Storey Drift Ratio					
Storey	**Elev.(mm)**	**Loc.**	**Building without soft storey**	**Top soft storey building strengthen by X- steel bracing**	**Ground soft storey building strengthen by X- steel bracing**
G+10	30	Top	0.000177	0.000198	0.000203
G+9	27	Top	0.000305	0.000301	0.00035
G+8	24	Top	0.000484	0.000484	0.000553
G+7	21	Top	0.000665	0.000667	0.000762
G+6	18	Top	0.000845	0.000848	0.000975
G+5	15	Top	0.001039	0.001041	0.001193
G+4	12	Top	0.001236	0.001239	0.001404
G+3	9	Top	0.001433	0.001437	0.001647
G+2	6	Top	0.001602	0.001606	0.001728
G+1	3	Top	0.001716	0.00172	0.002239
Ground	0	Top	0	0	0

Table G1. 2Storey displacements after strengthening of soft storey and building without soft storey

Storey Displacement					
Storey	**Elev.(mm)**	**Loc.**	**Building without soft storey**	**Top soft storey building strengthen by X- steel bracing**	**Ground soft storey building strengthen by X- steel bracing**
G+10	30	Top	29.716	29.856	30.219
G+9	27	Top	29.431	29.482	29.947
G+8	24	Top	28.764	28.812	29.28
G+7	21	Top	27.518	27.572	28.019
G+6	18	Top	25.691	25.745	26.183
G+5	15	Top	23.284	23.335	23.807
G+4	12	Top	20.295	20.341	20.941
G+3	9	Top	16.719	16.758	17.662
G+2	6	Top	12.545	12.575	13.999
G+1	3	Top	7.787	7.806	9.234
Ground	0	Top	0	0	0